Delimitation of the organizer from the posterior notochord: descriptive and functional studies in mouse and African clawed frog

Dissertation zur Erlangung des Doktorgrades
der Naturwissenschaften (Dr. rer. nat.)

Fakultät Naturwissenschaften
Universität Hohenheim

Institut für Zoologie

vorgelegt von

Philipp Andre

aus Stuttgart

2009

Dekan:	Prof. Dr. Heinz Breer
1. berichtende Person:	Prof. Dr. Martin Blum
2. berichtende Person:	Prof. Dr. Heinz Breer
Eingereicht am:	02.09.2009
Mündliche Prüfung am:	13.11.2009

Die vorliegende Arbeit wurde am 29.10.2009 von der Fakultät Naturwissenschaften der Universität Hohenheim als „Dissertation zur Erlangung des Doktorgrades der Naturwissenschaften“ angenommen.

Mein herzlicher Dank gilt Prof. Martin Blum für die Begeisterung, die er in mir für das spannende Feld der Entwicklungsbiologie geweckt hat und die Überlassung der interessanten Fragen, die ich bearbeitet habe. Sein Interesse und seine Motivation waren mir eine große Hilfe.

Ich danke Prof. Heinz Breer für sein Interesse an dieser Arbeit und die Bereitschaft, diese zu begutachten.

Ich möchte mich bei Dr. Axel Schweickert für seine Unterstützung und seinen wertvollen Rat gerade bei kniffligen und verworrenen Problemen, auch in letzter Minute, bedanken.

Vielen Dank an die gesamte Arbeitsgruppe Embryologie für lebhafte Diskussionen, die nette Atmosphäre und große Hilfsbereitschaft jedes einzelnen. Bei Bärbel Ulmer möchte ich mich besonderst für die große moralische Unterstützung und die Geduld, meine Arbeit zu verbessern bedanken. Ich danke Tina Beyer für die Unterstützung bei der Anfertigung und der Analyse der REM-Aufnahmen. Thomas Weber möchte ich für seine Hilfe bei der Analyse des Flows und anderen Herausforderungen danken. Bei Philipp Vick möchte ich mich ganz herzlich für die tolle, jahrelange Zusammenarbeit in zoologischer, embryologischer und ernährungswissenschaftlicher Hinsicht bedanken.

Ganz besonderst lieben Dank an meine Frau und Kollegin Verena für die große Liebe, Geduld und Unterstützung, auch wenn’s bei mir mal wieder länger gedauert hat. Dazu danke ich auch für den Rückhalt und die Motivation in den schwierigen Phasen und besonderst den letzten Tagen dieser Arbeit.

Vielen lieben Dank auch meiner Familie, die mir durch ihre vielfältige Unterstützung und ihrem Interesse an meiner Arbeit ein großer Rückhalt ist. Besonderer Dank an meine Mutter fürs Korrekturlesen dieser Arbeit

Abstract

During vertebrate development, gastrulation is probably the most important phase, as the future body plan is established. Thereby the three body axes anterior-posterior, dorsal-ventral and left-right are determined as well. A central role thereby is taken by the Spemann organizer, as this part of the embryo governs the above mentioned processes. The left-right axis is specified by an extracellular leftward fluid-flow, which results in asymmetric gene expression of the TGFβ factor *Nodal*. In mice the ciliated epithelium responsible for the fluid-flow as well as the organizer are denominated as 'node'. In contrast to that two distinct entities are thought to be responsible for organizer function and fluid-flow in zebrafish, *Xenopus* and rabbit embryos. In the present study, it could be shown that this also applies for mouse embryos. In order to prevent further confusion the ciliated epithelium responsible for the fluid-flow was denominated as posterior notochord (PNC) as it is in continuity with the notochord but located anterior to the organizer ('node'). The latter is characterized by the expression of the homeobox gene *Goosecoid* (*Gsc*). *Gsc* possesses, like the tissue of the organizer, the potential to induce an almost complete axis and became therefore famous as 'the organizer gene'. However upon knockout of *Gsc* in the mouse, surprisingly no gastrulation defects could be detected. Therefore the function of *Gsc* during gastrulation was investigated using a gain-of-function approach. The analysis of this, in the present and previous studies, indicated that *Gsc* acts as a switch between two modes of cell movement. Accordingly, *Gsc* promotes active cell migration and inhibits convergent extension movements.

Furthermore it was investigated whether the monoamines adrenaline and serotonin have an influence on the cilia and thus on the leftward fluid-flow, as it was reported in rat and *Xenopus* experiments. Thereby it could be detected that the addition of adrenaline led to a reduction of the ciliary beat frequency (CBF) and therefore the fluid-flow was attenuated. In contrast to that the addition of serotonin or its antagonists resulted only in minor changes of CBF and thus had no measurable effect on the fluid-flow.

The consequences of a malformed PNC were analyzed using embryos mutant for *Brachyury* (*T*). Thereby, it was shown that embryos homozygous for this mutation did not develop a functional PNC and thus lacked the fluid-flow. Furthermore a possible cause for the absence of asymmetric *Nodal* in these embryos was brought into

context of an attenuated expression of *Fgf8*. This indicated that *T* possesses two distinct roles in left-right development. On the one hand it is necessary for the correct formation of a PNC and on the other hand it is probably needed to maintain the expression of *Fgf8*, which is a prerequisite for the transcription of *Nodal*. Finally it was investigated whether these functions were conserved from the African clawed frog *Xenopus*. Thereby, it could be shown, that *Xbra*, the homologous gene of *T* in *Xenopus*, was also necessary for the formation of the gastrocoel roof plate, the homologous structure of the PNC. Additionally it was observed that the absence of *Xbra* led to an attenuation of *Nodal* expression in the midline of *Xenopus* embryos. This implied that not only the function of *Brachyury*, but also the process of laterality determination is highly conserved between mammals and amphibians.

Zusammenfassung

Während der Entwicklung der Wirbeltiere stellt die Gastrulation die vermutlich wichtigste Phase dar, da sie sich durch die Anlage des zukünftigen Körperbauplans auszeichnet. Dabei werden auch die drei Körperachsen Anterior-Posterior, Dorsal-Ventral und Links-Rechts bestimmt. Eine zentrale Rolle nimmt hierbei der sog. Spemann-Organisator ein, da dieser Teil des Embryos die oben genannten Prozesse steuert. Die Links-Rechts-Achse wird als letzte spezifiziert. Dies geschieht durch eine extrazelluläre, linksgerichtete Flüssigkeitsströmung, die eine links-asymmetrische Genexpression des TGFβ Faktors *Nodal* zur Folge hat. In Mausembryonen wird das für diese Strömung verantwortliche Epithel darüber hinaus als Homolog des Spemann Organisators betrachtet und als ‚node' bezeichnet. In den Wirbeltieren Zebrabärbling, Krallenfrosch und Kaninchen sind im Gegensatz dazu zwei verschiedene Strukturen für Organisatorfunktion und Flüssigkeitsströmung verantwortlich. In der vorliegenden Arbeit konnte gezeigt werden, dass es sich in der Maus ebenfalls um zwei verschieden Einheiten handelt. Um weitere Verwechslungen auszuschließen wurde das cilierte Epithel, das für den Flüssigkeitsstrom verantwortlich ist, als posteriores Notochord (PNC) bezeichnet, da es sich in Kontinuität mit dem restlichen Notochord befindet, aber anterior des Organisators (‚node') liegt. Dieser wird durch die Expression des Homöoboxgens *Goosecoid* (*Gsc*) charakterisiert. *Gsc* besitzt, wie das Gewebe des Organisators, die Fähigkeit eine

beinahe vollständige Körperachse zu induzieren und wurde daher als „das Organisator Gen“ berühmt. Durch den Funktionsverlust von *Gsc* in der Maus wurde überraschenderweise aber keine bemerkbare Beeinträchtigung der Gastrulation festgestellt. Daher sollte mittels Funktionsgewinn untersucht werden, welche Funktion *Gsc* während der Gastrulation besitzt. Die Analysen in dieser und in vorangegangen Arbeiten zeigte, dass *Gsc* vermutlich als Schalter zwischen zwei verschiedenen Zellbewegungsmodi fungiert, indem es die aktive Migration unterstützt und den Prozess der konvergenten Extension inhibiert.

Darüber hinaus wurde untersucht, ob die Monoamine Serotonin und Adrenalin einen Einfluss auf Cilien des PNCs und damit auf den linksgerichteten Flüssigkeitsstrom haben, da es dafür Hinweise aus Ratten- und Froschexperimenten gibt. Dabei zeigte sich, dass die Zugabe von Adrenalin in einer Reduktion der Cilienschlagfrequenz (CBF) resultierte und somit auch die Flüssigkeitsströmung abgeschwächt wurde. Im Gegensatz dazu veränderte die Zugabe von Serotonin oder dessen Antagonisten die CBF nur in geringem Maße und hatte daher keinen entscheidenden Einfluss auf die Flüssigkeitsströmung.

Die Fehlbildung eines PNCs wurde anhand der *Brachyury* (*T*) Mutante untersucht. Dabei zeigte sich, dass Embryonen, die diese Mutation homozygot tragen, kein funktionelles PNC ausbilden und daher auch über keinen Flüssigkeitsstrom verfügen. Darüber hinaus wurde nach einer Ursache für das Fehlen der asymmetrischen Expression von *Nodal* in diesen Embryonen gesucht. Dies konnte in Zusammenhang mit einer Abschwächung der Expression von *Fgf8* gebracht werden. Daraus folgte, dass *T* zwei verschiedene Funktionen bei der Entwicklung der Links-Rechts-Achse einnimmt. Einerseits wird es benötigt um ein funktionelles PNC auszubilden, andererseits ist es vermutlich dafür verantwortlich, dass die Expression von *Fgf8* erhalten bleibt und damit die Transkription von *Nodal* ermöglicht wird. Abschließend wurde *T* auf eine mögliche Konservierung seiner Funktionen im afrikanischen Krallenfrosch untersucht. Dabei zeigte sich, dass *Xbra*, das homologe Gen von *T* im Krallenfrosch, ebenfalls für die Morphogenese der Dachplatte des Archenterons, der homologen Stuktur des PNCs, notwendig ist und in Abwesenheit von *Xbra* die Expression von *Nodal* beeinträchtigt ist. Daraus konnte geschlossen werden, dass nicht nur die Funktion von *Brachyury*, sondern auch der Prozess der Links-Rechts Entwicklung zwischen Säugetieren und Amphibien hoch konserviert ist.

Table of contents

Introduction

The fertilization of an egg-cell demarcates the beginning of embryonic development of animals. This period is subdivided into different phases in vertebrates, beginning with the cleavages, in which the oocyte divides consecutively. The resulting sphere of cells is called morula and it further develops into the blastula. This stage is defined by the formation of a fluid filled cavity, the blastocoel, situated in the center of the sphere. Subsequently the gastrulation begins. In this stage the basic body plan is established. This is achieved by the formation of the three germ layers: the ecto-, meso- and endoderm. Furthermore the cells reach an orderly allocation through complex migrational movements. By this the three body axes dorsal-ventral, anterior-posterior and left-right are established as well. Gastrulation is followed by neurulation. This phase is characterized by the formation of the central nervous system. Embryonic development is concluded by the generation and differentiation of the organs, the phase of organogenesis (Wolpert et al. 1998).

Determination of the body axes during gastrulation

Gastrulation

During the development of the deuterostomes, gastrulation is of particular importance, as coordinated cell movements result in a dramatic rearrangement of the embryo. Thereby the three germ layers and the basic body plan are established. Of these the endoderm gives rise to inner surface of the intestines, whereas the mesoderm forms the musculature and the ectoderm is responsible for the development of the skin and the central nervous system. Thus gastrulation results in the formation of a bilateral symmetric, multi-layered organism which is characterized by a central gut.

Cell movements

During gastrulation embryonic cells undergo massive relocation. Thereby cells migrate actively. This is achieved in three steps, beginning with the formation of an actin rich protrusion (lamellipodium) at the front of the cell. The second step involves the attachment of the protrusion to the substratum. This is followed by contraction at the rear end of the cell which propels the cell forward (Alberts et al. 2002). A special mode of cell movement is represented by convergent extension which is driven by a cell-rearrangement within a tissue. Thereby the cells intercalate along a specific axis. This is achieved by cells crawling between one another using attachment to other cells in the same population as a substrate for the movement. A prerequisite for this movement is the polarity of the cells. Convergent extension results in a concomitant narrowing and lengthening of a tissue (Wallingford et al. 2002). The process of convergent extension is involved in the closure of the neural tube.(Ybot-Gonzalez et al. 2007). Therefore, a compromised convergent extension leads to neural tube closure defects. These malformations occur at an average rate of 1 per 1,000 human pregnancies and thereby are the second most prevalent congenital defects in human development (Copp et al. 2003).

The Spemann organizer

For gastrulation the organizer is of great importance in vertebrates. It was first described by Hilde Mangold and Hans Spemann in 1924 (Spemann and Mangold 1924). In their ground breaking work they found out that there is a specific region in amphibian embryos which has the ability to induce the formation of a complete axis. This was shown experimentally by transplantation of dorsal tissue from a donor newt embryo into the ventral region of another newt embryo. The experiment led to the formation of Siamese twin embryos as it consisted of the endogenous body axis which was accompanied by an induced secondary axis.

Intense studies were carried out to find equivalent structures in other vertebrates. In rabbit and chick embryos the Hensen’s node represented a possible candidate. This specific structure was named after its discoverer Victor Hensen. He described a thickening in the rabbit embryo which was characterized by a mass of cells in which the germ layers were indistinguishable. A similar thickening could also be found in

the chick embryo. After transplantation of this very structure from one chick embryo to another, the formation of a secondary axis was reported (Waddington 1933; Waddington and Schmidt 1933). Therefore Hensen's node is regarded as homolog of the Spemann organizer. The detailed molecular and embryological analysis of organizer function in recent years has shown that it is composed of a dynamic population of cells (Kinder et al. 2001). These cells are the progenitors of the notochord and the overlying floorplate. Although the cells of the organizer change during development, they share the temporary expression of genes such as *Goosecoid* (*Gsc*), *Follistatin*, *Chordin* and *Noggin* (De Robertis et al. 1992; Joubin and Stern 1999; De Robertis et al. 2000; Niehrs 2004).

Gastrulation in the mouse

Gastrulation in mouse embryos begins at embryonic day 6.5 (E6.5) and, like in other vertebrates, is manifested by the formation of the primitive streak (PS; Fig. 1). In contrast to other mammals and chicks, the rodent embryo does not develop from a blastodisc but from an egg-cylinder. This unique form derives from a folding of the blastodisc in a way that its center gives rise to the distal tip while its periphery is connected to extraembryonic tissue arranged in a small ring. Before the onset of gastrulation the epiblast, i.e. the future animal, of the mouse embryo faces the inside of the egg-cylinder and is surrounded by the hypoblast (visceral or extraembryonic endoderm). Therefore, gastrulation in the mouse appears inverted as the endodermal cells migrate towards the outside and not the inside of the embryo like in other vertebrates. This inversion is reversed at stage E8.5 when the embryo rotates in a manner that the endodermal cells finally reach the inside of the embryo.

During gastrulation the PS elongates towards the distal tip of the egg-cylinder and reaches it by E7.5. At that stage anterior to the PS an indentation, covered by a ciliated epithelium, is formed at the distal tip of the embryo. This ciliated indentation was originally denominated archenteron (Theiler 1972). Furthermore Theiler described it to be in continuity with the notochord. The region was then renamed in an attempt to find homologous structures of the amphibian Spemann organizer and

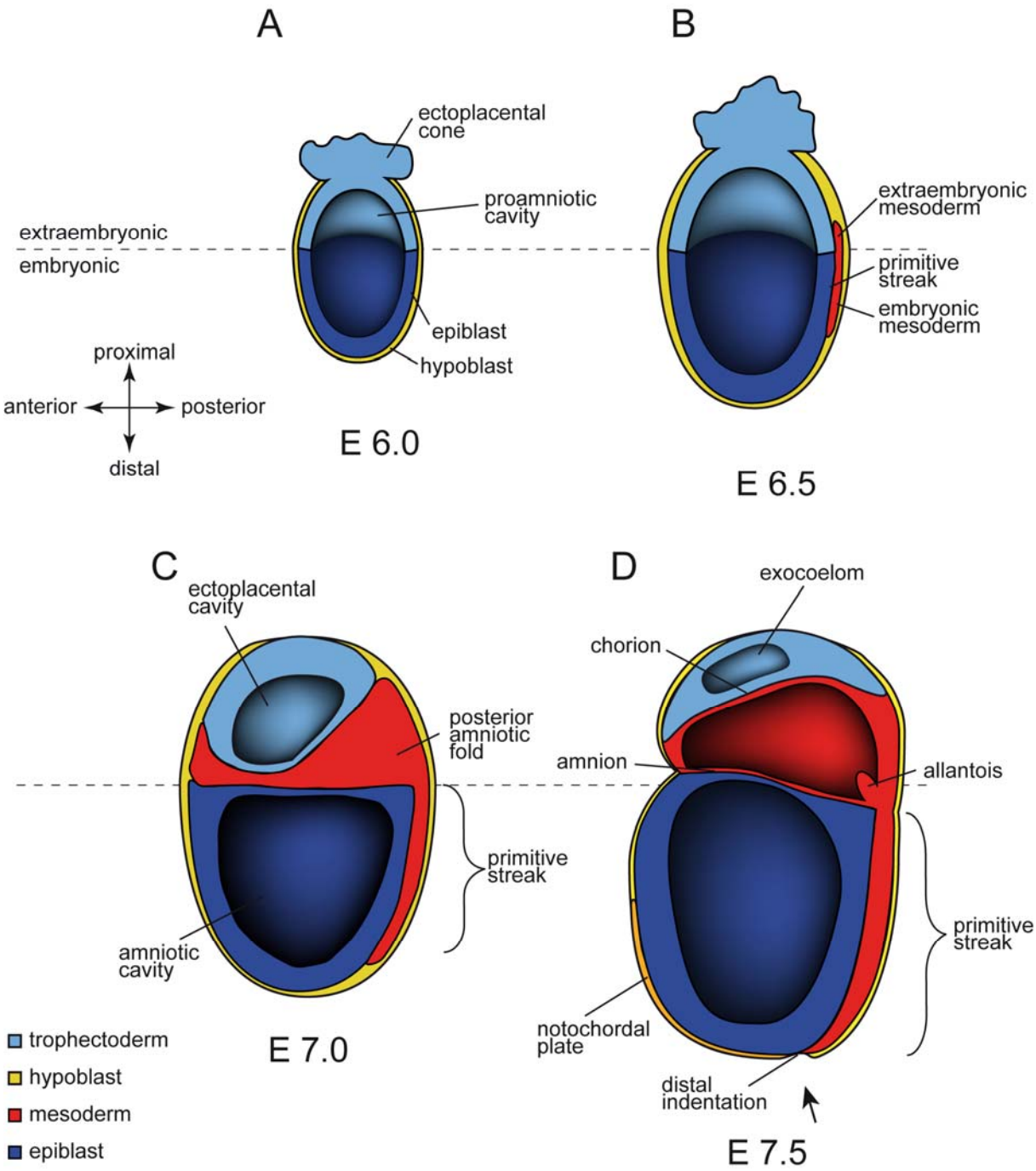

Fig. **1** Gastrulation in the mouse. Schematic drawing of mouse development from embryonic day (E) 6.0 to E7.5 (adapted from Nagy et al. 2003). (**A**) Before the onset of gastrulation the embryo consists of the epiblast (blue, the actual embryo) and the trophectoderm (light blue). It is surrounded by the hypoblast (visceral endoderm, yellow). The ectoplacental cone mediates the gas exchange between the embryo and its mother. (**B**) Gastrulation begins with the formation of the primitive streak at the posterior end of the embryo. Thereby nascent mesodermal cells (red) leave the epiblast and start to migrate in order to encompass the epiblast and to spread into the extraembryonic region. (**C**) In the 7.0 day old embryo the formation of the amniotic fold separates the proamniotic cavity into the ectoplacental and amniotic cavity. Concomitantly the primitive streak elongates toward the distal tip of the egg-cylinder. (**D**) On E7.5 the formation of the allantois and the chorion begins. These two structures are destined to give rise to the umbilical cord and the placenta, respectively. The primitive streak extends to its maximum length at this stage, as it reaches the distal tip of the embryo. In this region a distal indentation covered with a ciliated epithelium forms (also known as node). Anterior to this the notochord (orange) develops and extends, thereby the anterior / posterior axis of the embryo elongates. Besides mesodermal cells, endodermal cells also leave the primitive streak in order to replace the hypoblast and give rise to the foregut. The cells remaining within the epiblast are the precursors of the ectoderm. Arrow in (**D**) indicates view in Fig. 2.

Hensen's node in the chick (Beddington and K.A. and Herrmann 1992). Since then the indentation is commonly referred to as 'the node'. Recently the indentation has received additional interest as it is involved in laterality determination (Nonaka et al. 1998; Hamada et al. 2002).

The Spemann organizer in the mouse

Subsequently, the homeobox gene *Gsc* was described as the first organizer specific gene in the mouse (Blum et al. 1992). In addition the organizer function of the tissue expressing *Gsc* was demonstrated in heterologous grafts into *Xenopus* embryos (Blum et al. 1992). This finding could be confirmed in homologous grafts (Beddington 1994). The knowledge on the organizer in the mouse was further improved by Patrick Tam and colleagues as they transplanted the anterior aspect of the PS of different stages (Kinder et al. 2001). Thereby it could be shown that the inductive capacity of the organizer is dependent on the developmental stage of the donor tissue and therefore can be distinguished in early, mid and late gastrula organizers (Kinder et al. 2001). The mid gastrula organizer (E7.0) has the capacity to induce a complete secondary axis. It thus resembles the Spemann organizer in the newt. In contrast to that the early and the late gastrula organizers only have the ability to induce head and trunk or trunk and tail structures, respectively (Kinder et al. 2001).

The mentioned data indicates that an uncertainty exists about the midline structures of gastrulating mouse embryos, as both the organizer and the distal indentation are referred to as 'the node'. In order to avoid further confusion, it was investigated which entity is homologous to Hensen's node and thus deserves to be called the node.

The role of the organizer gene *Goosecoid*

Among the first genes that were discovered to be expressed in the Spemann organizer of the African clawed frog (*Xenopus laevis*) was the homeobox gene *Goosecoid (Gsc)* (Blumberg et al. 1991). The expression of *Gsc* in the dorsal marginal zone (DMZ), i.e. Spemann's organizer, was found to be conserved in all vertebrates examined to date (De Robertis et al. 1992). Studies in invertebrates revealed that homologous genes are present in *Drosophila* and even in the cnidarian *Hydra* (Broun et al. 1999). Upon injection of *Gsc* into the ventral side, which does not express *Gsc* endogenously, the formation of secondary axes could be induced in *Xenopus* embryos (Cho et al. 1991). With this the Spemann experiment was genetically mimicked and therefore *Gsc* became known as 'the organizer gene'.

Surprisingly, the knockout (KO) of *Gsc* in the mouse did not result in any gastrulation phenotype (Rivera-Perez et al. 1995; Yamada et al. 1995). *Gsc* deficient embryos display defective rib formation and craniofacial development is affected in a way that the newborn pubs are unable to feed and therefore do not survive more than 24 hours (Rivera-Perez et al. 1995; Yamada et al. 1995). The lack of a gastrulation phenotype was supposed to be attributed to a compensational mechanism. Therefore possible candidates were searched for. *Gsc2*, a close relative of *Gsc*, was identified but showed a different expression pattern and thus could not compensate for the loss of *Gsc* (Galili et al. 1997; Saint-Jore et al. 1998; Wakamiya et al. 1998). Up to date only genes that are negatively controlled by *Gsc* have been identified. Direct target genes are *Wnt8a* (*wingless-related mouse mammary tumor virus integration site 8A*) and the transcription factor *Brachyury* (*T*) (Artinger et al. 1997; Latinkic et al. 1997; Latinkic and Smith 1999; Boucher et al. 2000; Yao and Kessler 2001).

Furthermore, *Gsc* has been shown to be able to control cell migration during gastrulation (Niehrs et al. 1993). This finding was revealed using lineage labeling and video microscopy of *Gsc*-injected frog embryos. Thereby anterior movements of posterior cells could be detected (Niehrs et al. 1993). An influence on migration was also proven in cultured embryonic frog head mesenchyme, as the migratory behavior of these cells was improved upon *Gsc* activity under certain conditions (Luu et al. 2008). In addition to that, an upregulation of *Gsc* was reported in human breast

tumors (Hartwell et al. 2006). Ectopic expression of *Gsc* caused an epithelial-mesenchymal transition and therefore an invasion-associated mechanism was activated. Moreover *Gsc* enhanced metastasis to the lung when overexpressed in human breast cancer cells, which were transferred to mice (Hartwell et al. 2006). Taken together, these experiments suggest a general role of GSC in cell migration during development and disease, which only was revealed in gain-of-function experiments.

However a unifying hypothesis regarding the role of *Gsc* especially in the context of the conserved expression pattern remains elusive. Therefore a *Gsc* gain-of-function experiment in the mouse was designed in a way that *Gsc* should not only be expressed in the anterior but the complete PS. For this experiment the generation of a transgenic mouse was necessary. The experiment was attempted in a conditional way as the overexpression was supposed to be lethal for the embryo.

Conditional misexpression of *Gsc*

In order to achieve a conditional misexpression, the *Cre/LoxP* system was used (Hamilton and Abremski 1984; Hoess and Abremski 1984; Lewandoski 2001). This system is derived from the phage P1 and allows site specific recombination and therefore activation or knockout of genes of interest. For the recombination the *LoxP* (locus of x-over) sites need to be inserted into the genome. These specific domains function as a recognition site for the *Cre* (*causes recombination*) enzyme. Sequences in-between two *LoxP* sites are being cut out by the *Cre* enzyme. As long as *Cre* is not present, the *LoxP* sites have no effect. Normally the *Cre* is added by crossing in a *Cre*-expressing mouse line. For specific recombination in specific tissue or developmental stages, there are several mouse lines available which express *Cre* in a different manner (Lewandoski 2001; Kuhn and Torres 2002).

In a first approach, a construct was produced for which the *Brachyury* (*T*) PS promoter was chosen as it has been shown to be responsible for expression of T in the complete PS (Clements et al. 1996). The promoter was followed by a *LacZ* marker-gene which allowed the analysis of the transgene expression. Finally, the *Gsc* coding sequence was attached to the construct. The *LacZ* gene was flanked with *LoxP* sites in order to allow the removal of the marker-gene and thus enable the transgenic *Gsc* expression. Without recombination no ectopic *Gsc* was expressed

and only the *LacZ* gene was under the control of the *T*-promoter in this mouse line. The transgene expression was analyzed using *LacZ* staining and thereby activity in the PS could be detected (Deißler 2002). After this the *Deleter-Cre* mouse line was crossed in and recombination was performed during blastula stages, when *Cre* is expressed in this very mouse-line (Schwenk et al. 1995). As it has been shown that *Gsc* represses *T*, the transgenic construct repressed its own expression (Artinger et al. 1997; Latinkic et al. 1997; Latinkic and Smith 1999). This resulted in only a very faint overexpression which did not disturb gastrulation (Deißler 2002).

A second approach was made which differed from the first only in that the *Gsc* binding site within the *T*-promoter was mutated (Boucher et al. 2000; Deißler 2002). This prevented GSC from binding to the *T*-promoter and the resulting mouse line was named *mT-Gsc*. The analysis of the transgene expression using *LacZ* staining again revealed activity in the PS although at earlier stages and at a higher level compared to the first mouse line (Andre 2004). Crossing in of the *Cre* line lead to a massive overexpression of *Gsc* and resulted in a gastrulation phenotype (Andre 2004). Although the observed defects concerned all three germ layers, an anterior posterior polarity was established. The transgene expression and thus the severity of the phenotype varied in strength. Therefore different malformations could be detected, but a main feature of the transgenic embryos was the diminished over-all size often accompanied by excessive tissue filling the cavity of the epiblast. Besides this, the formation of the definitive endoderm was impaired and thus the visceral endoderm could not be replaced correctly (Kienle 2006). A third observation involved the compromised formation of the notochord in *mT-Gsc/Cre* embryos as revealed by scanning electron microscopy (SEM). In order to further understand the influence of *Gsc* on development of this embryonic structure, molecular markers were investigated. As the notochord is necessary for the elongation of the anterior-posterior axis, absence of the notochord could explain the mentioned shortened over-all size of the double transgenic embryos.

The development of the left-right axis in mouse and frog

Brachyury (*T*)

As mentioned above, *Brachyury* (*T*) is repressed by *Gsc*. The transcription factor *T* belongs to the family of T-box genes (Herrmann and Kispert 1994). It is expressed in the PS of mammals and chicks and in homologous structures of other vertebrates (Wilkinson et al. 1990; Smith et al. 1991; Schulte-Merker et al. 1994; Kispert et al. 1995). As the *T*-expressing cells adopt a mesodermal fate, *T* is known as a pan-mesodermal marker. After full extension of the PS, *T* is also expressed in the distal indentation and the forming notochord. *T* was one of the first morphogenetic mutants identified in the mouse and is characterized by heterozygous animals bearing shorter or even absent tails (Dobrovolskaïa-Zavadskaïa 1927). Homozygous mutants die during embryogenesis at about E9.5 of gestation. These embryos display multiple defects as the posterior mesoderm does not form correctly. This results in a defective notochord which is initially establish but not maintained (Gruneberg 1958). Furthermore, only the anteriormost somites are formed and the allantois, the precursor of the umbilical chord, is absent (Herrmann 1992). As the allantois is necessary for the connection between the embryo and the mother via the placenta, the lack of the allantois causes embryonic lethality. Additionally, homozygous *T* mutants display left-right defects as the heart fails to become asymmetric (King et al. 1998).

The left-right axis

With the onset of gastrulation the main body axes are established. As a consequence of the determination of the dorsal-ventral and the anterior-posterior axis the left-right axis is predestinated in vertebrates. Although the two other axes define the left-right axis per se, this is molecularly not manifested until late gastrulation (mouse) or neurulation (frog; Lowe et al. 1996). Before this the vertebrate embryo develops bilateral-symmetrically like all other members of the taxon bilateria. This ancient form remains for the outer appearance of all vertebrates. In contrast to that the inner organs are distributed asymmetrically within the body. For example the apex of the

heart points to the left side whereas the liver is located mainly on the right side. Furthermore the stomach is on the left side and even the lung that appears to be symmetric consists in the mouse of one lobe on the left side and four lobes on the right side. The determination of the laterality can be divided into three phases. First step thereby is the breaking of the bilateral symmetry, which is followed by asymmetric gene expression. Finally, the asymmetric expression of transcription factors gives rise to asymmetric organogenesis (Fig. 2).

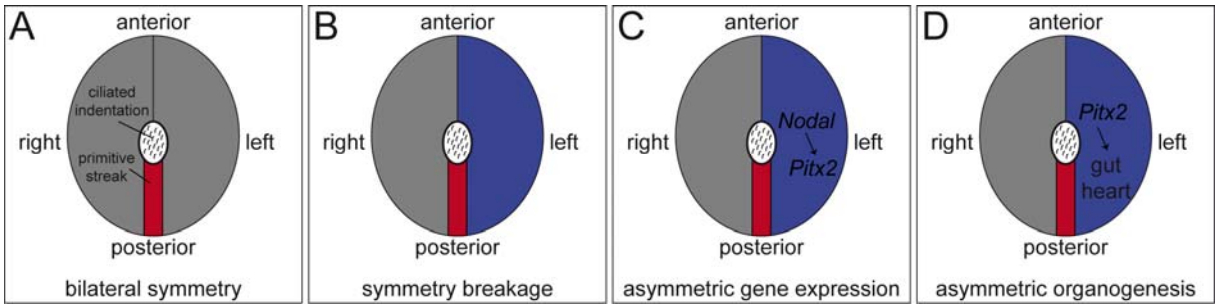

Fig. **2** Three phases of left-right development. Schematic drawings of a ventral view (indicated in Fig. 1D) at a mouse embryo during laterality determination (Modified from Blum and Fischer 2003). (**A**) At E7.5 the embryo is bilateral symmetric. Anterior to the primitive streak a ciliated indentation forms. (**B**) The breakage of the symmetry is governed by the ciliated indentation. (**C**) This is manifested by the onset of asymmetric gene expression of Nodal, which induces transcription of Pitx2. (**D**) Pitx2 is responsible for the asymmetric organogenesis.

In humans about 1 out of 10,000 persons displays a mirror image-like arrangement of the inner organs (Casey 2001). This situation is called *situs inversus* whereas a normal placement of the organs is called *situs solitus*. Individuals demonstrating a *situs inversus* do not suffer from any impairment. When only some of the organs are misplaced the phenotype is called heterotaxia. In contrast to situs inversus, heterotaxia are accompanied by health impairment often so severe, that the developing individual is non-viable. Heterotaxia are caused by the random arrangement of each organ. An additional impairing phenotype is represented by a left or a right isomerism, meaning that both sides adopt the fate of either the left or right side, respectively. This can result, in case of the spleen for example, in duplication or absence of the organ (Casey 1998).

Nodal – the key player in left-right development

In the mouse *Nodal* is expressed in the complete PS from the onset of gastrulation on (Varlet et al. 1997). Thus, it is also expressed in the organizer, which is located at

the anteriormost part of the PS (Kinder et al. 2001). Knockout experiments have shown that Nodal is necessary for gastrulation, as *Nodal* deficient mouse embryos fail to form a PS (Conlon et al. 1994). As soon as the PS reaches the distal tip of the embryo, *Nodal* is downregulated in the PS. *Nodal* is then expressed in a bilateral domain on the left and right side of the ciliated indentation mentioned above (Conlon et al. 1994). The bilateral expression, flanking the indentation, has been shown to be crucial for the subsequent laterality determination, as its absence leads to the absence of asymmetric gene expression ((Brennan et al. 2002; Saijoh et al. 2003)). *Nodal* is the first gene to be expressed asymmetrically and was first described 1995 in the chick (Levin et al. 1995). Later it was also found in all other vertebrate model organisms (Lowe et al. 1996).

The *Nodal* cascade

The *nodal* cascade consists of *Nodal* and its three identified downstream targets *Lefty1/2* (*left-right determination factor 1/2*, members of the TGF-β superfamily) and *Pitx2* (*paired-like homeodomain transcription factor 2*). The cascade is initiated by expression of *Nodal* in the left Lateral plate mesoderm (LPM) where it induces its own expression via a positive feedback loop. *Nodal* negatively regulates its own expression by inducing the *Nodal* repressors *Lefty1* in the midline and *Lefty2* in the LPM (Meno et al. 1996). *Lefty1* is thought to act as midline barrier preventing the Nodal signal from crossing over to the right side and inducing the cascade there (Meno et al. 1998). *Lefty2* is responsible for the regulation of *Nodal* expression in the LPM (Meno et al. 1999; Schier and Shen 2000). The regulation of *Nodal* resembles a ‘reaction diffusion system’, a theoretical model proposed by Turing in 1952 which allows for a short period of strong *Nodal* expression followed by a subsequent termination of this expression (Turing 1952). This system requires a faster diffusion of the feedback inhibitor (*Lefty2*) compared to the inducer (*Nodal*; Hamada et al. 2002). The third target of *Nodal*, *Pitx2*, is a transcription factor and remains expressed in the left LPM much longer than *Nodal*. It mediates the translation of the asymmetric signals into the left-sided morphogenesis of the organs (Logan et al. 1998; Campione et al. 1999).

Cilia – architecture and function

Cilia are ancient organelles that can be found throughout the kingdom animalia and share common function, structure and biogenesis. They are protrusions of the cell membrane and either motile or immotile. Motile cilia can serve as a motor to drive motion of the cell, like in unicellular organisms belonging to the Ciliata. Motion driven by cilia can also be found in numerous larvae of marine animals. In multicellular organisms cilia are responsible for the transport of fluid within the organism like for example for transportation of the mucus out of the respiratory system. Most of the motile cilia belong to the 9+2 type, which means that the microtubules are arranged in a circle consisting of nine doublet microtubules around a central pair of single microtubules (Davenport and Yoder 2005). Besides these cilia, there are also motile cilia which possess four central microtubules (9+4 type) or lack the central pair of microtubules (9+0 type: Sulik et al. 1994; Feistel and Blum 2006). The root of the cilium is called basal body and it consists of nine groups of microtubules triplets arranged in a cartwheel. Thus basal bodies share the same form as centrioles. The formation and maintenance of the cilium is governed by intraflagellar transport (IFT). This bidirectional movement of particles necessary for the formation and maintenance of the cilium along the microtubules is accomplished by two classes of motor proteins. Whereas kinesins are responsible for anterograde transport, the retrograde transport is performed by dyneins (Alberts et al. 2002).

There are two different patterns of cilia motion. In most cases the motion of the cilia resembles a biphasic, whip-like pattern, consisting of a fast and effective stroke and a slow non-effective recovery movement back to the initial position (Wemmer and Marshall 2004). In contrast to that motile monocilia can rotate in a clock-wise manner. Both types of motion are generated by motor proteins attached to microtubules. Powered by the hydrolysis of ATP, these proteins drive a sliding motion of two neighboring doublets of microtubules. As the neighboring microtubule doublets are interconnected to one another by linking proteins, the force generated by the motor proteins results in a bending of the cilium (Davenport and Yoder 2005).

Immotile cilia, i.e. primary cilia, can be found on almost all mammalian cells and have been shown to play a role during signal transduction and cell growth (Davenport and Yoder 2005). Beside these, specialized non-motile cilia can be found on sensory cells like the olfactory neurons or as a component of the photoreceptors (Alberts et al. 2002).

Cilia and left-right development

Cilia were first brought into the context of left-right development in 1976 when Afzelius described the human Kartagener syndrome (Afzelius 1976). Patients suffering from this genetic disorder display cilia with impaired motility. One of the symptoms of this ciliopathy is reduced or absent mucus clearance from the lungs resulting in chronic respiratory infections. This is often accompanied by male infertility due to immotile sperm and besides this, many of the patients also show a situs inversion.

As mentioned above the indentation at the distal tip of the gastrulating mouse embryo possesses monocilia. These cilia belong to the 9+0 type and are motile (Sulik et al. 1994). The rotation of the cilia results in a leftward flow of the extracellular fluid within the indentation (Nonaka et al. 1998). As rotation of the cilia alone would only result in many small vortices, a posterior tilt of the cilia is necessary for generating leftward the directionality of the flow (Nonaka et al. 2005). This is achieved by translocating the basal body from the center of the apical side of the cell to the posterior pole. The posterior pole of each cell is defined according to the anterior posterior axis of the embryo. As the apical surface of the cell is not flat but rather hemi-spherical, the translocation of the basal body to the posterior pole results in a posterior tilt of the cilium as it always protrudes orthogonally to the cell surface. In a ventral view, the cilia rotate in clockwise manner. Due to the tilt of the cilium, the rightward semicircle occurs in the vicinity of the cell surface and thus is exposed to strong friction. As consequence of this, the fluid is only affected marginally. In contrast to that, the leftward phase strikes through the extracellular medium, driving the fluid leftward (Nonaka et al. 2005).

The leftward fluid-flow model

The leftward fluid-flow (also known as ‘nodal flow’) was first described in 1998 (Nonaka et al. 1998). Since then, numerous mutant and KO mice have been identified lacking the flow and therefore developing left-right defects (Okada et al. 1999; Takeda et al. 1999; Beckers et al. 2007). Most of these genetic alterations affect the motor proteins responsible for cilia motility, IFT or genes involved in ciliogenesis in general. In 2002 a study involving two mouse-lines lacking the leftward

fluid-flow, demonstrated that laterality could be rescued by an artificial flow running above the indentation (Nonaka et al. 2002). Furthermore, wildtype mice developed left-right defects upon application of an artificial rightward flow (Nonaka et al. 2002). Thus the necessity of the leftward flow could be proven. In contrast to that, the direct effect of the flow remains elusive as basically two different models have been proposed.

The first model was published along with the discovery of the flow and favors a morphogen to be distributed by the flow (Nonaka et al. 1998). The morphogen then is accumulated on the left side where it induces the asymmetric gene expression. In 2005 this model was slightly modified in that the flow is not supposed to transport a morphogen but nodal vesicular parcels (NVPs; Tanaka et al. 2005). The NVPs are thought to contain retinoic acid (RA) and sonic hedgehog (Shh; Tanaka et al. 2005). Although both substances have been shown to be involved in left-right development, they lack the ability to act as left sided determinant (Shiratori and Hamada 2006). On the other hand the 'two cilia hypothesis' involves immotile, sensory cilia in the translation of the flow into asymmetric gene expression. These cilia are believed to sense the flow and subsequently induce a Ca2+ signal on the left side of the indentation (McGrath et al. 2003; Tabin and Vogan 2003).

With these findings the question arose whether the leftward fluid flow is a conserved mechanism among vertebrates or just the rodent or mammalian way of defining the left-right axis. Intense efforts lead to the discovery of a flow in rabbits, fish and recently also in *Xenopus* (Essner et al. 2002; Okada et al. 2005; Schweickert et al. 2007). Therefore, the flow is now regarded to be a general vertebrate mechanism. The only vertebrate model organism, in which no flow has been found so far, is the chick.

Flow in the frog

During gastrulation in *Xenopus*, the archenteron is formed inside the spherical embryo as a precursor of the gut. During neurulation a specialized epithelium forms ventrally to the neural plate, facing the archenteron, i.e. in the roof of the archenteron (Shook et al. 2004). Therefore, it is called gastrocoel roof plate (GRP) and characterized by monociliated cells. These cilia are motile and generate a leftward

fluid flow by their rotational movement (Schweickert et al. 2007). In order to show the relevance of the flow to left-right development, two approaches were performed. First, flow was inhibited by increasing the viscosity of the archenteron-liquid using methylcellulose and secondly, knockdown of ciliary components in the epithelium led to absence of flow. In both cases laterality defects resulted from the treatment, demonstrating the necessity of the flow for left-right development in *Xenopus* embryos (Schweickert et al. 2007).

Brachyury (*T*) and left-right development

As mentioned above the absence of *T* leads to left-right defects in mouse embryos. For these embryos it was reported that the ciliated indentation is malformed and that the expression of *Nodal* in the left LPM and in the midline is absent (Fujimoto and Yanagisawa 1983; King et al. 1998). The malformation of the indentation could lead to absence of the leftward fluid-flow and thus to laterality defects. However, it does not explain the absence of the *Nodal* cascade as the lack of the fluid-flow normally results in randomization of *Nodal* expression in the LPM. This means, that the transcription of *Nodal* occurs in the left, right or both LPMs. Therefore the *T*/*T* mutant embryos were investigated in this respect. Furthermore, it was investigated whether *Brachyury* is also necessary for laterality in *Xenopus* embryos. This question was addressed by using a loss of function of *Xbra*, the *Xenopus* homolog of *T. Xbra* is expressed in nascent mesodermal cells and thus resembles the transcription of *T* (Wilkinson et al. 1990; Smith et al. 1991). So far, loss-of-function of *Xbra* has only been investigated using antisense mRNA and no specific tissues have been targeted (Giovannini and Rungger 2002). Therefore, the published data only describe impaired mesoderm formation upon downregulation of *Xbra*. As an alternative method to antisense mRNA, antisense-oligonucleotide-morpholinos are available meanwhile. These synthetic molecules are much more stable and therefore the knockdown of genes can be performed more efficiently. The *Xenopus* system provides the possibility to target a specific region by an injection into its exact precursors and thus the GRP can be targeted specifically at the 4-cell stage. A specific knockdown of *Xbra* in the GRP revealed whether *Xbra* is necessary for *Xenopus* laterality development.

Monoamines and left-right development

Although much is known on the determination of laterality in vertebrates, there are still a couple of open questions. Among these the effect of monoamines on left-right development remains elusive up to date. In *Xenopus* embryos it has been reported that the serotonin neurotransmitter is crucial for correct laterality determination (Fukumoto et al. 2005). It is believed to be distributed asymmetrically during cleavage stages (Fukumoto et al. 2005). This early asymmetry is thought to be translated into asymmetric gene expression (Levin 2004). In sea urchins, mollusks and even mice and rat it has been reported that serotonin has the potency to increase ciliary beat frequency (CBF; Goldberg et al. 1994; Wada et al. 1997; Nguyen et al. 2001; Konig et al. 2009). Therefore, serotonin could also play a role in mammalian left-right development, as it might be necessary for the generation of ciliary motion. In order to provide data supporting this idea, serotonin should be investigated for a possible effect on cilia motility and thus on leftward flow. This experiment needed to be performed in the mouse, as visualization of frog GRP cilia is extraordinary laborious and thus hardly achievable. Furthermore, it was clarified whether the components, involved in serotonin signaling, like for example the receptor, are present during the leftward fluid-flow stage.

Serotonin is not the first monoamine neurotransmitter that could be identified having the potency to affect left-right development. In the beginning of the 1990s a series of papers was published by Baden and colleagues about their work on rat embryos (Fujinaga and Baden 1991; Fujinaga and Baden 1991; Fujinaga et al. 1992; Fujinaga et al. 1994). In these they report on the cultivation of late gastrula embryos. When phenylephrine, an adrenergic agonist, was present during this cultivation, about half of the embryos developed laterality defects. This was judged by the position in which the placenta formed and where the tail is located after embryonic turning. At that time it was not known that the investigated period of cultivation covered the leftward fluid flow and thus the crucial step for the onset of asymmetric gene expression. Therefore, the mechanism responsible for the outcome of these experiments could not be identified. Like other monoamines, adrenaline could have the potential to affect CBF. Thus the presence of adrenaline could have impaired the leftward fluid flow and hence affected laterality development.

Aim of this work

The aim of this work was the delimitation of the organizer from the distal indentation in the gastrulating mouse embryo. This was achieved through morphological and molecular characterization of both structures. New insights on the mode of operation of the organizer were obtained by analysis of gain-of-function experiments using the homeobox gene *Gsc*. This is of particular interest as *Gsc* is expressed in the organizers of all vertebrates, but astonishingly its knockout had no influence on gastrulation.
The distal indentation of the mouse embryo has been shown to be necessary for the development of the left-right axis. In order to further understand its functionality, the influence of the monoamines adrenaline and serotonin were investigated. Further evidence on the development of the indentation was gained by the analysis of embryos mutant for T-box transcription factor *Brachyury*, which suffer from left-right defects. Additionally, the conservation of the function of *Brachyury* was investigated using a knockdown of this gene in the frog.

Specific questions addressed in this thesis involved:

1. Is the distal indentation in the mouse known as ‘the node’ the homolog of Hensen’s node in the rabbit?

2. What is the role of *Gsc* during gastrulation?

3. How does monoamine signaling influence left-right development in the mouse?

4. Why do *T*/*T* mutant mouse embryos develop laterality defects?

5. Is *Xbra* necessary for Xenopus left-right development?

Results

The identification of midline structures

Expression of *Gsc* defines the organizer

At the beginning of gastrulation in the mouse, *Gsc* is expressed in the posteriormost part of the embryo. This is the region where the primitive streak forms. From there on the primitive streak elongates towards the distal tip of the embryo. During that period *Gsc* marks the anterior extension of the primitive streak. The region where *Gsc* is expressed is also known as gastrula organizer. Transplantation experiments of this tissue resemble the Spemann experiment, i. e. to induce the formation of body axes (Blum et al. 1992; Beddington 1994; Kinder et al. 2001).
At mid-gastrula, *Gsc* was expressed in the distal tip of the mouse egg-cylinder (Fig. 3A, A'). This region is characterized by a mass of cells in which the germ layers are indistinguishable (Fig. 3A''). As *Gsc* is also expressed in this region in rabbit embryos of corresponding stages, it thus shares the same morphological properties as described by Victor Hensen for the node in the rabbit and molecular as described by Blum and colleagues (Blum et al. 2007). According to Hensen the term 'node' was chosen to distinguish this area from the primitive streak posteriorly and the floorplate or notochord anteriorly (Blum et al. 2007).

As gastrulation proceeded the expression of *Gsc* in the organizer had declined strikingly at the zero bud stage (Fig. 3B, B'). Only very slight remnants could be detected as the *Gsc*-expressing cells began to migrate anteriorly. During this stage *Gsc* marked the prechordal mesoderm and thus the first cells that leave the organizer in the midline anteriorly (Fig. 3B''). These cells are destined to give rise to the prechordal plate as soon as they reach the anterior aspect of the embryo. In the late headfold stage depicted in Fig. 3C and C', *Gsc*-positive cells were found in the prechordal plate mesoderm and overlying neuroectoderm. No expression of *Gsc* in the organizer could be detected at this stage (Fig. 3C''). Anterior to the organizer the

formation of an indentation takes place (asterisk in Fig. 3C'; Sulik et al. 1994). This indentation could be distinguished from the organizer as it consisted of a cell layer which was in continuity with the notochordal plate and was dorsally separated from the floorplate by a basal membrane. Taken together, *Gsc* expression was detected in prechordal mesoderm and in the organizer but no expression could be found within the indentation at the distal tip of the late gastrula mouse embryo

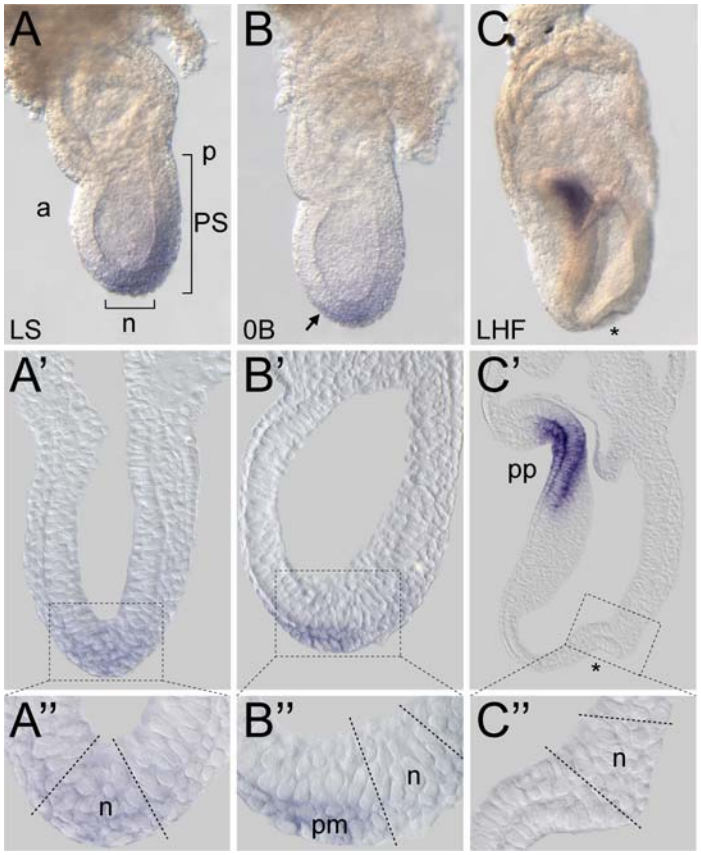

Fig. **3** Identification of the murine node by analysis of *Goosecoid* (*Gsc*) gene expression in mouse; lateral views (**A-C**) with anterior to the left and vibratome sections (**B'-C'**) of embryos hybridized in whole mounts using specific antisense *Gsc* probes. *Gsc* marked the node (n) and prechordal plate (pp) in the mouse. (**A**) At the late-streak stage (LS), *Gsc* was expressed in the anterior primitive streak and node. (**B**) At the zero-bud stage (0B) *Gsc* expression in the primitive streak and node has faded, and signals were strongest in the first presumptive prechordal cells leaving the node anteriorly (arrow). (**C**) At late-headfold (LHF), *Gsc* expression was confined to the pp and overlying neuroectoderm. Asterisks mark distal indentation (**C, C'**). Parasagittal (**A'**, **A''**) and sagittal (**B'**, **B''**, **C'**, **C''**) histological sections of embryos in (**A**-**C**) show the dense, epithelium-like cell arrangement in the node area and the separation between floor plate and prechordal mesoderm (pm; **B''**) or the notochordal cells (**C''**) anterior to the node. Dashed lines in **A''-C''** mark anterior and posterior limits of the node area. a, anterior; p, posterior.

Nodal expression occurred in two distinct domains

The expression of *Nodal*, a member of the TGF-ß (transforming growth factor ß), superfamily provided further information about the formation of the indentation in the vicinity of the organizer. At the zero-bud stage *Nodal* was expressed in the organizer and no signals could be detected in the prechordal mesoderm (Fig. 4A, A'). Subsequently *Nodal* remained to be expressed in the organizer (Fig. 4B). In addition to this, expression was detected adjacent to the organizer, flanking the forming indentation laterally and posteriorly. Together these two domains resembled a y-

shape seen in a ventral view of the embryo (inset in Fig. 4B). At the early head fold stage only slight changes in the expression pattern could be detected as the indentation and concomitantly the expression of *Nodal* increased in size (Fig 4C and inset). During this stage *Nodal* was also expressed in the organizer. This domain decreased during the following stages until expression only remained in the tissue flanking the indentation laterally and posteriorly resembling a horseshoe (Fig. 5C). In summary *Nodal* was expressed in two adjacent domains during mouse gastrulation, namely the indentation and the organizer, indicating that these structures are two different entities.

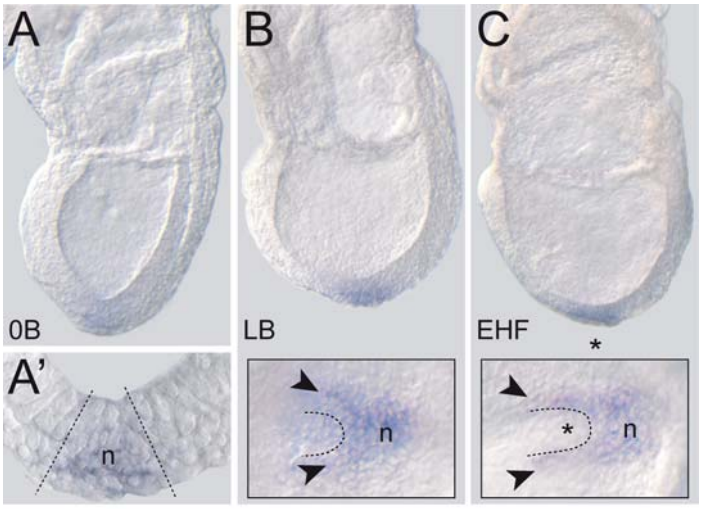

Fig. **4** *Nodal* expression defined the early node and the posterior notochord in mouse embryos. Whole-mount *in situ* hybridization of mouse embryos using specific antisense *Nodal* probes. (**A**-**C**) *Nodal* expression in the node and bilateral notochordal domain in the mouse. Embryos shown in lateral views, anterior to the left. (**A**) At the zero bud stage (0B), *Nodal* expression was restricted to the node (n). The sagittal section in (**A'**) shows expression of *Nodal* in the organizer; dashed lines indicate the anterior and the posterior border of the node area accordingly. During late-bud (LB) and early-headfold (EHF) stages (**B**, **C**), distal views of egg cylinders (insets in **B** and **C**) revealed *Nodal* signals in the node and in two lateral wings, extending anteriorly from the node (arrowheads). Asterisk in (**C**) indicates the location of the emerging ventral indentation. Dashed lines in (**B**) and (**C**) highlight the boundary between node and posterior notochord. r, right.

Conserved *Nodal* expression flanked a ciliated epithelium in frog, mouse and rabbit

In order to find out more about the relevance of the indentation, which is encompassed by *Nodal* expression, homologous structures were sought to be identified in embryos of the vertebrates *Xenopus* and rabbit. In *Xenopus* embryos *Nodal* expression was found in stage 17 flanking the gastrocoel roof plate (GRP, Fig. 5A, A'; Lowe et al. 1996). This structure is located on the inside of neurula embryos in the vicinity of Spemann's organizer. The GRP is destined to become a part of the notochord, hypochord and somites (Shook et al. 2004).

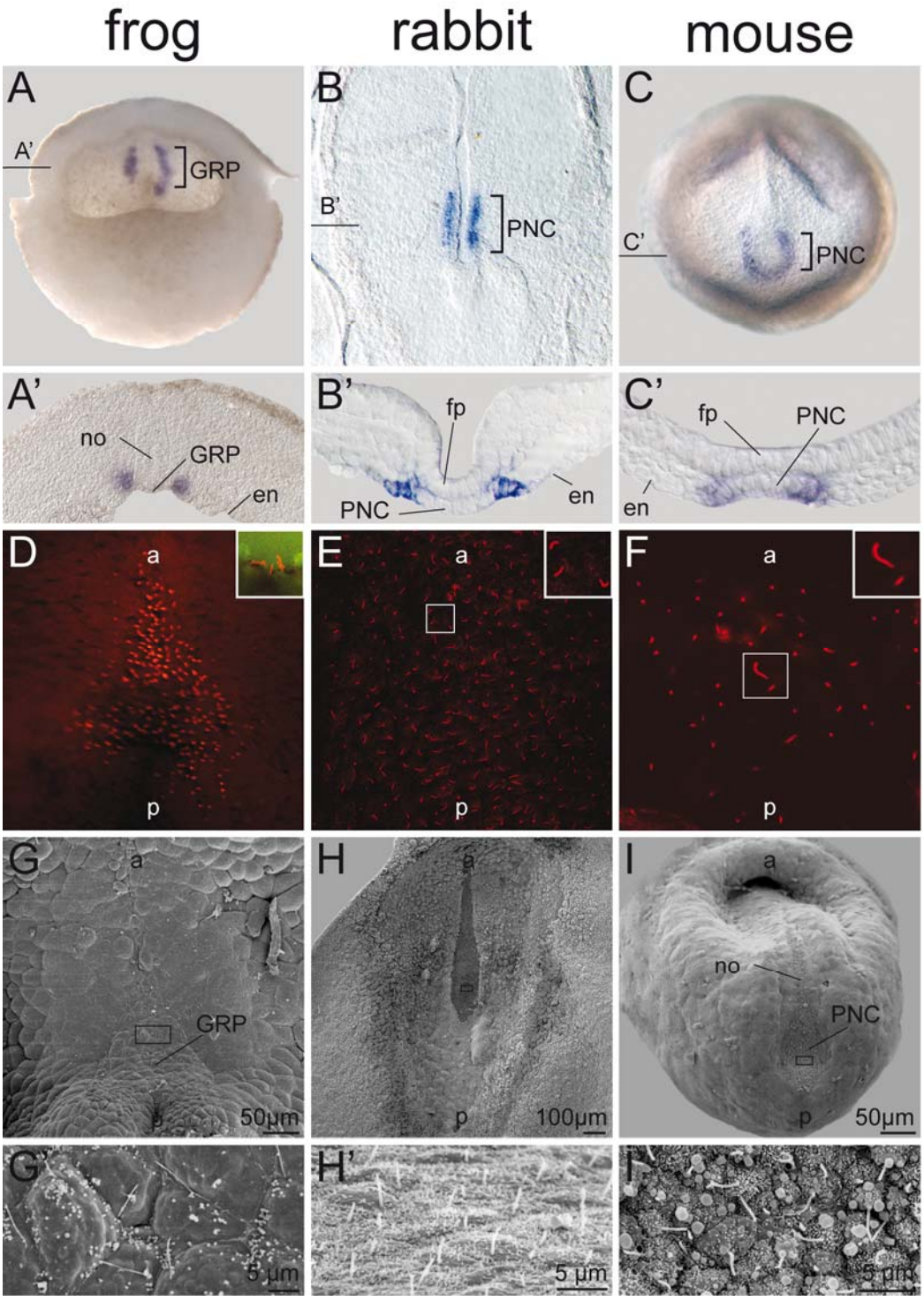

Fig. **5** Conserved bilateral *Nodal* expression encompassed a monociliated notochordal epithelium in frog, rabbit, and mouse embryos. (**A**-**C**) Ventral views of embryos hybridized with specific *Nodal* probes in whole mounts demonstrated bilateral *Nodal* expression encompassing the posterior aspect of the notochord (no) in all three species. Domains representing the gastrocoel roof plate (GRP) in frog (**A**) and the posterior notochord (PNC) in rabbit and mouse (**B**, **C**) are indicated by square brackets. (**A'**-**C'**) Transverse sections of embryos, levels indicated by horizontal lines in (**A**-**C**), confirmed the *Nodal* expression to reside in the ventral cell layer adjacent to the notochord or the notochordal plate in frog and mammals, respectively. Sections oriented with dorsal side up. Immunohistochemistry for acetylated tubulin (**D**-**F**) and scanning electron microscopy (**G**-**I**) revealed cilia on the ventral surface of GRP/PNC (**G'**-**I'**). Note that GRP cells were much larger compared to cells of the PNCs. Insets in (**D**-**F**) show higher magnifications of cilia. The inset in (**D**) depicts a confocal image of a transverse vibratome section. Frog: Posterior parts of embryos were cut transversally at about the middle of the embryos. (**A**) Cavity represents the archenteron; the dorsal

side is facing upwards. (**D**, **G**) Close-up views from archenteron onto GRP. Rabbit: overview (**B**) and close-ups (**E**, **H**) of the ciliated region in ventral views. Mouse: Embryos presented in distal views (**C**, **F**, **I**) to allow a close-up examination of cilia on the PNC (**E**, **H**). Picture (**D**) was kindly provided by Susanne Bogusch. Pictures (**B**, **B'** + **E**) and (**H, H'**) were kindly provided by Anja Rietema and Kerstin Feistel, respectively. a, anterior; en, endoderm; fp, floorplate; no, notochord; p, posterior.

In the rabbit a bilateral *Nodal* expression domain was observed just anterior to Hensen's node (Fig 5B, B'). It encompassed the posterior aspect of the notochordal plate laterally. As mentioned above, *Nodal* was expressed in a horseshoe-like pattern in the mouse (Fig. 5C, C'). As it has been published, cells within the indentation are ciliated in mice, immunohistochemisty (IHC) and scanning electron microscopy (SEM) were performed on rabbit and frog embryos (Sulik et al. 1994). Thereby further homologies of the regions marked by *Nodal* expression between these species could be identified. IHC with an antibody against acetylated tubulin revealed the presence of cilia in all three vertebrates in these specific regions (Fig. 5D-F, higher magnification in insets). Cilia were also detected using SEM on the areas which were encompassed by *Nodal* expression (Fig 5G-I). In addition, the continuity of the indentation to the notochordal plate could be observed in the mouse embryo, suggesting the indentation to be the posterior aspect of the notochord.
Taken together, the comparison of these vertebrate embryos revealed that the indentation at the distal tip of the mouse embryo shares the same molecular and morphological properties with the GRP of the frog and the posterior notochord (PNC) of rabbits. Therefore this very structure was labeled PNC in the mouse as well.

The role of *Gsc*

In order to find out more about the role of *Gsc* during gastrulation, a conditional gain-of-function approach was chosen. Therefore *Gsc* was misexpressed under the control of a *Brachyury* primitive streak promoter. As it has been shown that *Gsc* is a repressor of *Brachyury* the construct repressed its own expression, resulting only in a mild overexpression of *Gsc* (*GSC-T*) (Deißler 2002). In order to overcome this repression, the overexpression construct was mutated within the *Brachyury* promoter at the *Gsc*-binding site (Deißler 2002). This lead to massive gastrulation phenotype caused by strong *Gsc*-misexpression which was lethal at about E 8.5 (Andre 2004). The downregulation of *Brachyury* expression in these transgenic embryos confirmed

the finding that *Gsc* represses *Brachyury* (Andre 2004). SEM analysis showed that the PNC did not form when *Gsc* was overexpressed in the primitive streak (Andre 2004). To further substantiate this finding the expression of marker genes was analyzed.

Gsc-mediated repression of *Noto*

Noto is a homeobox transcription factor and is expressed in the precursors of the notochord at the distal tip of gastrulating mouse embryos (Fig. 6A-C) (Abdelkhalek et al. 2004). As soon as the PNC forms, it is thus marked by *Noto* expression. Knockout of *Noto* leads to malformation of the PNC, left-right defects and a truncated tail (Abdelkhalek et al. 2004; Beckers et al. 2007). Furthermore *Noto* has been shown to be one of the downstream targets of *T* (Abdelkhalek et al. 2004). Upon misexpression of *Gsc*, a strong downregulation of *Noto* expression in the transgenic embryos could be detected (Fig. 6D-F). The downregulation of *Noto* ranged from strong repression to complete absence of *in situ* hybridization (ISH) signals (Fig. 6D-F and not shown). This supports the finding that the PNC and the notochord had not formed in these specimens.

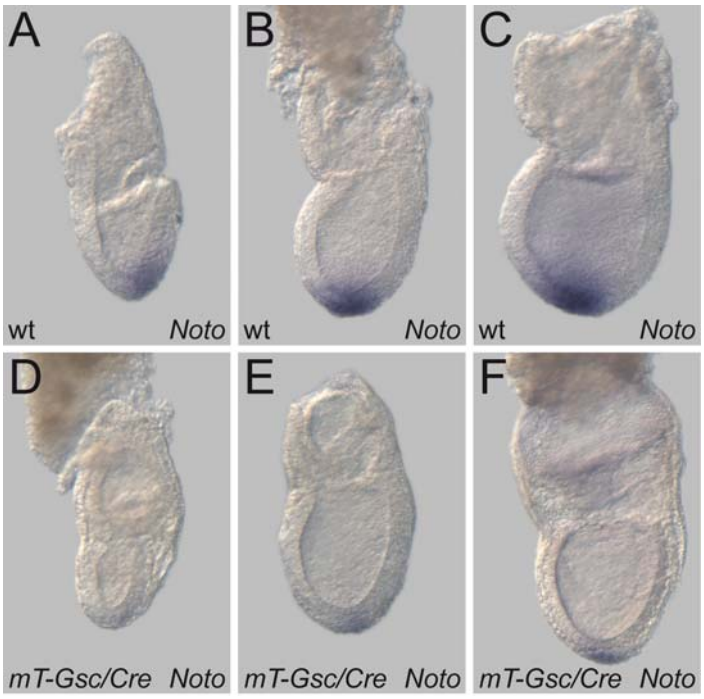

Fig. **6** *Gsc*-overexpression in the complete PS led to repression of *Noto*. (**A**-**F**) Lateral views of embryos hybridized with specific *Noto* probes, anterior to the left. In wt embryos *Noto* is expressed in the distal tip of gastrulating mouse embryos (**A**-**C**). In *Gsc*-overexpressing embryos the transcription of *Noto* is hardly detectable (**D**-**F**). Presented embryos are in the mid-streak stage (**A**, **D**), late-streak stage (**B**, **E**) and late-bud stage (**C**, **F**). PS, primitive streak.

Downregulation of *Tbx6* upon *Gsc* overexpression

The T-box containing gene *Tbx6* is expressed in the primitive streak of gastrulating mouse embryos from E7.25 - E7.75 (Fig. 7A-D) (Chapman et al. 1996). Although *Tbx6* is closely related to *T* it has been shown that their expression is not dependent on one another during the stages shown in Fig. 7 (Chapman et al. 2003). Absence of *Tbx6* expression leads to defective presomitic mesoderm and thus the somites do not form correctly (Chapman and Papaioannou 1998). Concomitantly, there is an increase of cells adopting an ectodermal fate which results in excessive neural tissue and the formation of additional neural tubes (Chapman and Papaioannou 1998).

Fig. **7** Misexpression of *Gsc* in the complete PS led to downregulation of *Tbx6* expression. (**A**-**H**) Lateral views of embryos hybridized with specific *Tbx6* probes, anterior to the left. In wt embryos transcription of *Tbx6* can be found in the complete PS of gastrulating mouse embryos (**A**-**D**). In the late-bud stage *Tbx6* is also expressed in the paraxial mesoderm (**D**). Upon overexpression of *Gsc*, expression of *Tbx6* is almost absent (**E**-**H**). Depicted embryos are in the mid-streak stage (**A**, **E**), late-streak stage (**B**, **F**), zero-bud stage (**C**, **G**) and late-bud stage (**D**, **H**).

In *Gsc*-misexpressing embryos the formation of additional neural grooves, the precursors of neural tubes, has been observed (Andre 2004). As this phenotype could be connected to overexpression of *Gsc*, transgenic embryos were examined for *Tbx6* expression (Fig. 7E-H). During the examined stages (E7.25 - 7.75), a strong downregulation (Fig. 7F, G) or even absence of *Tbx6* signals (Fig. 7E, H) were detected. The analysis of the *Tbx6* expression showed that overexpression of *Gsc*

resulted in a repression of *Tbx6*. Therefore the absence of *Tbx6* could be responsible for the formation of additional neural grooves in *Gsc*-misexpressing embryos.

The function of the PNC

In order to further characterize the PNC, its properties were analyzed in detail. As a first approach, the untreated cilia were investigated. In a second step, it was attempted to affect cilia behavior and thus, the leftward fluid-flow. For the analysis of ciliary beat frequency (CBF) and the fluid-flow a closed chamber as shown in Fig. 8A was set up. Mouse embryos of about E 8.0 were isolated, placed in culture medium (F10) with the ventral side facing up and analyzed under a microscope. The effects of different substances were assessed by addition to the medium and the pattern of ciliary beating was videographed. In untreated wt embryos about 10-20% of cilia either moved in an irregular pattern like wiggling back and forth or did not move at all. These cilia were not taken into account for CBF calculation.

Ciliary beat frequency (CBF) in the PNC of the mouse

Cilia of embryos of the mouse-line C57Bl76j were analyzed as reference. It has been previously reported that cilia rotate at about 10 Hz (Okada et al. 2005). The analysis of 385 cilia in 29 wt embryos led to an average CBF of 9.65Hz ± 2.16Hz (Fig. 9). In Fig. 9A the mean CBF is shown in relation to exact developmental stages. The CBF increased during development in such that CBF of embryos before onset of leftward flow (early headfold to presomite stage) was assessed at 9.0 Hz. Embryos which had already reached flow stages (2-4 somite stages) showed a significant increase in CBF to 10.3 Hz (Fig 7A, $p<0.001$).

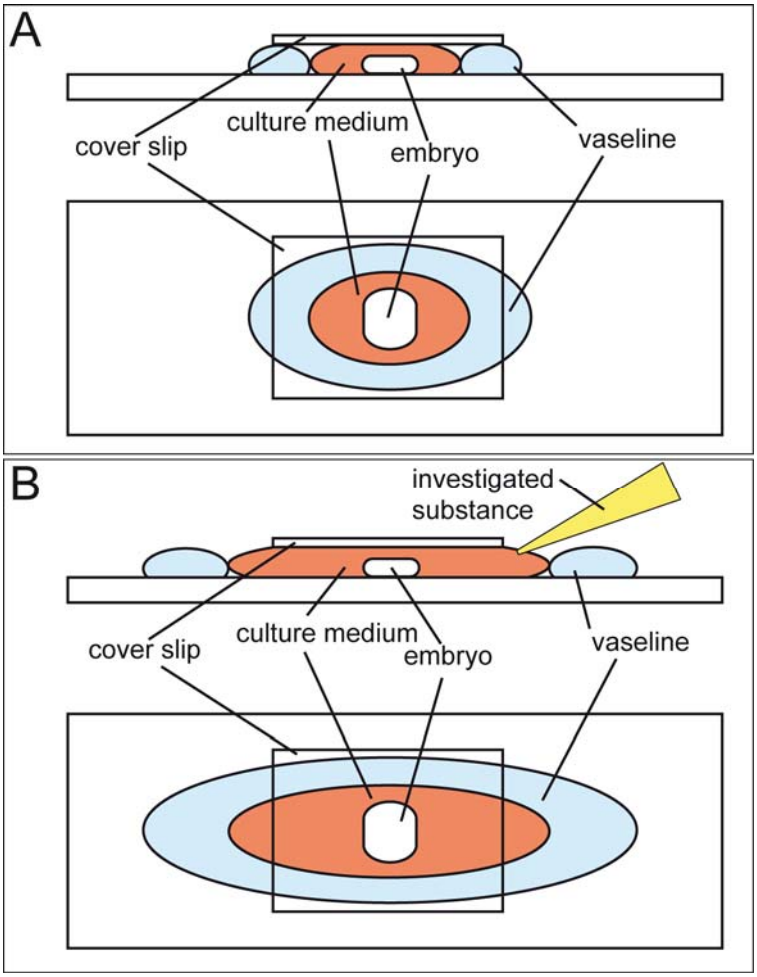

Fig. **8** Schematic drawing of a reaction chamber for the assessment of ciliary beat frequency and leftward fluid-flow. (**A**) The closed chamber consisted of an object slide with a circle formed of Vaseline. Inside the circle the specimen was placed within about 100µl of F10 culture medium. The substance to be investigated was added to the medium. The chamber was closed by a cover slip. (**B**) In the open camber system space remained open laterally, thus the specimen could be investigated before and after the addition (yellow pipette tip) of a substance.

Adrenaline reduced the CBF and attenuated the leftward fluid-flow

As adrenergic effectors have been shown to influence the left-right asymmetry in rat embryos, adrenalin was investigated for its possible effect on CBF and thus on leftward flow (Fujinaga and Baden 1991). Adrenaline was added to the medium at a final concentration of 1.8 mM. Subsequently, the CBF was analyzed and compared to the CBF of untreated littermates. Upon addition of adrenaline the CBF dropped to about half of its usual value (Fig. 9B, $p<0.001$). As adrenaline reduced the CBF in the PNC, it was taken into account that the leftward fluid-flow would also be affected by addition of adrenaline to the medium. Therefore embryos of flow stages (1-4 somites) were treated with adrenaline and the fluid-flow was compared to untreated littermates (Fig. 10A, B).

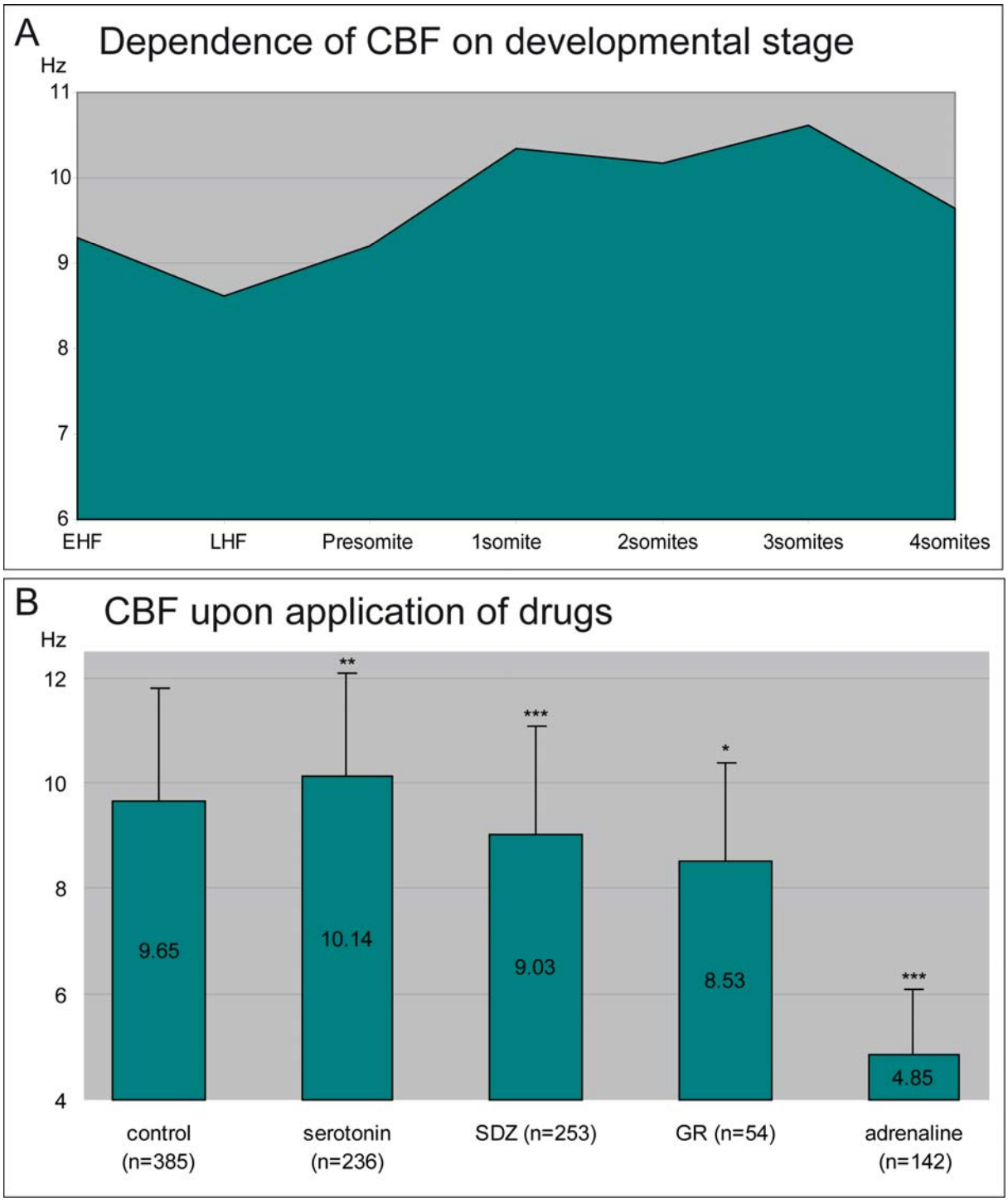

Fig. **9** Ciliary beat frequency (CBF) changed during development and was influenced by serotonin, serotonin antagonists and adrenaline. (**A**) In the course of development the CBF increased from about 9Hz in pre-flow-stages to beyond 10Hz in flow-stages. (**B**) Upon addition of 2.4 mM serotonin CBF increased to 10.14Hz. The presence of the serotonin antagonists SDZ-205,557 (10µM) and GR113808 (1µM) decreased CBF by about 5%. The addition of adrenalin (1.8mM) led to decrease of the CBF by about 50%. EHF**,** early-headfold; LHF late-headfold.

Therefore fluorescent latex beads were also applied to the medium and embryos were observed as indicated in Fig. 8A. Embryos were focused, so that ciliary effect on beads (beads being accelerated suddenly) could be seen and then filmed for 1min at 10fps. Afterwards the procedure was repeated with the same embryo. Both movies

were analyzed and for further comparison the movie with either more traced beads or better quality of flow was chosen. In order to visualize the quality of the leftward fluid-flow, the result of the analyzed data is shown in gradient time trails (GTT; Schweickert et al. 2007). The images show a time period about 5s (Fig. 14A, C) and and thus visualize the trails the beads have moved along. The colored bar indicates which color corresponds to which point in time. This means that the individual beads that were present at the end of the investigated lapse of time are highlighted in red and those present at the beginning are green. Thus, if a particle was present throughout the complete time span, its trajectory represented the complete color gradient.

Furthermore, the quality of the flow was assessed by analyzing the directionality of the trajectories. Therefore the directions were pooled into 8 different main directions. The size of each petal indicates the amount of particles summarized in it. As indicated in the wt GTT image, about 80% of the particles moved basically to the left side of the embryo, whereas more than 40% of the particles moved directly to the left (Fig 10B). In adrenaline treated embryos (Fig. 10C, D), the analysis shows a decreased number of fluorescent beads which were transported to the left side of the embryo compared to the control (Fig. 10A, B). Besides the decrease in the number of transported particles, the overall direction of particle trails was altered, represented by the value of rho. The value of rho can reach 0-1 and represents the mean resultant length of all particle trajectory directions. A value around 1 represents the situation in which nearly all particle trails point towards the same direction. A value around 0 represents randomness of particle motion (Analysis developed by Thomas Weber, cf. methods and Maisonneuve et al. 2009). Calculating the quality of flow, rho dropped to 0.43 compared to 0.71 in the control. This indicated that, although the leftward fluid-flow still occurred, it was markedly attenuated in the presence of adrenaline.

Taken together, it could be shown that adrenaline has the potency to influence the CBF and thus the leftward fluid-flow in mouse embryos.

Role of serotonin signaling for the leftward fluid-flow

In the following experiments the effect of serotonin signaling on mouse left-right development was investigated. The question whether serotonin plays a role arose from published results showing that serotonin is distributed asymmetrically in *Xenopus* embryos during cleavage stages. Furthermore it could be shown that influencing serotonin signaling resulted in left-right defects (Fukumoto et al. 2005).
A first approach was made by applying serotonin to PNC explants of mouse embryos shortly before and during flow stages. This was done using a concentration of 2.4 mM serotonin in F10 medium. By this the CBF increased significantly ($p=0.0015$) from 9.65 Hz to 10.14 Hz which equaled a gain of 4.3% (Fig. 9B). In order to rule out the possibility that this difference was caused by diversity of embryos and not due to serotonin the open chamber system was used (Fig. 8B). In this attempt the untreated embryos were videographed first and following serotonin addition, a second CBF-movie was acquired. Only a very mild increase of CBF from 10.07 Hz to 10.13 Hz could be detected which was statistically not significant (not shown).

Inhibition of serotonin signaling reduced the CBF marginally

Serotonin signaling is mediated through various receptors. In *Xenopus* the responsible receptors could be narrowed down to class 3 (*Htr3*) and class 4 (*Htr4*) type receptors (Fukumoto et al. 2005). For these receptors specific drugs that block the binding of serotonin are available.
Blocking of receptors was accomplished by applying the substances GR113808 and SDZ-205,557 which block the serotonin receptor 4 or receptors 3 and 4 together, respectively (Fludzinski et al. 1987; Bockaert et al. 2004). To test the influence of these pharmacological inhibitors regarding CBF, the closed chamber system was used to gather control and treated movies of murine CBF at the PNC. All substances were able to reduce CBF (Fig 9B). First the application of the *Htr4* antagonist GR113808, diluted to a final solution of 1 μM, led to a reduction of CBF by 11.6% ($p=0.0176$). For these experiments 4 embryos were evaluated and the CBF of 54 cilia was analyzed. In a next step, SDZ-205,557 at a concentration of 10 μM was examined.

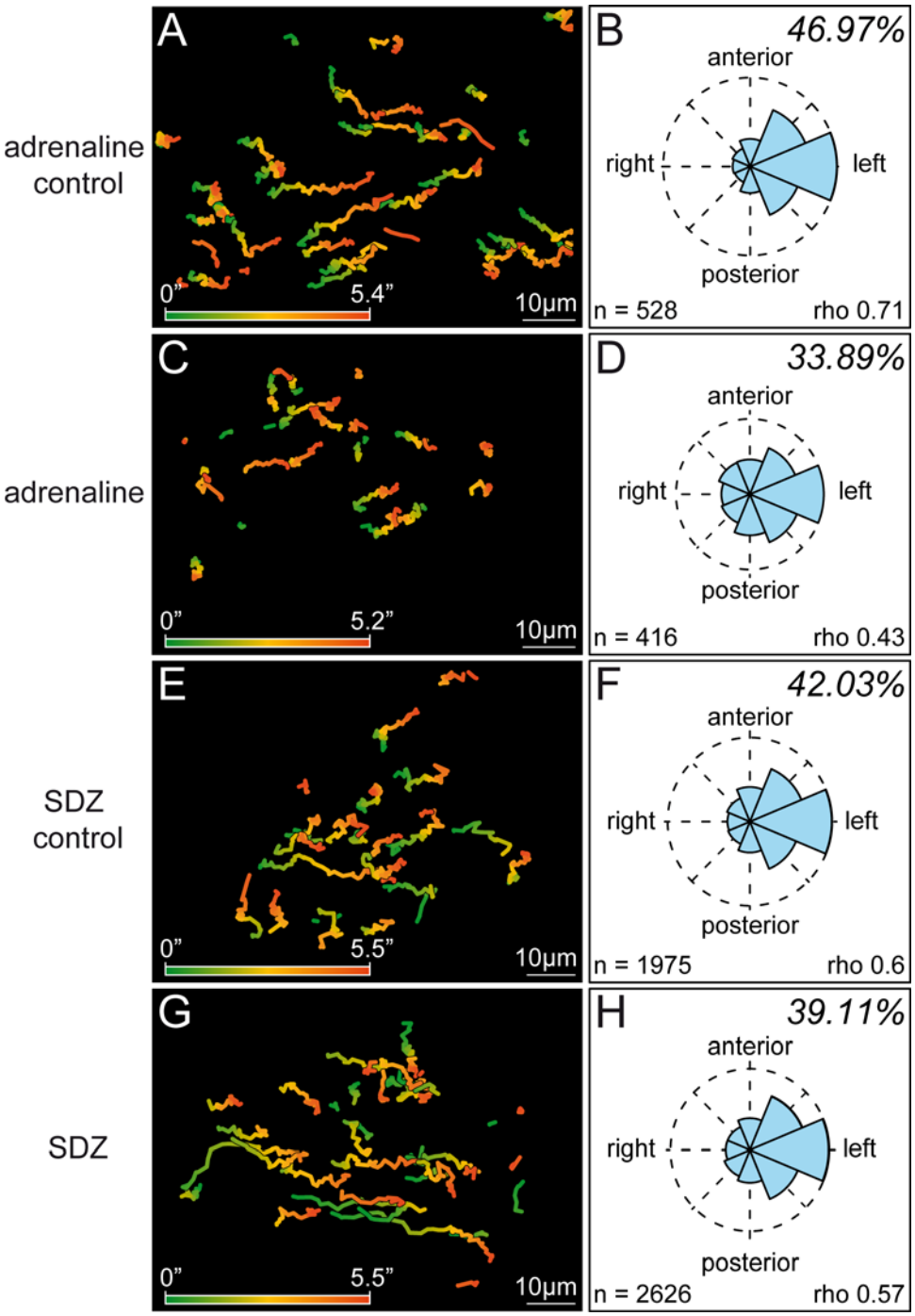

Fig. **10** Leftward fluid-flow was attenuated by addition of adrenalin but not due to the presence of a serotonin antagonist. (**A**, **C**, **E**, **G**) Particle movements displayed as gradient-time trails (GTTs), representing about 5s from green to red (cf. gradient bar). The analysis indicated that GTTs were shortened and reduced, thus the flow was attenuated upon the addition of 1.8 mM adrenaline (**C**) compared to the control (**A**). Quantitative analysis of GTT directionality over the area of the PNC (**B**, **D**, **F**, **H**) demonstrated strong leftward flow in the control (**B**, n=5 embryos) but weakened flow after addition of adrenaline (**D**, n=7 embryos), judged by the value rho, which indicated the quality of the directionality. No effect on the flow was measured in the presence of serotonin antagonist SDZ-205,557 (10µM; **G**, **H**) compared to the control (**E**, n=16 embryos, F, n=12 embryos).

Therefore 17 different embryos with 253 cilia were analyzed, resulting in a significant (p= 0.0009) decreased CBF by 6.5% through blocking *Htr3* and *Htr4.* In summary the

monoamine serotonin increased the CBF slightly, whereas CBF was reduced by serotonin antagonists.
These results raised the question if the serotonin antagonist had the potency to alter the leftward fluid-flow. Hence SDZ-205,557 was applied to embryos during flow stages and analyzed for a possible effect on the flow. Although SDZ-205,557 was used again at a concentration of 10 μM (Fig. 10G, H), no effect on leftward fluid-flow could be detected in comparison to untreated control embryos (Fig. 10E, F).

Taken together the slight effect on CBF was irrelevant, as leftward fluid-flow occurred normally when serotonin receptor antagonists were applied to the PNCs of mouse embryos.

Expression of serotonin receptors during laterality determination

A prerequisite for the observed effect is the presence of components of the serotonin signaling pathway within the PNC. This aspect was investigated using reverse transcriptase polymerase chain reaction (RT-PCR).Therefore cDNAs of different mouse embryo stages were produced. The examined stages were E7.5 (pre-flow stage) E8.0 (flow stage) and E8.5 (post-flow stage). As a positive control, a cDNA derived from a head of an E14.5 embryo was used. For further specificity the embryos which were used for the E8.0 cDNA were dissected into different parts, namely head, trunk, extraembryonic tissue and the PNC including surrounding tissue. Of these parts most attention was paid to the PNC cDNA.
Seventeen serotonin receptors have been identified to date in the mouse and nineteen in humans. As some of these are possibly just different isoforms of the same receptor and others have not been identified yet, this numbers are probably not final. The receptors were subdivided into seven families. The type 3 receptors differ from the others as these are subunits of a ligand-gated ion channel. The remaining receptors are G-protein coupled receptors (GPCR) that activate an intracellular second messenger cascade in order to produce a response.
Specific primers were created for all of the 17 known mouse serotonin receptors. As the quality and amount of RNA isolated from the mentioned tissue (especially the PNC) was very poor, no DNase digestion was performed. This approach did not

prevent the presence of genomic DNA in the cDNA and therefore could be responsible for false positive results. In order to rule this out, primers were chosen in a manner that the result of the PCR was different whether deriving from cDNA or genomic DNA. This was achieved by designing primers for different exons, so that the amplified product either contained introns (genomic DNA) or not (cDNA).

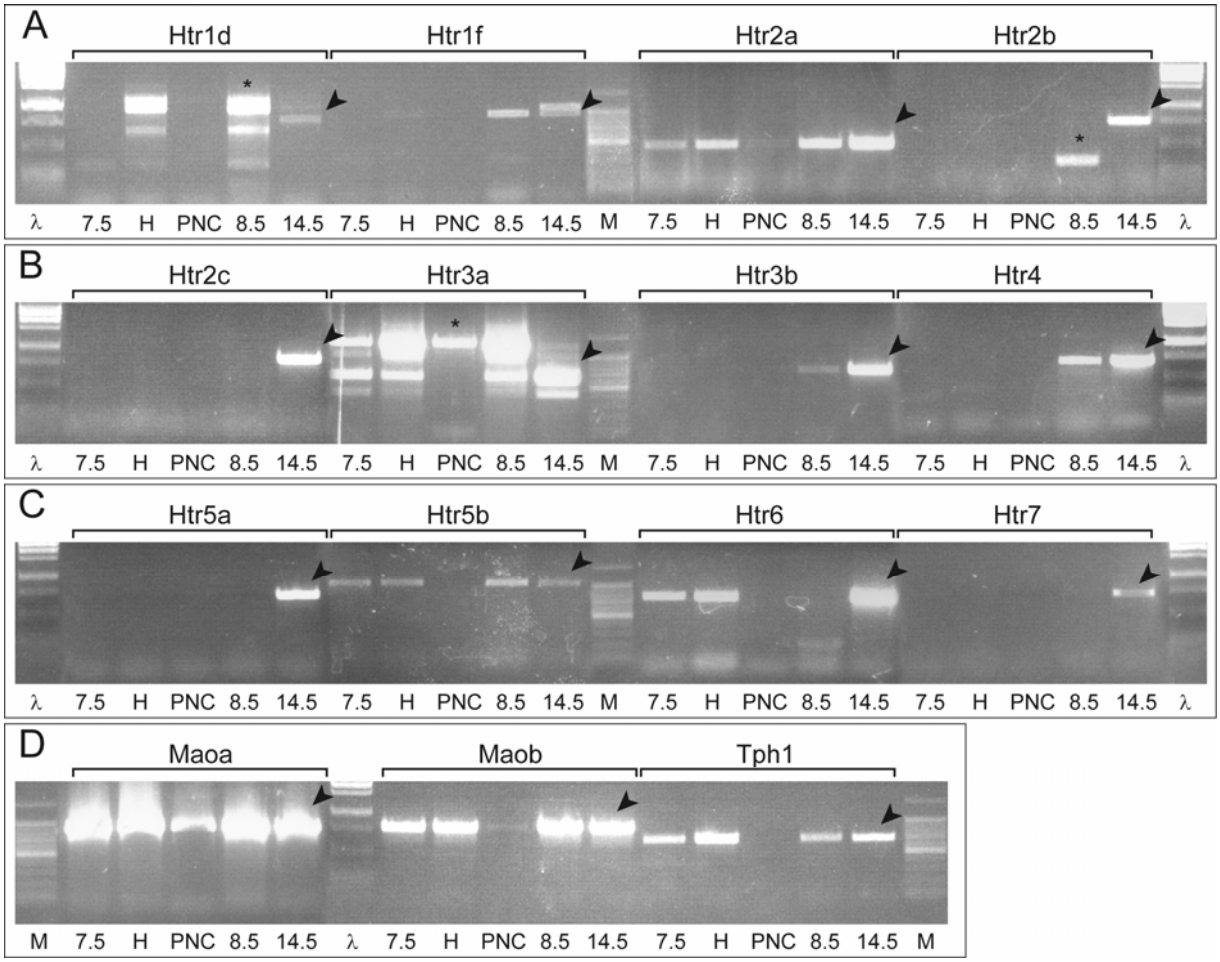

Fig. **11** Expression of serotonin receptors during flow stages. Expression was analyzed using RT-PCR with specific primers for *Htr1d, Htr1f, Htr2a, Htr2b* (**A**), *Htr2c, Htr3a, Htr3b, Htr4* (**B**), *Htr5a, Htr5b, Htr6, Htr7* (**C**), *Maoa, Maob, Tph1* (**D**). As template cDNA of the stages E7.5 (7.5), head of E8.0 (H), PNC of E8.0 (PNC), E8.5 (8.5) and head of E14.5 (14.5) were used. As markers λPst (λ) and 100bp step ladder (Promega, M) were used. Expression during flow stages (E8.0) were shown for *Htr2a, Htr3a, Htr5b, Htr6, Maoa*, *Maob* and *Tph1* (**A**-**D**). Transcription of *Htr2a* (very faint), *Maoa* and *Maob* were detected in the PNC cDNA (**B**, **D**). Bands caused by genomic DNA contamination are marked by asterisks and arrowheads mark bands of the expected size in E14.5 cDNA.

The receptors *Htr1a* and *Htr1b* only consist of one exon and thus no reliable statement could be made concerning the expression of these. For all other receptors with the exception of *Htr1f*, positive signals could be detected in E14.5 cDNA (Fig. 11 arrowheads). There was only one receptor which could be detected in the PNC cDNA namely the receptor *Htr2a* (very weak, red arrow, Fig. 11A). Furthermore *Htr2a*

was expressed in all other examined stages. The receptors of the class 3 type were detected in one RT-PCR but these results could not be reproduced. The *Htr3a* receptor was detected in stages before, during and after the flow event occurs.

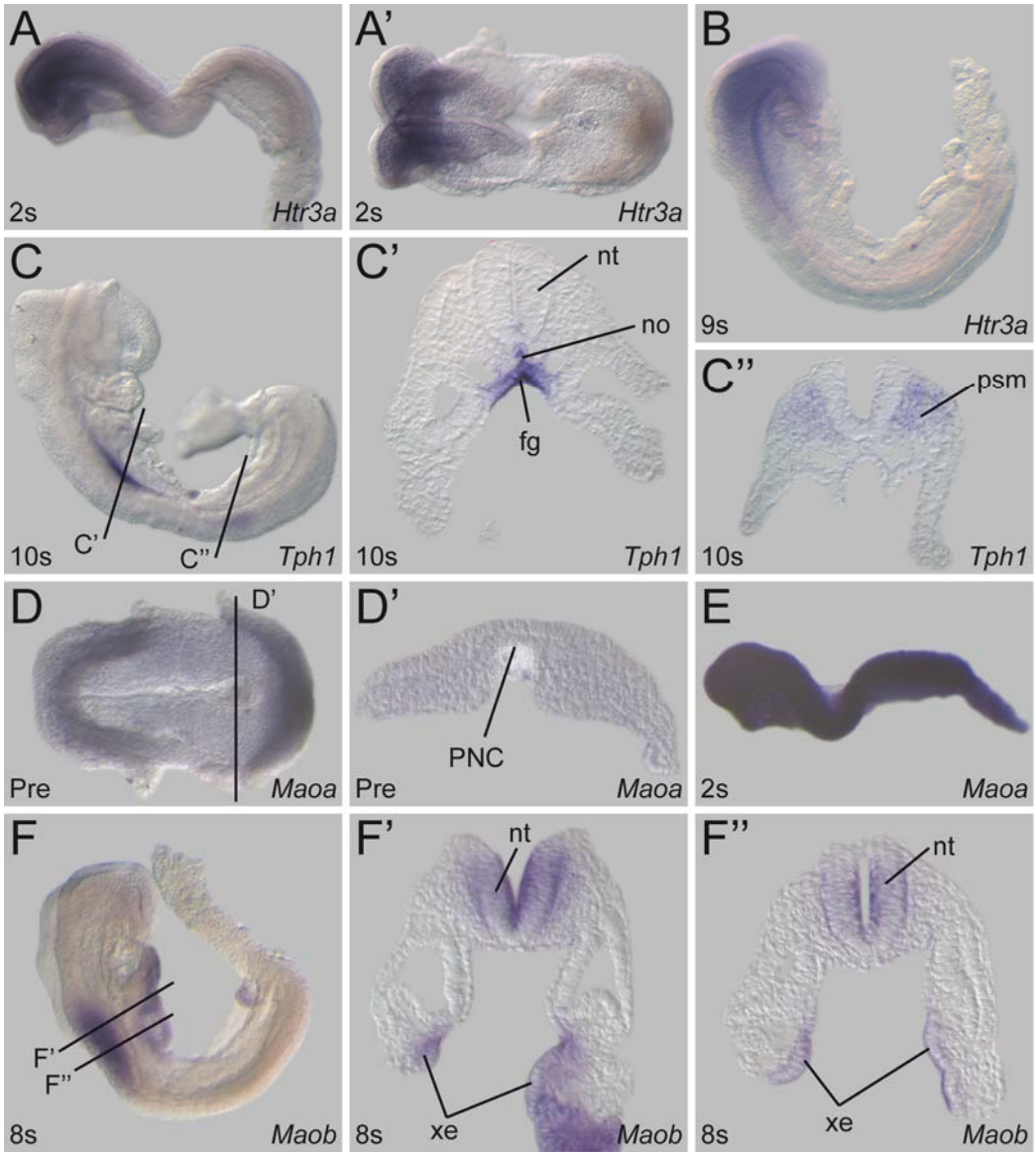

Fig. **12** Expression of serotonin signaling components could not be detected in the PNC. Lateral (**A**, **B**, **C**, **E**, **F**) ventral (**D**) and dorsal (**A'**) views and vibratome sections (**C'**, **C''**, **D'**) of embryos hybridized with specific probes for *Htr3a* (**A**, **B**), *Tph1* (**C**, **C'**, **C''**), *Maoa* (**D**, **D'**, **E**) and *Maob* (**F**, **F'**, **F''**); anterior to the left and dorsal up in sections. Expression of *Htr3a* was detected in the forming head but not in the PNC (**A**-**B**) in 2-somite stage (2s) and 9somite stage (9s). *Tph1* was transcribed in the foregut (fg), notochord (no) and in presomitic mesoderm of an 10-somite (10s) stage embryo (**C**, **C'**, **C''**). Ubiquitous expression of *Maoa* in presomite (Pre) and 2-somite stage embryos. No downregulation of expression of *Maoa* in the PNC (**D'**). (**F**) Transcription of *Maob* in neural tube ectoderm in the region of neural tube closure (**F'**, **F''**) and in extraembryonic tissue (xe) in 8-somite stage (8s). Bars indicate level of sections (**C**, **D**, **F**). nt, neural tube; psm, presomitic mesoderm.

In Fig. 9B the result of the *Htr3a* RT-PCR is depicted, which revealed the presence of genomic DNA in the cDNA as the upper bands (marked by asterisk) could only be derived of genomic DNA. The lower band represented the expected size of 653bp (marked by arrowhead) and thus indicated expression in all examined stages but in the PNC (Fig. 11B). The *Htr5b* receptor was detected in a similar way, as it was detected in all cDNAs except the one derived from the PNC (Fig. 11C).Although the *Htr6* receptor was expressed during flow stages, it could not be detected in the PNC cDNA (Fig. 11C). The receptors *Htr2b*, *Htr2c*, *Htr3b*, *Htr4*, *Htr5a* and *Htr7* could only be substantiated in post-flow stages (Fig. 11A-C).

As the RT-PCR indicated that the *Htr2a* class receptor was expressed at or in the vicinity of the PNC, this result should be validated using ISH. Therefore the gene was cloned and a specific probe for the receptor was synthesized. In order to prevent that the detection of the receptors failed due to problems caused by the RT-PCR the other receptors were also cloned and specific probes were made as well. Of all investigated serotonin receptors only for *Htr3a* an *in-situ* signal could be detected during flow stages. *Htr3a* was expressed in the forming head (Fig. 12A, B). No transcription of *Htr3a* could be found in the PNC. In sections the spots seen in Fig. 12A' turned out to be artifacts (not shown). No expression of *Htr3b* could be detected (not shown). As a preliminary RT-PCR showed that this receptor was expressed, ISH was performed with the double amount of digoxigenin-labeled uracil labeling within the probe in order to enhance the signal. Unfortunately, this approach did not improve the ISH and thus no expression could be visualized (not shown). In summary evidence for serotonin signaling in or close to the PNC could not be found using ISH.

Expression of components for serotonin synthesis and degradation

The biosynthesis of serotonin involves L-tryptophan which is processed by the *tryptophan hydroxylase 1* (*Tph1*). TPH is necessary for the synthesis of serotonin and represents the rate-limiting step in this pathway. A local source for serotonin in or near the PNC could be used in order to control or activate ciliary beating and thus regulating the leftward fluid-flow. Expression of *Tph1* has been reported to be first detectable at stage E14.5 in the pineal gland (Cote et al. 2007). In contrast to that,

expression was detected during flow stages using RT-PCR (Fig. 11D). It was substantiated from E7.5 on and remained expressed in all investigated stages, although it was not found to be transcribed in the PNC. In order to exactly localize the tissue where *Tph1* is transcribed, an ISH was performed. No expression could be found during flow stages (not shown). Directly after the flow event had occurred (E8.5), two distinct expression domains were detected (Fig. 12C). One of these was located in the notochord and the foregut in the mid-trunk, directly at the region where the neural tube was about close (Fig. 12C'). The other domain resided in the posteriormost somite and the region where the somites condense of presomitic mesoderm (Fig. 12C''). On E9.5, transcription of *Tph1* could still be detected in the region where the somites form and another domain was located in the vicinity of the tail bud (not shown).

The genes *monoamine oxidase A* and *B (Maoa / Maob*) encode the enzymes responsible for serotonin degradation. Serotonin signaling can thus be affected by the presence or absence of one of the two MAOs. Both *Mao* genes could be substantiated in all investigated cDNAs using RT-PCR (Fig. 11D). The expression of *Maoa* occurred in all stages relatively uniform and no downregulation within the PNC could be shown. *Maoa* was expressed throughout the embryo (Fig. 12D). In the ventral view the PNC and the notochord appeared to be free of *Maoa* transcripts. Lateral section through this embryo revealed that *Maoa* was expressed uniformly thus even in the PNC and the notochord (Fig. 12D, D'). *Maoa* remained to be expressed ubiquitously in the E8.5 embryo (Fig. 12E). In contrast to that only very weak signals of *Maob* transcription were detected in the cDNA of the PNC while it was expressed at much higher levels in the other investigated tissues (Fig. 11D). Expression of *Maob* could be detected in post flow-stages in the neural tube ectoderm in the region where the neural tube was about to close (Fig. 12F).

Taken together, the analysis of the expression of molecules involved in synthesis or turnover of serotonin did not provide any hints for a presumed role of serotonin in left-right development.

Reduction of serotonin levels in *Sert*-deficient mice did not result in laterality defects

A recent study showed that the amount of serotonin present in the serum of pregnant female mice is crucial for the development of the embryos (Cote et al. 2007). This finding raised the possibility that left-right development could also be affected by the maternal serotonin level. A candidate for an analysis of this aspect is the serotonin transporter (*Sert*). This enzyme is responsible for serotonin reuptake from the synaptic cleft after signal transduction. In *Sert* knockout mice it was shown that the serotonin level is reduced in adult animals (Bengel et al. 1998). Therefore the embryos of a *Sert* -/- x *Sert* -/- mating were isolated at stage E14.5 and examined for left-right defects. The inner organs of all examined embryos (n= 9) displayed *situs solitus* (not shown). As the litters were relatively small and remnants of decidual tissue indicated that embryonic lethality already had occurred, earlier stages were examined. The analysis of *Pitx2* expression using ISH revealed transcription in a wt manner in E8.5 and E9.5 embryos (n=15, not shown). In summary, the reduction of the maternal serotonin level did not result in left-right defects in the offspring of *Sert* knockout mice.

Taken together, the analysis of serotonin signaling during laterality determination in the mouse did not provide any striking evidence for a direct effect of serotonin on the leftward fluid-flow.

Brachyury (T)

In order to gain information on the formation of the PNC and the effects of a defective PNC, *T*-deficient embryos were analyzed. Loss of function of *Brachyury* in *T/T* mutant mouse embryos leads to multiple mesoderm associated defects. Among these, the formation of the somites, the allantois and the notochord is disturbed. The defects result in embryonic lethality at mid-gestation and left-right development is impaired (Herrmann 1992; King et al. 1998). As the formation of the PNC has also been reported to be affected by the mutation, the leftward fluid-flow was investigated in *T*-deficient embryos (Fujimoto and Yanagisawa 1983).

SEM analysis confirmed malformation of the PNC in *T/T* mutants

Scanning electron microscopy (SEM) analysis of E8.0 *T/T* mutant embryos in comparison to heterozygous and wt littermates is shown in Fig. 13. The characteristic features of a wt PNC are monociliated cells arranged in an indentation at the distal tip of the cup shaped E8.0 mouse embryo (Sulik et al. 1994). The ciliated cells were detected at the expected location in wt embryos and possessed a hemispherical apical shape, which made the cells easily distinguishable from the surrounding endodermal cells (Fig. 13A-A'').

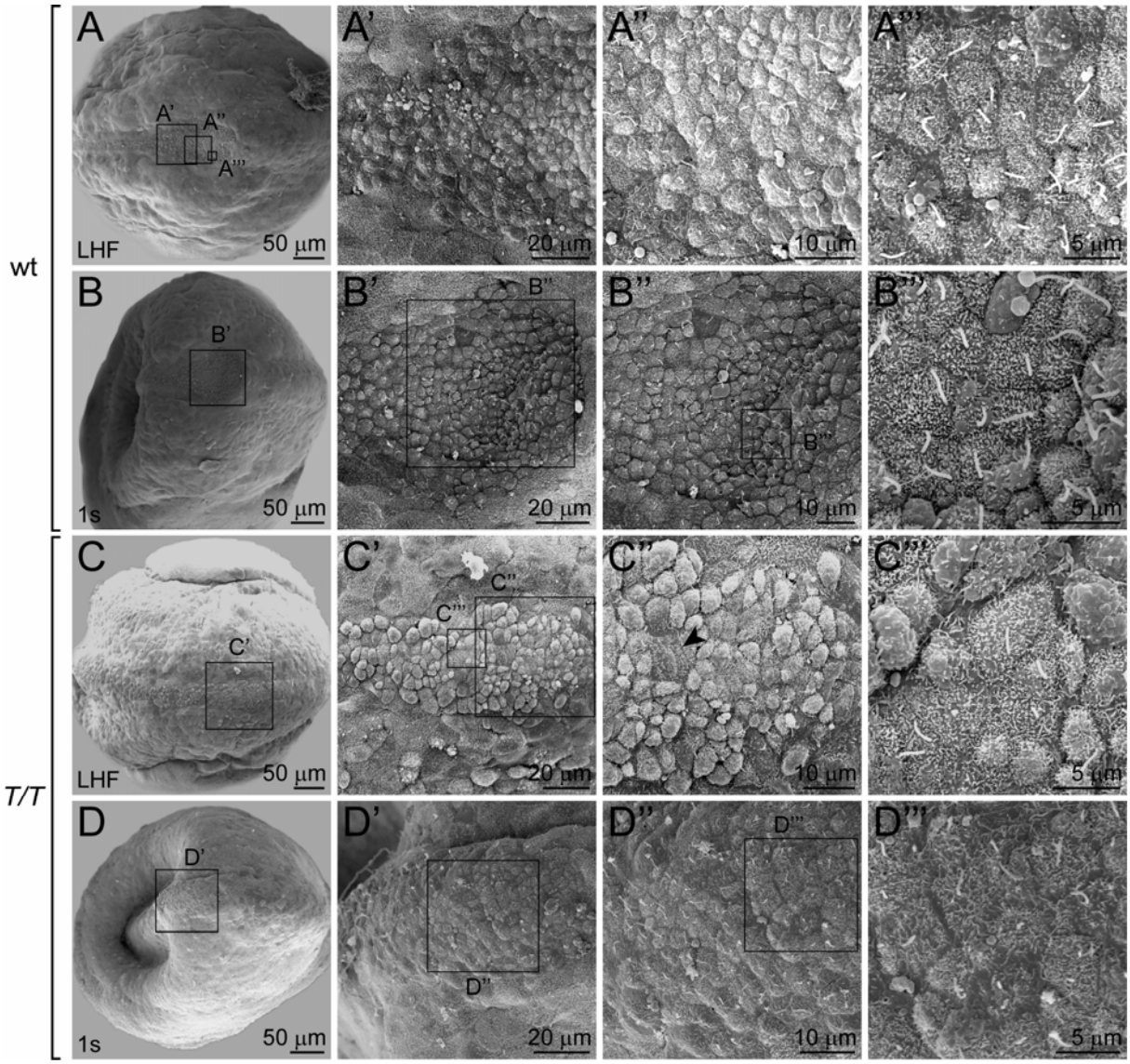

Fig. **13** Abnormal PNC formation in *T/T* mutant mouse embryos. Scanning electron microscopy of E8.0 wt or heterozygous (**A**-**B'''**) and *T/T* mutant (**C**-**D'''**) embryos. The PNC consisted of several monociliated cells arranged in a dense cluster forming an indentation. *T/T* mutant embryos possessed less ciliated cells with shorter cilia and lacked the indentation (**C**-**D'''**). Ciliated cells were intermingled with endodermal cells (judged by outer appearance; arrowhead in **C''**). Depicted stages are late-headfold (LHF, **A**, **C**) and 1 somite (1s, **B**, **D**). Boxes indicate areas shown in higher magnification.

The indentation had not completely formed in the late headfold stage (Fig. 13A-A’’’) but could clearly be detected in the 1-somite stage (Fig. 13B-B’’’). In contrast to that no indentation at the distal tip of *T/T* embryos of corresponding stage could be found (Fig. 13C-D’’’). Ciliated cells were found in all investigated specimen (n=18), however the amount of ciliated cells differed severely between homozygous mutant and wt / heterozygous embryos. Furthermore, only a few cilia appeared normal in *T/T* embryos and reached an average length of 2.2µm (n=183). In wt or heterozygous littermates cilia possessed an average length of 3.2µm (n=142). The usual dense cluster of cells in the PNC could not be detected in *T/T* mutants. In these specimens cells with a rather endodermal shape, judged by the size and flattened cell shape, could be found between remaining ciliated cells (arrowhead in Fig. 13C’’). Taken together, the PNC had not formed correctly in *T/T* mutant embryos but ciliated cells were not completely absent.

Ciliary motility was affected by the absence of a functional T-protein

The motility of the cilia in mutant *T/T* embryos was studied using light microscopy. In order to visualize the motility of the cilia, the area at the distal tip was filmed. The movies were then processed in a way that the difference between two consecutive frames was calculated. The subtraction of grey-levels of corresponding pixel of subsequent frames resulted in a blackened pixel, if the pixel was not altered. When altered, the resulting pixel shows the aberration of grey-levels. This method can be used to mathematically subtract the background and non-moving parts from a movie. This method allowed to visualize ciliary motion and made it distinguishable from moving particles.

The result of this processing is shown in Fig. 14. In a wt PNC most of the cilia rotated in a clockwise manner. Cilia are exemplarily marked by arrowheads in one of the 500 frames of the movie (Fig. 14A). In Fig. 14B the same region is shown in a processed movie where light spots indicate that cilia or particles have moved. The rotational movement of cilia resulted in spoke-like circles. The movie in Fig. 14E and 14F was filmed at a higher magnification and with more frames per second increasing the comprehensibility of ciliary motion.

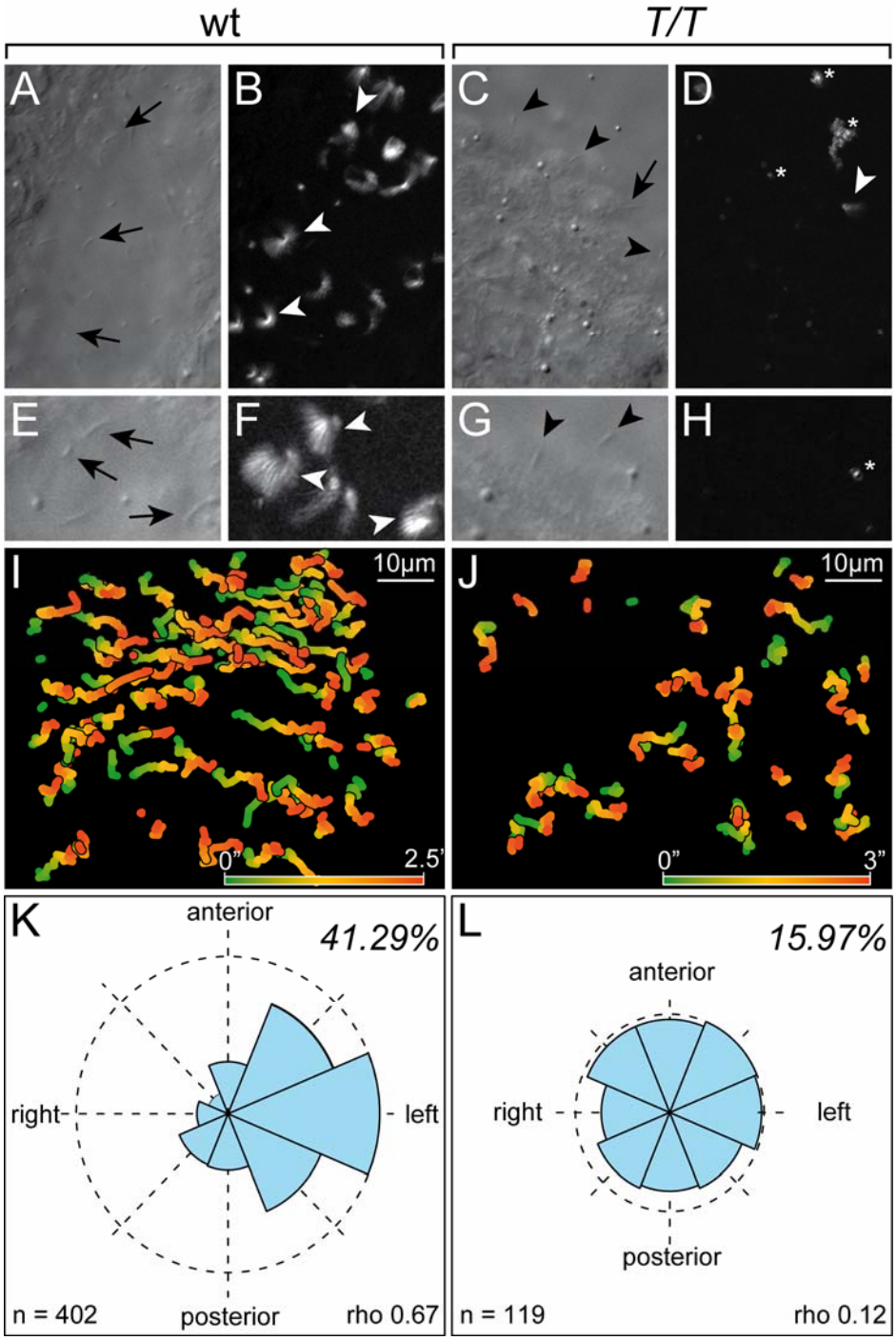

Fig. **14** Immotile cilia in malformed PNC caused absence of leftward fluid-flow in *T/T* mutant embryos. Still pictures of video-microscopy of *T/T* mutant (**A**, **B**, **E**, **F**) embryos and heterozygous littermates(**C**, **D**, **G**, **H**) revealed that most cilia were immotile in T-deficient embryos. Collapsed movies of frame-by-frame pixel changes showed light spots only in areas where changes had occurred (**B**, **F**, **D**, **H**). Higher magnification provided improved comprehension of ciliary motion (**F**, **H**). Motile cilia produced a circle of stripes around a light spot (arrowhead in **B**, **F**) Representative frames (**A**, **C**, **E**, **G**) of processed movies enabled distinction between motile (arrows in **A**, **E**, **C**) and immotile cilia (arrowheads in **C**, **G**). Artifacts caused by moving particles are marked by asterisks (**D**, **H**). Particle movements displayed as gradient-time trails (GTTs), representing about 2.5 to 3s from green to red (cf. gradient bar). The analysis indicated that the flow was absent in *T/T* mutant embryos (**J**) compared to the control (**I**). Quantitative analysis of GTT directionality over the area of the PNC demonstrated strong leftward flow in the control (**K**) but only randomized distribution of directions of moving particles in *T/T* mutants (**L**).

As the cilia were tilted posteriorly, the corresponding bright spot (base of cilium) did not mark the center of the motion-circle, but was localized anterior to it. In *T/T* mutant embryos cilia could be found using light microscopy (marked by arrowheads, Fig. 14C). Only about a fourth of the observed cilia were motile. In the processed and collapsed movie shown in Fig. 14D one cilium was motile (marked by arrowhead). The other light spots (marked by asterisks) derived from moving particles.
This light microscopic study of *T/T* embryos revealed also the decrease of ciliary length compared to wt specimens like observed in the SEM analysis (Fig. 14G). Furthermore, the notion that the ciliated cells were arranged in a lower density could be confirmed. None of the cilia filmed in the movie in Fig. 14G was motile as Fig. 14H showed. The bright spot was caused by a moving particle (marked by asterisk).

Leftward fluid-flow was absent in *T/T* mutant embryos

After showing that cilia were hardly motile and the PNC had not formed correctly the leftward fluid-flow in *T/T* embryos was analyzed as explained above.
In wt embryos most particles moved to the left side in a ventral view of the PNC (Fig. 14I). In contrast to that, the particles in a *T/T* mutant embryo did not move in one particular direction (Fig. 14J). In Fig. 14K and L the distribution of trajectory-directions of the traced beads is indicated. In wt and heterozygous embryos more than 40% of the particles moved directly to the left side of the PNC (Fig. 14K). In *T/T* mutants no preferred direction of the beads could be detected (Fig. 14L). The distribution of the direction appeared random. Along with this, the quality of flow dropped from 0.67 in wt to 0.12 in *T/T* embryo. In summary, in *T/T* mutant embryos very few motile cilia could be detected but these were not able to produce a leftward fluid-flow.

Absence of asymmetric gene expression in *T*-deficient embryos

In *T/T* mutants it was published that *Nodal* expression is absent around the PNC and in the lateral plate mesoderm (King et al. 1998). As the asymmetric expression of the transcription factor *Pitx2* was shown to be a downstream target of *Nodal*, it is very likely that *Pitx2* is also absent in *T/T* mutants. In order to investigate this, ISH was

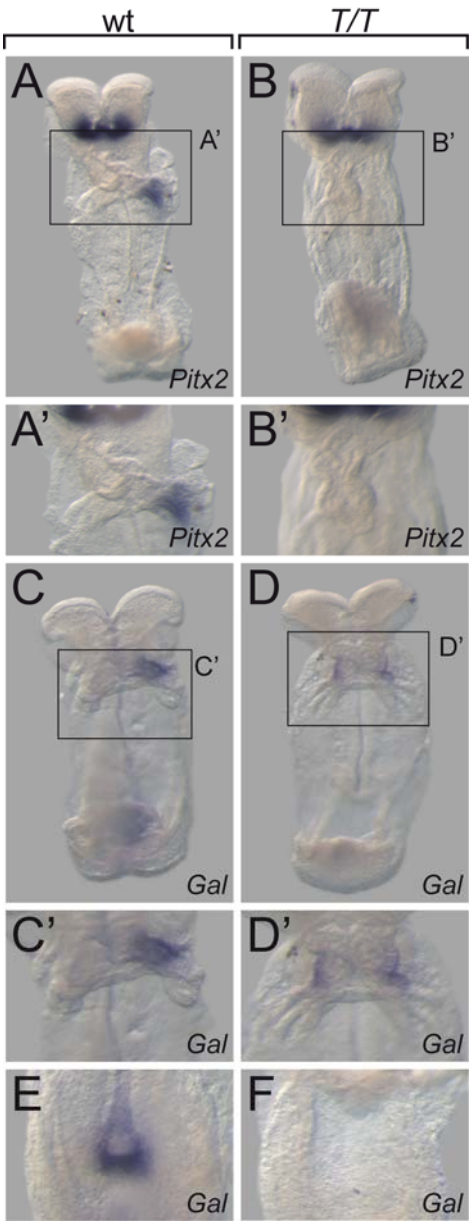

performed on *T/T* embryos and on heterozygous and wt littermates. *Pitx2* was expressed in the head mesenchyme in all examined embryos at E8.5 (Fig. 15) (Mucchielli et al. 1997). Asymmetric expression of *Pitx2* was observed in the left myocardium of the heart in heterozygous or wt embryos (Fig. 15A, A'). No transcription of *Pitx2* could be detected in the heart anlage of *T/T* mutant embryos (Fig. 15B, B').

Fig. **15** Absence of asymmetric gene expression in *T/T* mutant mouse embryos. Ventral views of heterozygous (**A**, **C**, **E**) and *T/T* mutant (**B**, **D**, **F**) E8.5 embryos hybridized with specific probes for *Pitx2* (**A**-**B'**) and *galanin* (*gal*, **C**-**F**), anterior directs at top. Expression of *Pitx2* in the head was independent of *T* (**A**, **B**). Asymmetric transcription of *Pitx2* in the heart (**A'**) was missing in *T/T* mutant embryos (**B'**). *gal* was expressed asymmetrically in the heart of heterozygous embryos (**C**, **C'**) and symmetrically in *T*-deficient embryos (**D**, **D'**). The expression of *Gal* at the PNC in heterozygous animals (**E**) was not detected in *T/T* mutants (**F**). Boxes indicate areas shown at higher magnification.

The signaling peptide *galanin* has recently been published to be a novel asymmetric expressed gene (Schweickert et al. 2008). Like *Nodal* it is expressed in a horseshoe like pattern close to the PNC (Fig. 15E) and additionally, in the left side of the heart (Fig. 15C, C'; Schweickert et al. 2008). In homozygous *T/T* mutants the expression of *Galanin* could be detected on both sides of the forming heart (Fig. 15 D, D'). In contrast to that, no expression of *galanin* around the PNC could be visualized (Fig. 15F).

The analysis of the two asymmetric expressed genes *Pitx2* and *galanin* revealed the expected absence of *Pitx2* but, surprisingly, *galanin* was expressed bilaterally.

Downregulation of *Fgf8* in *T/T* mutants

As thus far no data has been published that indicated that *T* can induce the expression of *Nodal*, it is very unlikely that the absence of *Nodal* is a direct effect of the loss of *T*. Therefore, other genes are probably involved in the regulation of *Nodal* which are dependent on *Brachyury* expression. One possible candidate for this purpose is the *Fibroblast growth factor 8* (*Fgf8*). In zebrafish it has been shown that *Nodal* expression is dependent on *Fgf8* expression (Griffin and Kimelman 2003; Mathieu et al. 2004). Furthermore, a transgenic mouse which only expresses a hypomorphic *Fgf8* lacks the transcription of *Nodal* in the midline as well (Meyers and Martin 1999). A connection between *Fgf8* and *notail*, the zebrafish homolog of *Brachyury* has been shown to exist in form of a positive feedback loop (Griffin and Kimelman 2003). In *Xenopus* this regulation has been reported for *Fgf4*, a close relative of *Fgf8* (Saka et al. 2000). Therefore the absence of *Nodal* expression in *T/T* embryos could be caused by absence or downregulation of *Fgf8* expression. Expression of *Fgf8* was analyzed in *T/T* embryos and heterozygous littermates using ISH.

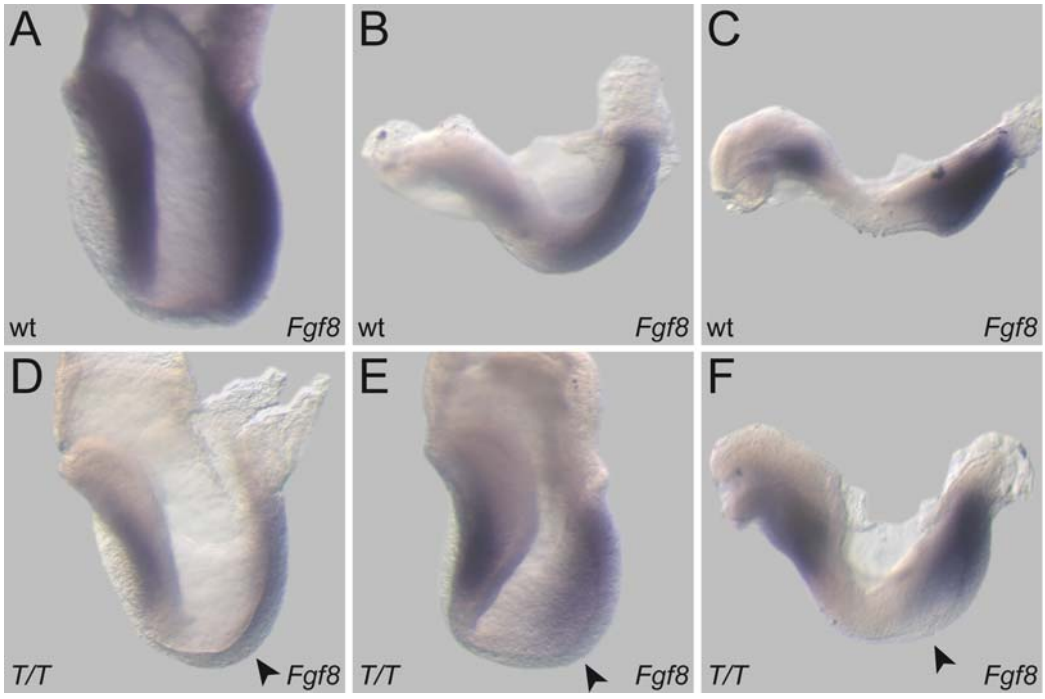

Fig. **16** *Fgf8* was downregulated in *T/T* mutant embryos. Lateral views of heterozygous (**A**-**C**) and *T/T* mutant (**D**-**F**) embryos hybridized with specific probes for *Fgf8*, anterior to the left. Expression of *Fgf8* in the PS was downregulated and almost absent in the anterior PS of *T*-deficient embryos (marked by arrowheads in **D**-**F**). Presented stages are early-headfold (**A**, **D**), late-headfold (**B**, **E**) and 1somite (**C**, **F**).

Fgf8 is expressed in the complete PS and in the mesenchyme of the forming headfolds of E8.0 to E8.5 (Fig. 16A-C; Crossley and Martin 1995). In *T/T* embryos, *Fgf8* was expressed in the PS and in the headfolds but the overall expression level appeared to be reduced (Fig. 16D-F). Moreover, the expression of *Fgf8* in the anterior PS was markedly reduced in the *T/T* embryos (arrowheads in Fig. 16D-F). This implied that *Fgf8* in the anterior PS is dependent on *T* expression. As this is the region where the PNC forms, the absence of *Nodal* expression around the PNC could be due to the downregulation of *Fgf8*.

Xenopus Brachyury (Xbra)

In order to investigate whether the role of *Brachyury* during left-right development is conserved from frog to mouse, knockdown experiments of *Xbra*, the *Xenopus* homolog of *Brachyury* were performed. Therefore an antisense morpholino was designed in a way that the morpholino binds to start codon of *Xbra* mRNA, thus preventing the initiation of *Xbra* translation. At first the morpholino was injected into the two dorsal blastomeres in the region of the dorsal marginal zone of 4-cell stage *Xenopus* embryos (Fig. 17C). Upon injection into this region the dorsal midline was targeted and thus the floorplate, the notochord and the GRP were aimed at (Blum et al. 2009). As a lineage tracer, the fluorescent dye rhodamine-B-dextran was coinjected into the embryos. The analysis of the distribution of the lineage tracer allowed for the validation of the targeting (Fig. 17F).

Laterality defects in *Xbra* morphants

As a first attempt, 2x0.25pMol of *Xbra* morpholinos were injected and the embryos were cultivated to tadpole stages. The embryos were then analyzed for correct development of the left-right axis. Hence the heart, the gut and the gall bladder were analyzed for proper formation. Fig.18C shows that in about 15% (n=14/90) of the embryos left-right defects were caused by knocking down *Xbra* expression. These defects were accompanied by a high rate of mortality, which occurred primarily during gastrulation and after st. 35.

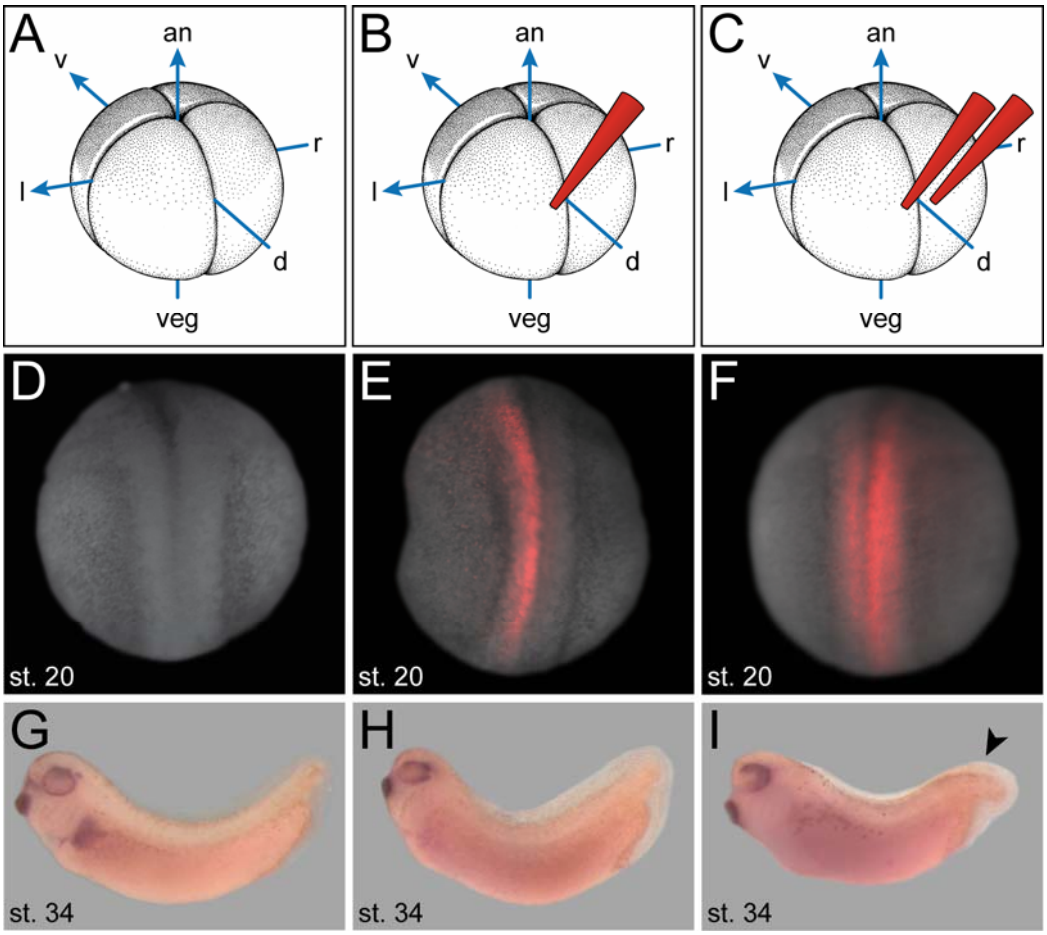

Fig. **17** Knockdown of *Xbra* in *Xenopus* embryos resulted in absence of *Pitx2c* expression and midline defects. Schematic drawings of *Xenopus* 4-cell stage (**A**) embryos with indicated injection of morpholinos and lineage tracer into the left (**B**) and the complete dorsal marginal zone (DMZ, **C**). (**D**-**E**) Distribution of the lineage tracer in neurula stages after injection shown in **A**-**C**: uninjected embryo (**D**); embryo with lineage tracer in the left portion of the midline after injection into the left DMZ (**E**); presence of lineage trace in entire midline after injection into complete DMZ (**F**). Lateral views of uninjected (**G**) and injected embryos (**H**, **I**) hybridized with specific probes for *Pitx2c*, anterior to the left. Upon unilateral injection of 1pMol *Xbra*-morpholino (XbraMo) the asymmetric expression of *Pitx2c* in the left lateral plate mesoderm was lost (**H**). Bilateral injection of 6pMol XbraMo led to absence of asymmetric *Pitx2c* expression and midline defects (arrowhead in **I**). Schematic drawing (**A**-**C**) was produced by Bernd Schmidt. st, stage.

Therefore embryos were only cultured to st. 30-34 and subsequently analyzed for asymmetric gene expression (Fig. 18D). This changed procedure allowed to use a higher dose of the morpholino as even at 2x0.75pMol less than 6% (n=10/190) of embryos died prior to analysis (data not shown). The injection of the morpholino led to left-right defects in about 40% (n=63/159) of the embryos. Of these, the predominant effect was absence of *Pitx2c* expression (n= 59/159, Fig18D). In order to show that this did not only result from unspecific effects of the morpholino or mechanical stress of the injection, a control morpholino was used. It was injected in embryos of the same batch and at the same concentration. About 5% (n=7/161) of control morpholino injected embryos expressed *Pitx2c* other than wt manner (Fig.

18D). In morphants it could be observed that about 20% of the embryos expressing *Pitx2c* in wt manner had a markedly reduced level of expression. This reduction ranged from almost normal expression levels to hardly detectable ISH signals (cf. Fig. 17H).

Unilateral knockdown of *Xbra* enhanced left-right defects

In order to further increase the effects of the *Xbra* knockdown and the persistence of the outcome, improvements of the experimental procedure were attempted. A higher persistence should allow rescue experiments which are necessary to prove the specificity of the morpholino. Vick et al. could show that a loss of function of ciliary dyneins on the left side of the midline is sufficient to induce left-right defects (Vick et al. 2009). As the artifacts caused by mechanical stress of the knockdown procedure were supposed to be reduced by unilateral compared to bilateral injection, the dose of the morpholino was raised to 1pMol per injection (Fig. 17B, E). The unilateral injection of 1pMol *Xbra* morpholino into the marginal zone of the left dorsal blastomere resulted in more than 50% (n=59/113) of embryos not expressing *Pitx2c* in the lateral plate mesoderm (Fig. 18E). As these results derived from 7 different experiments, each showing very similar results, the persistence of the phenotype could be improved. As described before, a control morpholino was used to show specificity of the knockdown. The injection of the control morpholino resulted in less than 1% (n=1/107) of embryos expressing *Pitx2c* not in a wt manner.

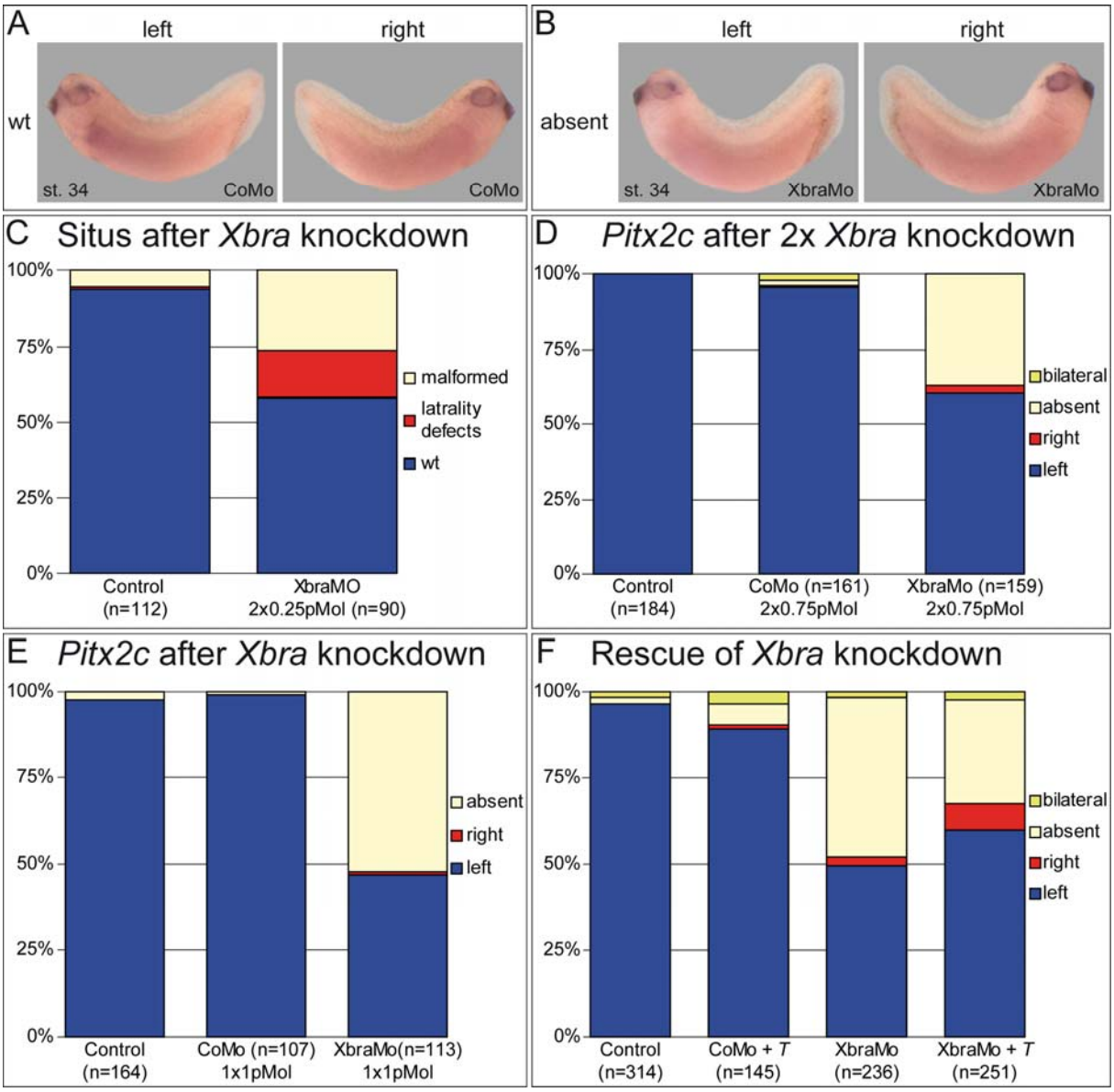

Fig. **18** Knockdown of *Xbra* in *Xenopus* embryos resulted in laterality defects. Lateral views of control-morpholino (CoMo, **A**) and *Xbra*-morpholino (XbraMo, **B**) injected embryos hybridized with specific probes for *Pitx2c* revealed absence of asymmetric *Pitx2c* expression. (**C**) Analysis of the situs of stage 45 embryos injected bilaterally with 0.5pMol XbraMo showed 15% left right defects. Asymmetric expression of *Pitx2c* was lost in 37% of embryos injected bilaterally with 1.5pMol XbraMo (**D**). Upon unilateral injection of 1pMol XbraMo 52% of embryos lost asymmetric *Pitx2c* expression (**E**). Asymmetric expression was regained in 60% of embryos by co-injection of mouse *T* mRNA and XbraMo compared to 50% when *T* mRNA was not present (**F**). Injections were controlled by application of a control-morpholino (CoMo) which did not result in more than 5% of embryos with changed expression of *Pitx2c* (**A**, **D**-**F**). st, stage.

Gain-of-function using mouse *Brachyury*

In order to show that the effects of the morpholino resulted from a knockdown of *Xbra*, a heterologous rescue experiment was designed. Therefore, the full length coding sequence of mouse *Brachyury* was cloned into a CS2+ expression vector. In order to prevent any confusion, the construct was named *T-cod*. The plasmid was then used to produce murine *Brachyury* mRNA. The mRNA was first analyzed in a gain of function experiment in embryos and compared to results in literature. Cunliffe and Smith injected 5ng in the animal pole at the one-cell stage. This resulted in the formation of additional mesodermal tissue and a perturbed gastrulation (Cunliffe and Smith 1992). In a second publication, the formation of tail-like protrusions was reported upon overexpression of 10pg of a hormone inducible *Xbra* construct into the animal pole of 32-stage embryos (Tada et al. 1997). Furthermore, they reported that the presence of these protrusions close to the head lead to absence of the eye (Tada et al. 1997). The injection of *T-cod* mRNA into the marginal zone of the left dorsal blastomere at a concentration of 20ng/µl led in about 13% (n=20/149) of embryos to the formation of protrusions. In 26% of left-sided injected embryos an absence of the left eye could be detected. On the left side of the embryo, the side that received the mRNA, the eye had not developed correctly (not shown). No relation between the presence of the protrusions and the malformation of the eye could be detected. In summary, the gain-of-function of mouse *Brachyury* resulted in similar changes as described for *Xbra*.

Rescue of *Xbra* knockdown

In order to show that the morpholino specifically inhibited the translation of *Xbra*, rescue experiments were necessary. Therefore the morpholino was injected simultaneously with *T-cod* mRNA into the marginal zone of the left dorsal blastomere (Fig. 18F). For a better comparability the *T-cod* mRNA was also injected together with the control morpholino. In about 11% (n=16/145) the injection of *T-cod* mRNA together with the control morpholino resulted in left-right defects. The overall morphology of these specimens resembled the changes described in the gain-of-function of *T-cod*. Thus the presence of the control morpholino had no considerable

effect on the development. The injection of the *Xbra* morpholino led, as described above, to the absence of *Pitx2c* expression in about 50% of the embryos (n=109/236). When the *T-cod* mRNA was also present at the same time, this portion dropped to about 30%. In contrast to that, the amount of embryos expressing *Pitx2c* in wt manner raised significantly from 50% without mRNA to 60% with RNA at a p-value of 0.024. Together with this increase the amount of embryos expressing *Pitx2c* bilaterally also raised from 2.5% (n=6/236) to 7.5% (n=19/251). Taken together, the co-injection of mouse *Brachyury* mRNA could rescue the effects of the *Xbra* morpholino partially and thus, the specificity of the morpholino was demonstrated.

Nodal expression was affected by *Xbra* knockdown

The mutation in the mouse *T/T* embryos leads to absence of *Nodal* expression (King et al. 1998). Therefore the expression of *Nodal* in the frog was analyzed after knockdown of *Brachyury*. *Nodal* expression flanks the GRP in frog embryos before and during the flow event (Schweickert et al. 2007). Fig. 19A and B show expression of *Nodal* in control morpholino and *Xbra* morpholino injected embryos, respectively. In control morpholino injected embryos, the bilateral transcription of *Nodal* remained unchanged (Fig. 19C). In contrast to that, only weak and therefore clearly affected expression of *Nodal* on the left side of the GRP could be detected in about 44% (n=26/59) of *Xbra* morpholino injected embryos. Thus, like in mouse embryos, the loss of a functional *Brachyury* protein resulted in a downregulation on the expression of *Nodal* in the frog.

Defective GRP in *Xbra* morphants

As the analysis of the *T/T* mutant embryos revealed that the PNC did not form correctly, the question was raised whether knockdown of *Xbra* has the same effect on the development of the GRP. A possible conservation of the role of the gene *Brachyury* from frog to mouse was thereby investigated. Therefore embryos injected with *Xbra* morpholino or control morpholino were fixed at st.18 and dorsal explants were dissected (Blum et al. 2009).

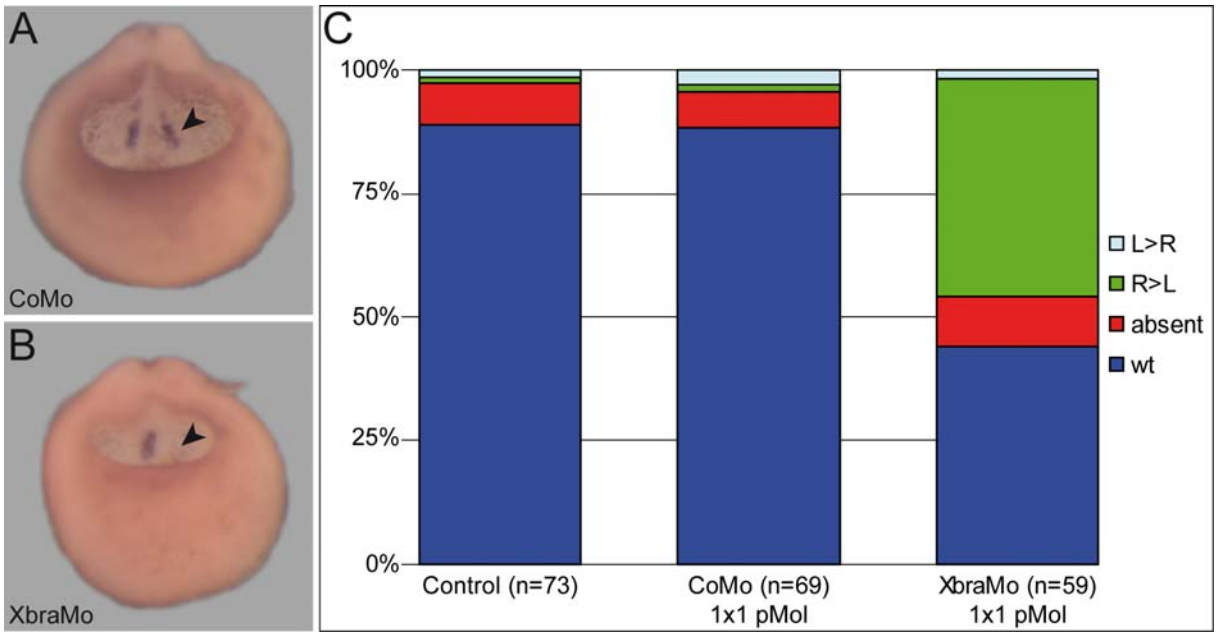

Fig. **19** Knockdown of *Xbra* in *Xenopus* embryos resulted in attenuation of *Nodal* expression. Ventral views of hemi-sections of control-morpholino (CoMo, **A**) and *Xbra*-morpholino (XbraMo, **B**) injected embryos hybridized with specific probes for *Nodal*. Upon unilateral injection of 1pMol XbraMo the left-sided *Nodal* expression at the gastrocoel roof plate was attenuated or even absent in 45% of embryos (arrowhead in **A**, **B**). In 5-10% *Nodal* expression could not be detected in all investigated groups.

The SEM analysis of the control morpholino injected embryos showed the archenteron (Fig. 20A). Higher magnification of the same region revealed the triangular shape of the GRP (Fig. 20A'). Closer view at the GRP showed that the cells were monociliated and that these cells differed in shape from the lateral endodermal crest (LEC) cells (Fig. 20A'') (Shook et al. 2004). In Fig. 20B, an embryo in which 1pMol of the *Xbra* morpholino was injected into the left dorsal marginal zone is displayed. Higher magnification of the same embryo indicated that some of the cells on the left side of the GRP adopted a shape resembling that of LEC cells (Fig. 20B'). At even higher magnification, the cilia on the GRP cells were visible (Fig. 20B''). Only few cilia could be detected in the region where the morpholino was expected. Most of these cilia appeared shortened in length. In summary the GRP did not form correctly in *Xbra* morphants (n=4).

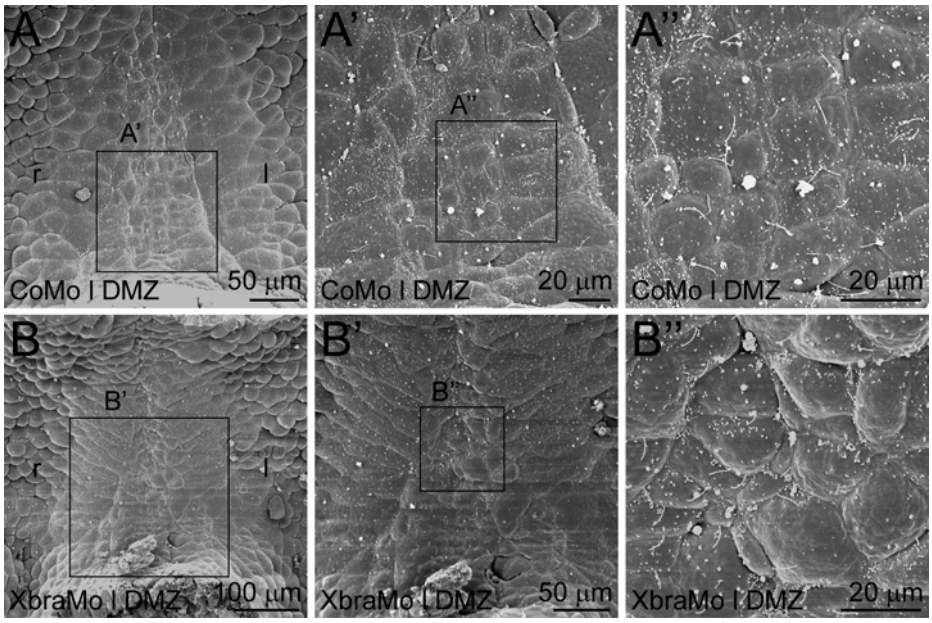

Fig. **20** Knockdown of *Xbra* in *Xenopus* embryos resulted in malformation of the gastrocoel roof plate (GRP). Scanning electron microscopy of *Xenopus* dorsal explants unilaterally injected with control-morpholino (CoMo, **A**-**A''**) or *Xbra*-morpholino (XbraMo, **B**-**B''**) into the left dorsal marginal zone. The GRP was not affected by injection of CoMo (**A**). The cells of the GRP possessed cilia and cells were distinguishable from lateral endodermal crest (LEC) cells in CoMo injected embryos (**A'**, **A''**). The knockdown of *Xbra* impaired the development of the GRP (**B**). Cells in the left GRP (the cells targeted by the XbraMo) appeared to have shorter cilia and adopted the shape of LEC cells (**B'**, **B''**). Boxes indicate areas shown at higher magnification.

Leftward fluid-flow was attenuated upon knockdown of *Xbra*

The finding that the PNC had not formed correctly upon knockdown of *Xbra* indicated that the leftward fluid-flow was affected as well in these specimens. Thus the fluid-flow was analyzed in control and *Xbra* morphants. Again, the unilateral injection of 1pMol into the left dorsal marginal zone was performed. Fig. 21A and B show explants of these embryos injected with control morpholino and *Xbra* morpholino, respectively. The lineage tracer indicated that in both cases the left side of the GRP was targeted (not shown). In Fig. 21C-F qualitative analysis of the leftward fluid-flow of embryos after injection of the control morpholino (C, D) and *Xbra* morpholino (E, F) is shown. The flow over the right side of the GRP was not affected in both experiments (Fig. 21C, D). In contrast to that, the flow on the left side of the GRP was attenuated in the *Xbra* morphant (Fig. 21D) while it remained normal in the control morphant (Fig. 21F). Taken together the knockdown of *Xbra* in the GRP resulted not only in defective morphology of the GRP but also the leftward fluid-flow was affected.

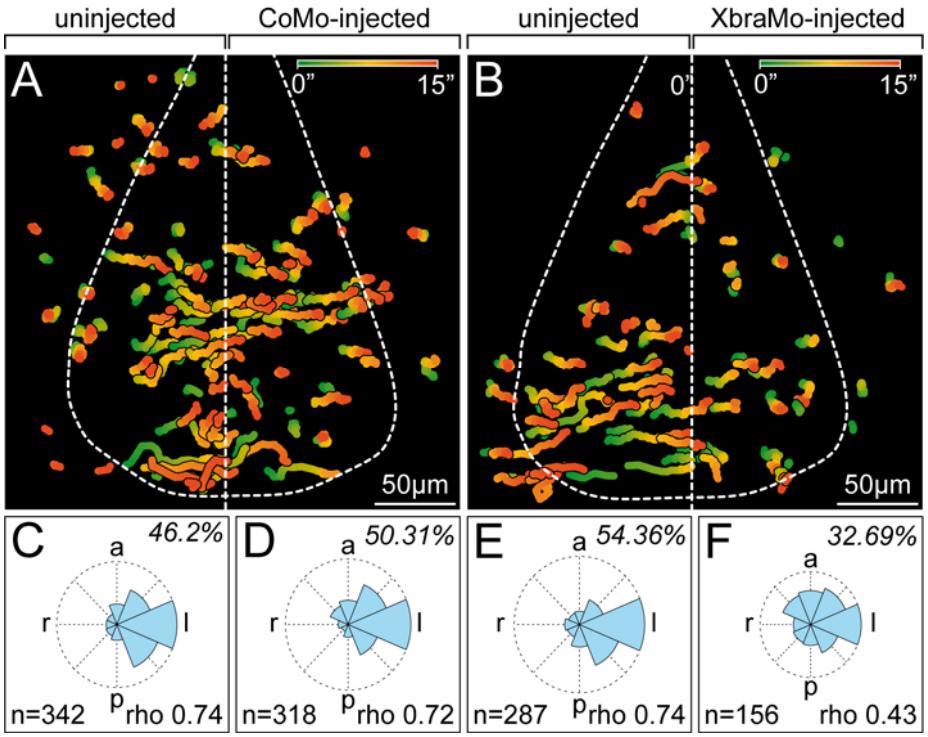

Fig. **21** Knockdown of Xbra attenuated leftward fluid-flow. Particle movements displayed as gradient-time trails (GTTs), representing 15s from green to red (cf. gradient bar). Explants of Xenopus gastrocoel roof plates (GRP) targeted with Control-morpholino (CoMo, **A**) and Xbra-morpholino (XbraMo, **B**). The embryos were injected in a way that only its left side of the GRP was affected, as judged by lineage tracer (not shown). Quantitative analysis of GTT directionality over the area of the GRP (**C**, **D**, **E**) demonstrated strong leftward flow in complete GRP of CoMo and in right side (i.e. the side that was not targeted) of XbraMo injected embryo. In contrast to that weakened flow in left GRP of XbraMo injected embryo (**F**), judged by the value rho, which indicated the quality of the directionality. Dashed lines in **A** and **B** indicate the area of the GRP. a, anterior; l, left; p, posterior; r, right.

Discussion

In the course of the present work the ciliated indentation of gastrulating mouse embryos could be allocated to the posterior part of the notochord. Furthermore, it could be shown that the monoamine adrenaline but not serotonin affected the ciliary beat frequency and thus the leftward flow. Finally, two distinct roles for Brachyury in left-right development could be identified in frog and mouse.

On the organizer of the vertebrate embryo

The posterior notochord (PNC)

The analysis of histology, SEM and gene expression revealed that the midline of a gastrula stage mouse embryo can be subdivided into five regions (Fig. 3-5). These are, from caudal to cranial, the PS, the organizer, the PNC, the anterior notochord and the prechordal plate. This distinction between organizer and PNC differs from published literature, as the PNC was formerly known as ‘the node’ and thought to be the homolog of the Spemann organizer (Beddington 1994). The PNC is in continuity with the notochord, which was indicated by SEM and is furthermore shown by several genes that are expressed in both regions (Wilkinson et al. 1990; Ang et al. 1993; Echelard et al. 1993). But some of the properties of the PNC are unique and therefore suggest that it should be regarded as a special structure in the midline of gastrulating mouse embryos. One of these is the expression of *Nodal* which demarcates its lateral and posterior boundaries (Lowe et al. 1996). Additionally, its ventral surface is characterized by a monociliated epithelium, which gives rise to the leftward fluid-flow necessary for correct laterality development (Sulik et al. 1994; Nonaka et al. 1998). Beyond that, the PNC is characterized by an indentation and is much wider compared to the anterior notochord.

The mouse organizer is not located within the PNC

The tissue responsible for axis induction in amphibian embryos is known as Spemann organizer (Spemann and Mangold 1924; Niehrs 2004). The term organizer includes the ability of a tissue to induce a complete secondary axis upon transplantation (Niehrs 2004). Therefore transplantation experiments have revealed the location of the organizer in many species before molecular markers were available. For example in chicks, the homolog of Spemann's organizer is could be identified to correspond to Hensen's node (Hensen 1876; Waddington and Schmidt 1933). As in rodents the PNC was known as 'the node', it was supposed to possess the characteristics of a full organizer. However in rodents transplantation experiments are very challenging not only due to the embryo's size but also due to the special mode of gastrulation. Thus the location of the mouse organizer has remained unknown until the discovery of *Gsc* expression and the transplantation of the corresponding tissue (Blum et al. 1992; Beddington 1994). Up to now, *Gsc* remains to be the best molecular marker of the organizer as it marks the homologous structures of the Spemann organizer in all investigated vertebrates (De Robertis et al. 1992). Furthermore the regions expressing *Gsc* have been identified for their organizing capacities in detail by Patrick Tam and colleagues (Kinder et al. 2001). Thereby full organizer capacity was detected for the so-called mid gastrula organizer which can be found only temporally before the formation of the PNC. The finding that no expression of *Gsc* could be detected in the PNC argues against organizer ability of this structure. In contrast to that, it is more likely that the region just posterior to the PNC possesses these capacities because it shares the properties of Hensen's node as it consists of a mass of cells and no germ layers can be identified (Hensen 1876). The precise analysis of *Nodal* expression in the gastrulating mouse embryo provided an excellent tool as it marked the organizer and outlined the forming PNC at the same time. Therefore, it showed that these are two different entities which resided next to each other (Fig. 22; Blum et al. 2007).This finding could explain the results produced by Rosa Beddington and colleagues which led to the renaming of the archenteron (Beddington and K.A. and Herrmann 1992; Beddington 1994). The transplanted tissue exhibited organizing capacity as it was obtained by excising the region of the PNC, which was further processed enzymatically until only a clump of cells remained. Therefore the tissue analyzed corresponded probably to the organizer and not only to the PNC. In order to completely rule out the possibility that

cells of the PNC have organizing capacity, a difficult transplantation experiment would be required as only the thin epithelium should be used. This could be accomplished by taking advantage of the *Noto* KO mouse. In this mouse-line the coding sequence of the *Noto* gene was replaced by a *green fluorescent protein* (*GFP*) marker. Thus, the cells of the PNC express *GFP* in addition to *Noto* in heterozygous embryos (Abdelkhalek et al. 2004; Beckers et al. 2007). Thereby the cells of the PNC could be identified assessing the fluorescence of the dissected tissue and thus sorted that only the fluorescent cells are used for the transplantation. To prevent further confusions, the term 'node' should be reserved for structures homologous to Hensen's node or the organizer and therefore the PNC should not be addressed in this way.

Gsc inhibits convergent extension

As the role of *Gsc* in the organizer remained unknown even after the KO of the gene, a conditional overexpression was performed (Deißler 2002). The construct used for this experiment turned out to repress its own expression and therefore only resulted in a mild overexpression. This led to neural tube closure defects (NTD), which initially did not tell much on the function of *Gsc*, as it was in sharp contrast o the expected role of *Gsc* as an organizer and thus axis inducing gene. In a second mouse-line the massive overexpression of *Gsc* resulted in multiple defects concerning all three germ layers (Deißler 2002; Andre 2004). These multiple defects complicated the analysis as the embryos died very early in gastrulation. The finding that the PNC had not formed upon *Gsc* overexpression was supported by the observation that *T* and *Noto* were downregulated (Fig. 6). As *Noto* is a marker for the forming PNC, the almost complete absence indicated that the axial mesoderm did not form. Additionally *Noto* has been shown to be downstream of *T*, whereas *T* is a direct target of *Gsc* (Artinger et al. 1997; Latinkic and Smith 1999; Boucher et al. 2000). Therefore the observed defects could be attributed to absence of *T* upon *Gsc* overexpression. As the defects did not resemble the loss-of-function of *T*, it is very likely that there is a further function of *Gsc* (Herrmann 1992). A possible hint therefore was obtained by the analysis of *Tbx6* expression in Gsc-overexpressing embryos (Fig. 7). *Tbx6* belongs, like *T*, to the t-box genes, a family of closely related genes. *T* has not been shown to be upstream of *Tbx6* as heterozygous *T/T* mutants initially express *Tbx6* (Chapman

et al. 2003). But as these embryos lose the expression of *Tbx6* in later stages, it was proposed that *T* is necessary for the maintenance of *Tbx6* expression (Chapman et al. 2003). Therefore, it is unlikely that *Tbx6* is almost absent in *Gsc*-overexpressing embryos just because of the downregulation of *T* in these specimens. In case there is a GSC binding site within the *Tbx6* promoter, *Tbx6*, like *T*, could be directly repressed by *Gsc* (Artinger et al. 1997; Latinkic and Smith 1999; Boucher et al. 2000). If the repression of *Tbx6* does not occur directly, an indirect mechanism involving other genes is also conceivable. The KO of *Tbx6* results in the formation of additional neural tubes (Chapman and Papaioannou 1998). Therefore, the observed additional neural groves, the precursor of a neural tube, can probably be attributed to the downregulation of *Tbx6* in *mT-Gsc/Cre* embryos (Andre 2004).

The axial mesoderm is responsible for the elongation of the anterior posterior axis. This process is mediated through convergent extension movements. Convergent extension is a cell behavior that leads to the concomitant narrowing and lengthening of a tissue (Wallingford et al. 2002). Furthermore the neural tube closure is also governed by convergent extension (Ybot-Gonzalez et al. 2007). A repression of convergent extension could explain the finding that *Gsc*-overexpressing embryos were smaller in size and filled up with cells. It seemed that the cells formed but behaved differently. Therefore, the midline did not elongate like it was supposed to and the embryo remained its size instead of expanding. Thus the ectodermal cells probably proliferated normally but the available space was limited, resulting in folding of this germ layer. Additionally, the repression of convergent extension would be in good correlation with the observed NTDs in the mildly *Gsc*-overexpressing embryos (Deißler 2002). In order to test this hypothesis, the gain-of-function of *Gsc* was tested in a comparable way in *Xenopus* embryos (Ulmer 2008). Thereby the blastopore closure and the neural tube closure were compromised (Ulmer 2008). As these two processes underlie convergent extension, the experiments in the frog confirmed the idea derived from mouse data (Keller and Danilchik 1988; Ewald et al. 2004). For the endogenous role of *Gsc* this proposes a completely new function for *Gsc* as a repressor of convergent extension in the prechordal plate. The cells of the prechordal plate have been shown to migrate actively and thus do not undergo convergent extension (Kwan and Kirschner 2003). This is in agreement with the finding that *Gsc* has the potential to induce cell migration (Niehrs et al. 1993). In contrast to that, cells of the notochord elongate through convergent extension. These cells express

Brachyury, which has been shown to be able to induce convergent extension (Conlon and Smith 1999; Tada and Smith 2000). Thus the two modes of cell behavior are likely to be governed by *Gsc* and *Brachyury* (Fig. 22). In summary, the organizer gene *Gsc* has been assigned a very new role in embryonic development as it is seems to be responsible for the repression of convergent extension.

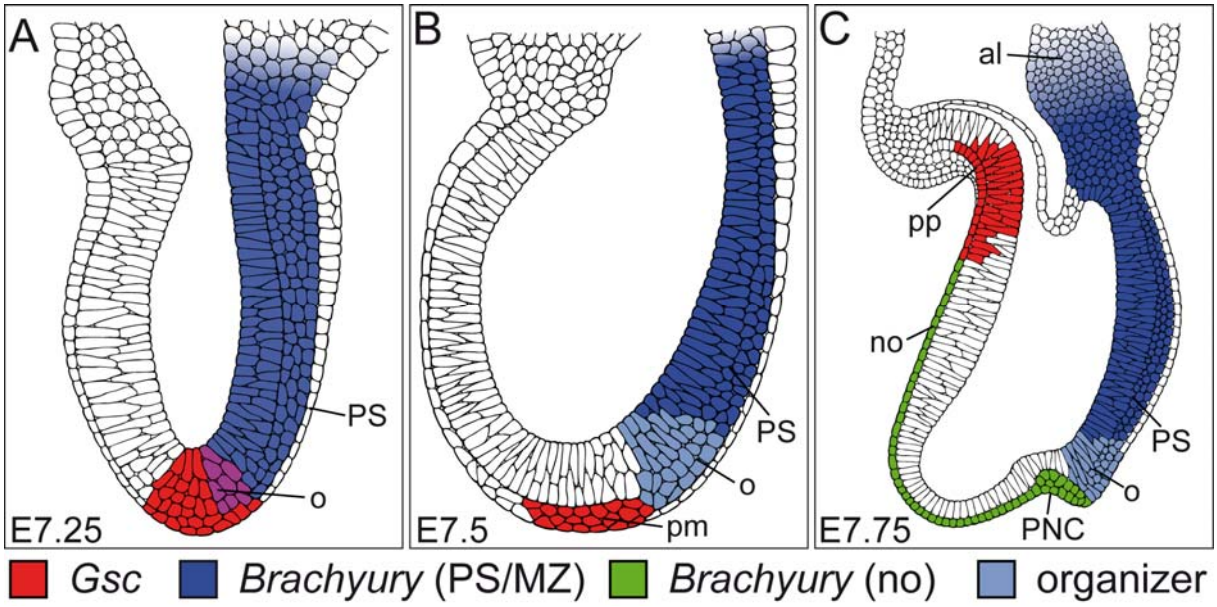

Fig. **22** Proposed role for the endogenous Gsc protein as a negative regulator of convergent extension. At mid- to late gastrula stages, *Gsc*- and *Brachyury*-expressing cells segregate into prechordal and notochordal domains. These are characterized by single cell migration and absence of CE (red, prechordal cells; *Gsc*) and by convergent extension (green, notochord; *Brachyury*), respectively. Gene expression patterns correlate with inhibition of PCP-mediated CE in migratory cells, and with activation of PCP-governed CE in notochordal cells. (**A**) Mid-gastrula at E7.25. (**B**) Early bud stage at E7.5. (**C**) Late gastrula (headfold stage) at E7.75. al, allantois; no, notochord; o, organizer; pm, prechordal mesoderm; PNC, posterior notochord; pp, prechordal plate; PS, primitive streak. Schematic drawings were produced by Bernd Schmidt.

The PNC as left-right coordinator

The function of the PNC

Many mutant and KO mice have shown that the PNC is necessary for correct laterality development (Nonaka et al. 1998; Okada et al. 1999; Takeda et al. 1999; Beckers et al. 2007). As the GRP in frog embryos possesses very similar properties, it probably represents the homologous structure to the PNC. Furthermore it has also been shown to be essential for the establishment of the left-right axis in *Xenopus* embryos. Therefore, the function of the PNC and its homologous structures can be regarded as a left-right coordinator (Blum et al. 2009). For this purpose the cilia within the PNC need to rotate. In the following the effect of monoamines on the ciliary beat frequency are discussed.

Ciliary beat frequency (CBF) within the PNC

As soon as cilia emerge within the PNC, they begin to rotate. Thereby the ciliary beat frequency (CBF) increased from initially about 9 Hz in pre leftward fluid-flow stages up to above 10 Hz in flow stages (Fig. 9). This could indicate that a frequency above 10 Hz is necessary to produce a robust flow. Besides the increasing CBF, the beat pattern of the cilia becomes more uniformly with ongoing development. Nascent cilia sometimes change the direction of rotation although most of the time it is clockwise (Nonaka et al. 1998; Okada et al. 2005; Hilfinger et al. 2009). Furthermore, the length and the number of cilia are also increasing (Lee and Anderson 2008). And finally, the posterior location on the cell and thus the posterior tilt is established during pre-flow stages (Nonaka et al. 2005). Therefore, all of the mentioned factors should be regarded as a prerequisite for a robust flow.

Adrenaline reduced the CBF

For quite a long time, the experiments of Baden and colleagues remained without an explanation why the laterality of rat embryos was disturbed upon exposition to adrenaline and therefore threatened to fall into oblivion (Fujinaga and Baden 1991; Fujinaga et al. 1992). The finding that adrenaline reduced the CBF and thus led to an attenuation of the leftward fluid-flow is a good explanation for which process has been affected in Baden's experiments (Fig. 9, 10). As it was shown that absence of flow leads to laterality defects, it is very likely that this happened in the rat embryos as well. For the present study, the concentration of the adrenaline used is 1.8 mM. This is about 35 fold more than mentioned in the publications, which was denoted to be 50µM (Fujinaga et al. 1992; Fujinaga et al. 1994). In contrast to that, in the first publication of this series a range of concentrations was tested for its potency to change the laterality and a dose-dependent effect could be shown (Fujinaga and Baden 1991). The dose at which more than 50% of the embryos developed laterality defects was stated to be between 0.6 and 3 mM. This resembles approximately the dose used in this study and the observed effect of the adrenaline appeared to be dose-dependent as well. Another explanation why a lower dose could be used in the original experiments might be the time the embryos were exposed to the adrenergic agonist. In these experiments, the agonist was applied before the formation of a PNC and thus present during the complete phase of laterality determination. Therefore, the effect of the agonist could be stronger than in the experiments presented in this work, which lasted only for some minutes.

No effect of serotonin signaling on the leftward fluid-flow

As the monoamine adrenaline had a negative effect on CBF, a second monoamine, namely serotonin, was analyzed for a possible role in the regulation of CBF (Fig. 9). This neurotransmitter has been identified as a key player for the determination of laterality in *Xenopus* embryos (Fukumoto et al. 2005; Levin 2006). Therefore, serotonin signaling might also be important for mammalian left-right development. The application of serotonin and two of its antagonists resulted only in minor changes of CBF. Furthermore, the blocking of the serotonin signaling was not sufficient to

impair the leftward fluid-flow. Therefore, it is not very likely that serotonin is needed for the regulation of CBF within the PNC.

In *Xenopus* recent data indicated that serotonin signaling is necessary for the morphogenesis of the GRP (A. Schweickert, unpublished data). Thus in mammals serotonin could also be necessary for the formation of the homologous structure, the PNC and therefore implicated in left-right development. In order to test this hypothesis, the development of mouse embryos should be investigated *in vitro*, in the absence of serotonin. This goal could be very difficult to achieve because for the cultivation of mouse embryos for a longer period the presence of serum (usually rat serum) is necessary (Tam 1998). As serotonin is a component of mammalian serum, a serotonin-free serum would be needed for the cultivation, which has not been described in the literature so far. Thus one possibility to overcome these difficulties would be the cultivation of embryos in the presence of drug cocktail which antagonizes all serotonin receptors. Blocking of the signaling could also be achieved by applying the serotonin antagonist to pregnant mice. The negative aspect of this approach is that it would require a large series of testing of different doses and inhibitors. On the other hand the result of such testing would also be very interesting for the human application of these antagonists, as an effect on laterality in developing embryos could lead to abortion or the substances might even have a teratocarcinogenic capacity.

Another approach to this problem could be achieved by loss-of-function of the serotonin receptors in transgenic mice. So far most of the serotonin receptors have been knocked out (Saudou et al. 1994; Tecott et al. 1995; Heisler et al. 1998; Grailhe et al. 1999; Nebigil et al. 2000; Zeitz et al. 2002; Compan et al. 2004; Bonasera et al. 2006; Weisstaub et al. 2006; Witkin et al. 2007). Of these only the absence of *Htr2b* led to embryonic lethality by malformation of the heart and laterality defects have not been published at all in this context (Nebigil et al. 2000). No data is available on the knockout of *Htr1e*, *Htr1f*, *Htr3b* and *Htr5b*, although the transgenic animals have already been generated (Mouse Genome Informatics). Therefore the published data suggests that the function of serotonin in left-right development is not conserved from frogs to mice. Nevertheless, this does not necessarily prove that serotonin is not involved in mammalian left-right development, as the many closely related receptors could compensate for the loss of a single receptor type. In order to rule out this

possibility the generation of double or even triple knockouts would be necessary. As this is very work-intensive, it would be advisable to narrow down the possible candidates first in inhibitor studies before using transgenic animals.

Expression of serotonin receptors

The analysis of the expression of the serotonin receptors provided only very little insight into the function of serotonin during left-right development (Fig. 11, 12). The only receptors that have been shown to be expressed at the late gastrula stage in literature are the receptors *Htr2a* and *Htr2b* (Choi et al. 1997). The expression of *Htr2a* was confirmed in this work. Furthermore, it could be shown that it was also transcribed at low level within the PNC. Therefore blockers of this receptor could also be investigated for their potency to alter CBF. In contrast to the published data no expression of *Htr2b* was detected (Choi et al. 1997). The presence of the receptors *Htr3a*, *Htr5b* and *Htr6* during flow stages indicated that serotonin signaling had not only occurred through *Htr2a* at this stage. The receptors *Htr3a* and *3b* were found to be expressed in one PNC cDNA but this result could not be reproduced with another cDNA derived from the same RNA. This could be due to problems during cDNA synthesis and therefore it remained possible that these receptors were expressed in the PNC. The evidence gained by ISH is reliable but is limited by the detection level. This means that genes expressed at a very low level cannot be visualized using this method unless probes labeled with radioactivity are utilized. Therefore only for the receptor *Htr3a* positive signals could be detected. It was expressed in the head and hence it could be important for the correct development of the brain although the knockout of this gene does not result in obvious developmental defects of the brain (Bhattacharya et al. 2004). Thus the precise regions where the receptors *Htr2a*, *Htr5b* and *Htr6* were expressed at late gastrula stage remained elusive.

In case that serotonin in the mouse is needed for correct formation of the PNC, the receptors should be present at E7.5. This was applicable for the receptors *Htr2a*, *Htr3a*, *Htr5b* and *Htr6*. Therefore, these receptors could be antagonized *in vitro* in order to investigate a role of serotonin signaling on the formation of the PNC.

Serotonin synthesis and degradation during laterality determination of the mouse

In contrast to the published data that *Tph1*, the enzyme responsible for serotonin synthesis, is only expressed from E14.5 on, transcription could be detected from E7.5 on and thus much earlier (Fig. 11, 12). Unfortunately, although *Tph1* was expressed in flow-stage mouse embryos, it could not be detected in or close to the PNC. In post flow stages *Tph1* was found to be transcribed in the foregut and the notochord. As the notochord is in close relation to the PNC, the possibility remains that the expression of *Tph1* was below detection limits in the PNC and therefore could not be found. Since this is rather unlikely, serotonin is probably not synthesized by the embryo but by the mother as it has been shown that maternal serotonin is crucial for embryonic development (Cote et al. 2007). The second expression domain of *Tph1*, which was observed in the forming somites, indicates that serotonin is also important for the somitogenesis. A connection between somitogenesis and serotonin has already been shown as the blocking of the *Htr1b* receptor using SB-236057 in cultured rat embryos led to defective somites (Augustine-Rauch et al. 2004). Furthermore, the presence of the serotonin receptors *Htr2a* and *Htr2b* in the somites of E9.0 embryos has also been reported (Lauder et al. 2000).
Maoa, one of the enzymes responsible for the degradation of serotonin, could be detected in all investigated stages and tissues. ISH showed a ubiquitous expression of *Maoa* during flow-stages. As no downregulation could be observed within the PNC, the idea of regulation of the serotonin level by degradation seems not to be likely. The expression of *Maob* indicated that there is a function of serotonin in the neural tube. Interestingly, the expression of *Maob* occurred close to where *Tph1* transcription was detected. As this occurred in the region where the neural tube is about to close, serotonin signaling might be implicated with this important step in vertebrate development (Copp et al. 2003).

Lowered maternal serotonin level had no effect on laterality determination

The analysis of the expression of the serotonin signaling pathway indicated that it is rather synthesized by the mother than by the embryo. As the serotonin level was reported to be lowered in *Sert* deficient mice this could have an effect on the laterality

development of the offspring (Bengel et al. 1998). Unfortunately, no defects regarding this could be detected. Therefore, it seems that the lowered serotonin level of about 20-40% of the wt level is still sufficient for the needs of the correct laterality determination or serotonin is not necessary regarding this process (Bengel et al. 1998). In order to find out whether serotonin is relevant for left-right development the *Tph1* KO mice could be analyzed for laterality defects. These animals exhibit an even stronger reduction of the serotonin level which ranges from 3-15% of the wt level (Cote et al. 2007). As the description of the malformed offspring of *Tph1* deficient mice is not very detailed, the presence of defects of this type could have been missed. Furthermore, the analysis of the CBF within the PNC of *Tph1-/-* embryos could also be educational.

A dual role for *Brachyury* in left-right development

Absence of leftward fluid-flow in *T/T* mutants

As reported earlier, the PNC of *T/T* mutant embryos is defective ((Fujimoto and Yanagisawa 1983)). The PNCs of these embryos lack the typical indentation and the specialized cells bordering the PNC could not be identified (Fig. 13). Therefore, it seems that fewer cells adopt the fate of PNC cells or are defective when *T* is absent and hence the usually dense cluster of cells within the PNC could not be detected. This is in agreement with findings from *T*-deficient embryos, stating that the mutant embryo has the ability to form the precursors of the notochord, but these cells fail to proliferate or differentiate (Conlon et al. 1995). For normal formation of the PNC, this could mean that a specific amount of cells is necessary to build the indentation. Furthermore, a slight apical constriction of the PNC cells, resulting in a rhomboid shape, seems to be a prerequisite for the indentation. The detailed analysis showed that there are cells that resemble the morphology of wt cells. Surprisingly, some of these also possess cilia which, in rare cases, were also motile (Fig. 14). Thus cilia can be assembled in the absence of *T*, but only very few are functional as shown by the analysis of the ciliary motion. Many of the cilia were almost or even completely immotile. This finding indicated that most of the cilia lack essential components like

the motor proteins or that the microtubules are not arranged properly. This could be investigated by analyzing the expression of the *Forkhead transcription factor Foxj1* which is believed to be master regulator for the formation of motile cilia in mouse, frog and zebrafish and thus might also be affected in *T/T* mutant embryos (Blatt et al. 1999; Brody et al. 2000; Stubbs et al. 2008; Yu et al. 2008).

The phenotype of the PNC resembled the defects observed in *Noto* deficient embryos. This finding confirms the idea that *Noto* is a downstream target of *T*. Therefore, *Noto* is responsible for the correct formation of the PNC while *T* is necessary for the correct formation of the mesoderm and for the induction of *Noto* expression. As only very few cilia were able to rotate at the right frequency, the motility did not suffice to generate a leftward fluid-flow. In the absence of the leftward flow laterality determination is disturbed. Therefore, the malformed PNC in *T/T* mutant embryos is one of the causes of the left-right defects in these specimens. In conclusion this means that one of the purposes of *T* in left-right development is the induction of *Noto* expression and thus the correct formation of the PNC.

Absence of asymmetric gene expression in *T/T* mutant embryos

Nodal expression close to the PNC and in the left LPM was reported to be absent in *T/T* mutants. Therefore the downstream targets of *Nodal* are supposed to be absent as well. As expected *Pitx2* was only expressed in the head of E8.5 in these embryos (Fig. 15). Due to this absence of asymmetric expression, the heart is unable to loop asymmetrically and remains as a linear tube. In *galanin*, a putative downstream target of *Nodal* was investigated in this work (Schweickert et al. 2008). The idea that *galanin* is a target of *Nodal* signaling derived from the analysis of the knockout of the *Nodal* co-receptor *Cryptic*. These animals are unable to express *Nodal* in the LPM although transcription occurs in the midline, thus the left-sided *Nodal* cascade is not activated, which means that *Pitx2* is not expressed asymmetrically (Gaio et al. 1999; Yan et al. 1999). Therefore, the *Cryptic*-deficient embryos develop left-right defects. Nevertheless *galanin* is expressed in wt-manner in these specimens arguing that the asymmetric activation of *galanin* expression is *Pitx2* independent. Hence, it could be dependant on an asymmetric signal generated in the PNC. According to the morphogen hypothesis this asymmetric signal is produced by *Nodal* itself (Hamada et

al. 2002; Oki et al. 2007). As the *Nodal* signal can only be transduced in the presence of a co-receptor, the second *Nodal* co-receptor, *Cripto*, was presumed to be involved in the regulation of *galanin* (Schweickert et al. 2008). Surprisingly, instead of being absent, *galanin* was expressed bilaterally in *T*-deficient embryos. This result indicates that the induction of *galanin* in the heart can also be achieved without asymmetric *Nodal* expression. As the expression of *galanin* in *T/T* mutants was observed to be bilaterally and thus differed from wt, it clearly lacked asymmetric signals. These could also be achieved by right sided repression, which is not present in *T*-deficient embryos. This would imply that *galanin* is not downstream of *Nodal* but in order to be expressed correctly, the PNC needs to give rise to asymmetric signals. In order to find out more about the induction of *galanin* expression in the heart, transgenic mice could be analyzed. One candidate therefore would be the mouse homozygous for a hypomorphic *Nodal* allele, which lacks expression of *Nodal* close to the PNC (Saijoh et al. 2003). In contrast to the expression in the heart, *galanin* could not be detected in the vicinity of the PNC in *T*/*T* mutant embryos. This observation is in agreement with the finding that the PNC did not form properly and therefore expression of *galanin* cannot be induced. It could also indicate that *galanin* expression around the PNC is dependent on *Nodal* transcription or that the cells, which normally express *Galanin* and *Nodal* close to the PNC, are lacking in *T/T* mutant embryos.

The relation between *T* and *Nodal*

The analysis of *Fgf8* expression in the *T/T* mutants revealed that it was downregulated in the anterior aspect of the PS (Fig. 16). This is the region which is important for the formation of the PNC and furthermore, the midline expression of *Nodal* occurs close to it. Therefore, *T* seemed to be necessary for correct expression of *Fgf8*. This is in good correlation with a finding in zebrafish, stating that there is a positive feedback-loop between the *Brachyury* homolog *Ntl* and *Fgf8* (Griffin and Kimelman 2003). The observation suggested that *T/T* mutant embryos lack expression of *Nodal* because of a downregulation of *Fgf8*. This would be suitable to the finding that compound heterozygous mice carrying only a hypomorphic *Fgf8* allele also lack expression of *Nodal* close to the PNC and in the left LPM (Meyers and Martin 1999).

The results gained from the analysis of *T/T* mutant embryos indicated that *T* possesses a dual role in left-right development of the mouse. On the one hand it is necessary for the induction of *Noto* and thereby the correct formation of the PNC. On the other hand *T* is needed to enable bilateral *Nodal* expression at the PNC. This is likely to be achieved through a feedback loop involving *Fgf8* signaling (Fig. 23). In order to further substantiate this idea, frog experiments could be used to clarify whether an overexpression of *Fgf8* is sufficient to compensate for the loss of *Brachyury*. Furthermore, the frog system could also be used to find out whether the lateral plate mesoderm (LPM) has the potency to activate the *Nodal* cascade in the absence of *Brachyury*. As all mesodermal cells express *Brachyury* when being differentiated it is very likely that the cells of the LPM are affected as well. In contrast to the mouse, this could be achieved relatively easily in the frog with a knockdown of *Xbra* in the left LPM and simultaneous injection of *Nodal* mRNA. Beyond that, this experiment could also reveal a possible third role of *Brachyury* in left-right development. In another mouse mutant lacking a functional notochord it was shown that this impairment results in absence of the midline barrier (Tsukui et al. 1999). Since the notochord is defective in *T/T* mutant embryos, it is very likely that the midline barrier is not established or maintained correctly in these specimens. Thus, the activation of the *Nodal* cascade in the left LPM in the absence of *Brachyury* could result in an additional activation of this cascade in the right LPM.

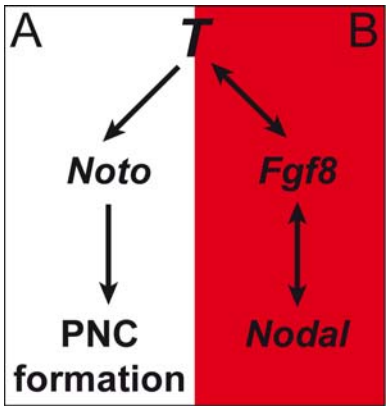

Fig. **23** Proposed two roles of *T* in left-right development. (**A**) *T* is necessary for the induction of *Noto* and thus for the formation of a functional PNC. (**B**) *T* is also needed in order to enable the expression of *Nodal* adjacent to the PNC. This could be mediated in a feedback-loop with *Fgf8*, which has been shown to be a prerequisite for *Nodal* expression at the PNC.

Knockdown of *Xbra* in the midline induced laterality defects

By knockdown of *Xbra* in the midline of *Xenopus* embryos left-right defects were induced. The vast majority of these specimens did not express *Pitx2c* in the LPM

(Fig. 17, 18) Thus the phenotype of frog embryos resembled the one of *T/T* mutant mouse embryos. Therefore, like in the mouse *Xbra* is not only necessary for correct laterality development but also *Pitx2c* is not expressed asymmetrically in the absence of *Xbra*.

At high doses, the embryos developed a shape which indicated that posterior mesoderm did not form or was defective (Fig. 17I). This observation was also described for the *T/T* mutant mouse embryos and thus showed again the conserved function of *T*. The investigated morphants completely lacked expression of *Pitx2c* in the left LPM. This effect was accompanied by a malformation of the anterior-posterior axis. Such specimens were not taken into account, as these two defects often coincide because laterality defects can also result from a defective anterior-posterior axis.

In some of the morphants, which showed transcription of *Pitx2c* in wt manner, a reduction of this expression in comparison to control embryos was mentioned. This reduction could indicate that a threshold of *Nodal* signal exists which is necessary for correct induction of *Pitx2c*. It would be very interesting to find out whether these specimens develop left-right defects or not.

Attenuated expression of bilateral *Nodal* after knockdown of *Xbra*

The analysis of *Nodal* expression revealed that *Xbra* is necessary for the induction of the bilateral midline transcription of *Nodal* (Fig. 19). Again this result was very similar to the described findings in *T* deficient mouse embryos. The unilateral knockdown of the *Xbra* allowed a very easy way to compare this effect as the side which was not targeted served as internal control. In most cases, the expression of *Nodal* was not completely lost but clearly attenuated upon knockdown of *Xbra*. The effect is probably partial because a knockdown of a gene, in contrast to a knockout, cannot be accomplished completely and thus remnants of the endogenous *Xbra* were likely to be translated. Furthermore, the cells might have not been reached by the same amount of morpholino or even not at all. The remnants could also be responsible for the observed weak induction of *Pitx2c* in some of the morphants. These results would argue against a theory based on findings in the mouse that a weak difference in the expression of the bilateral *Nodal* is the result of the left sided flow. According to the theory, the left sided domain becomes larger than the right one and this

difference is sufficient to induce expression of *Nodal* only in the left LPM. If this was true the knockdown of *Xbra* in the left domain together with the attenuation of the left sided *Nodal* transcription should have resulted in inversed expression of *Pitx2c* and not in absence.

Xbra is necessary for the formation of the GRP

The malformation of the GRP upon knockdown of *Xbra* showed that the T-box gene is needed in order to build this epithelium (Fig. 20). Due to this malformation, the flow is also absent and therefore, even if *Nodal* was not impaired, laterality defects would be caused (Fig. 21). Again these two findings showed that the malformations caused by the knockdown of *Xbra* resembled the phenotype of *T/T* mutant mouse embryos. Especially when the effects on the GRP are compared to the defective PNC of *T* deficient mouse embryos, the similarity is very obvious as in both cases typical cells were missing and cilia appeared shorter and less in number. Whether the cilia in frog were still motile to some extent remains elusive.
Furthermore, the results of Vick and colleagues could be confirmed to the extend that a left-sided knockdown of genes necessary for the correct formation or function of the GRP or the midline expression of *Nodal* was sufficient for the induction of left-right defects (Vick et al. 2009).

Conserved left-right development of amphibians and mammals

The comparison of the *Brachyury* loss of function phenotypes between mouse and frog indicated that the prerequisites for correct left-right development are very similar in both species. This implicated *Brachyury* into two distinct functions in laterality development as it is responsible for proper formation of the epithelium necessary for the leftward flow and furthermore needed for the induction of the midline expression of *Nodal* (Fig. 23). In addition to that, these findings provided further evidence that the GRP is the frog homolog of the PNC as *Brachyury* is necessary for the formation of these epithelia (Blum et al. 2007). This conservation comprises even zebrafish, as in the *notail* mutant the fish homolog of *T* the formation of Kupffer's vesicle, the homolog of the PNC, is impaired (Amack and Yost 2004). The similarities between

the different classes of vertebrates suggest that the mechanism for the formation of the epithelium responsible for the flow is universal. This implies that the leftward fluid-flow is also a universal mechanism for left-right development within vertebrates.

Material and Methods

Embryological procedures

Mouse

All mouse embryos used in this work were derived from timed matings of C57Bl/6j, *mT-Gsc* x *Deleter* or *T* x *T*. All steps involving isolation and culture of embryos were conducted under sterile conditions using sterile buffers, media, lab-ware and instruments. Fixation in a solution of 4% paraformaldehyde in PBS^- (4% PFA) was conducted for 1h at room temperature (RT) or overnight at 4°C.

Dissection and storage of embryos

Animals were sacrificed by cervical dislocation. After the abdominal cavity of the dead animal had been opened, the uterus was removed as a whole and transferred to PBS^+.

Dissection and fixation of mouse embryos

Uteri were transferred to fresh PBS+ where the uterus was separated into individual deciduas and subsequently removed under a stereomicroscope using watchmaker's forceps. The deciduas were transferred to another culture dish with fresh PBS^+ carefully dissected in half and the embryos were isolated. Staging of the embryos was performed according to Downs and Davies (Downs and Davies 1993). For the analysis of ciliary beat frequency (CBF) or left-ward fluid flow embryos were transferred to a culture dish containing F10 culture medium above a thin layer of agarose. Alternatively embryos were either fixed in 4% PFA or processed further for electron microscopy.

Dehydration and storage

If desired, all embryos fixed in PFA could be stored until further utilization. After fixation had been completed, they were washed three times for 5min in PBS^- and

then dehydrated in an ascending methanol series (25, 50, 75% methanol in PBS^-, 100% methanol). Embryos were stored in 100% methanol at -20°C.

Analysis of CBF and left-ward fluid flow

After isolation embryos were maintained in F10 culture medium in agarose coated culture dishes at room temperature. For the analysis objective slides were prepared with a circle of vaseline. The circle was filled with F10 medium together with 500nm fluorescent beads at a dilution of 1/125 (flow analysis) or a drug (CBF analysis). Embryos were then dissected in a way that a flat circle of tissue containing the PNC remained. This tissue was subsequently transferred into the medium within the circle of vaseline and covered by a cover slip. The slide was then investigated under a microscope. For CBF the embryos were filmed with more than 100fps and the movies were analyzed manually.

Xenopus

Extraction of *Xenopus* embryos

In order to obtain embryos *Xenopus* females were stimulated for ovulation. This was achieved by injection of a hormone. Therefore the females were injected subcutaneous with 50µl of human chorionic gonadotropin one week prior to oviposition. On the evening before the desired oviposition the females were injected again subcutaneous with 400-600µl (depending on the size of the animal) of human chorionic gonadotropin. On the following day the spawning was supported by manual massage of the frog.

In vitro fertilization

The spawn was in vitro fertilized by sperm extracted from *Xenopus* testes. The testes were isolated from adult males and kept in 1xMBSH at 4°C for up to two weeks. For the fertilization about $1mm^3$ of the testis was placed in 1ml 1xMBSH, cut into small pieces and subsequently added to the eggs. After the addition of DDW the fertilization began and about 40min later the eggs were incubated for 7min in 2% cystein (pH 7.99) in order to be dejellied. The cystein solution was then removed by several washing steps in 0.1xMBSH followed by washing it twice with 1xMBSH. Afterwards the fertilized eggs were used for injection of RNA or morpholinos.

Injection experiments

For the injection the embryos were transferred to 2% Ficoll solution in a Petri dish coated with agarose. The mRNA or the morpholino was diluted to the desired concentration in Gurdon's-buffer and injected into 4cell stage embryos with a thin glass-needle (5-10µm diameter). The embryos were then cultivated in the Ficoll solution for about 1h and subsequently transferred to 0.1xMBSH for further cultivation. Rhodamine dextrane was utilized as a lineage tracer (1/30 dilution) and embryos were checked for correct tissue targeting by assessing the fluorescence of the lineage tracer.

Fixation of embryos

Embryos were cultivated to the stage of interest and then transferred into 4ml of freshly prepared 1xMEMFA for fixation. After incubation for 2h at room temperature or overnight at 4°C embryos were washed with ethanol. 30min later the embryos were washed again in ethanol and stored at -20°C

Knockdown of *Xbra* using a specific morpholino

Morpholinos are synthetic molecules used to bind complementary mRNA. As thus the correct translation is blocked a transient knockdown is caused. The *Xbra*-morpholino (XbraMO) was designed to bind to the start codon of *Xbra* and the exact sequence was: 5'-GTAATGAGTGCGACCGAGAGCTGCG -3'.

Flow analysis in frog and mouse embryos

Frog embryos were raised to stage 16–18 in 0.1xMBSH, dorsal explants were prepared, placed in a closed chamber and the extracellular flow at the GRP was recorded following addition of fluorescent latex beads (500nm FluoSphere®, Molecular Probes) in dilution of 1:2500 in 1xMBSH as described (Schweickert et al., 2007). Mouse embryos were isolated at E8.0 and the distal tip was cut off. A closed chamber was used and the explant was mounted with the ventral side facing up (Fig. 6). Flow at the PNC was recorded following addition of fluorescent latex beads (500nm FluoSphere®, Molecular Probes) in dilution of 1:125 in F10 culture medium (Gibco). Movies were acquired on a Zeiss AxioMot2 mounted with the CCD via AxioCam Hsc (Zeiss) and Axiovision 4.6 under the green fluorescent channel at 2 fps for frog and 10fps for mouse embryos, respectively.

For the analysis, particles were tracked by the ImageJ plugin ParticleTracker (Abramoff et al. 2004; Sbalzarini and Koumoutsakos 2005) and qualitative and quantitative measurements were calculated with a custom-made program (Thomas Weber, University of Hohenheim) written in statistical-R (R Development Core Team, 2008).

Flow was analyzed as follows: trajectories with less than 10 frames duration were excluded because necessary information was not gained on short tracks. Masks covering the GRP/PNC or GRP/PNC halves were introduced to calculate the flow parameters of trajectories above the GRP/PNC exclusively. To exclude particles not driven by flow (Brownian motion), a Rayleigh's test of uniformity was performed on each trajectory to tell particles with directed movement from random particle motion. Particles were considered ‘directed’ when they reached a mean-resultant-length (rho) of >0.6. To determine the general direction of flow, a second Rayleigh's test of uniformity was performed comprising the mean angles of ‘directed’ particles above the GRP/PNC.

To visualize particle movement, gradient-time-trails (GTT) for each trajectory meeting the above criteria were produced. GTTs represent a span of particle coordinates that is colored time-dependently according to the color-gradient green (start of time span), yellow (mid of time span), red (end of time span). The exact time span is visualized by the color gradient for each analysis respectively (cf. figure legends).

Visualization of ciliary motion

To visualize motion, the grey-levels of corresponding pixels of subsequent frames were subtracted using a custom made extension to ImageJ (Thomas Weber University of Hohenheim). This results in a blackened pixel, if there was no difference in between the brightness of the two corresponding pixels. Moving objects cause pixel based alterations of grey levels. A subtraction thus leads to a differential grey-level.

Collapsing of such processed frames leads to a greyscale image resembling the motion in such a movie. A rotating cilium therefore results in a spoke wheel-like structure.

Polymerase Chain Reaction (PCR)

Isolation of RNA from embryos

E7.5 – E14.5 stage embryos were dissected and subsequently transferred into Peqlab peqGold Trifast solution. Total RNA was extracted following the peqGold Trifast protocol for a guanidinium thiocyanate-phenol-chloroform extraction. 1ml of the solution was used for the isolation of RNA of 10 x E 7.5, 5 x E8.5 or the head of one E14.5 embryos. RNA was eluted in 25µl sterile DDW, measured photometrically and stored at -80°C.

First strand synthesis of cDNA

cDNA was synthesized from total RNA preparations by reverse transcription using MMLV Reverse Transcriptase. A standard protocol started with 1µg of total RNA to which 0.5µl of random hexamers was added and filled up with sterile water to a total volume of 14µl. In case the RNA concentration did not suffice to reach 1 µg, 13.5 µl were used. The solution was heated to 70°C for 5min to melt secondary structures within the template. Immediate cooling on ice thereafter prevented these structures from reforming. The reagents were then supplemented with 5µl 5x M-MLV Reaction Buffer, 1.25µl 10mM dNTPs, 1µl (200units) of M-MLV RT and filled up to a volume of 25µl. After an initial incubation for 10min at room temperature, the reaction was put to 50°C for another 50min to complete first strand synthesis. The reaction was stopped by a final step at 60°C. The cDNA was stored at -20°C.

Standard PCR protocol

For a 25µl PCR reaction 1µl of previously prepared template cDNA was mixed with 2mM dNTPs, 1U of Taq DNA polymerase, 5µl 5x Buffer, 1µl of each forward and reverse primer at a concentration of 10µM and filled up to 25µl with sterile double distilled water (DDW). A standard PCR cycling program started with (1) 1’ at 95°C, followed by (2) 30’’ at 95°C, (3) 30’’ or 1’ at the annealing temperature indicated below and (4) 1’ at 72°C. Steps (2) to (4) were repeated for 35 times before the reaction was (5) stopped and kept in the cycler at 8°C. Step (1) and (2) yield a denaturation of the double-stranded template DNA, step (3) allows hybridization of the primers to the single-stranded DNA and during step (4) the Taq polymerase elongates the sequences at the primer’s 3’ end. For the detection of gene expression

using Reverse Transcriptase-PCR (RT-PCR) the steps (2) to (4) were repeated 37 times.

If the PCR product was intended to be further amplified in bacteria, an extra 15min at 72°C were added after the 40 cycles to make use of the Taq Polymerase's Terminal Transferase activity, that adds an extra deoxyadenosine onto each 3' end of already existing double-stranded PCR product. This creates a single 3'-A overhang that can be utilized for ligation into a cloning vector. The RT-PCR differed from the protocol in that a 'hot start' was performed. This was achieved by using the Promega Go Taq hot start polymerase or manually by adding normal Taq polymerase only after an additional step at 95°C for 2min before the start of the normal PCR program.

Oligonucleotides and PCR conditions

For the design of primers, sequences were obtained from NCBI database. Primers were designed using the Primer3 Input program (http://frodo.wi.mit.edu/primer3/). The following primer combinations and PCR conditions were used:

Primers used for RT-PCR

Htr1d (902)

forward: for1 5' TGT TTC CGG ATC TCC CTA TG 3'

reverse: rev1 5' TGG AGG AGA CAT GCT CAG TG 3'

annealing temperature: 56°C

Htr1f (961bp)

forward: for2 5' GGG AAG CTG AGT TGA GAT GG 3'

reverse: rev2 5' TCC GAT CTG GGA CTT TTC AC 3'

annealing temperature: 56°C

Htr2a (500bp)

forward: for5 5' AAG CCT CGA ACT GGA CAA TTG ATG 3'

reverse: rev5 5' AAG ATT TCA GGA AGG CTT TGG TT 3'

annealing temperature: 56°C

Htr2b (819bp)

forward: for1 5' GGA GAA AAG GCT GCA GTA CG 3'

reverse: rev1 5' TTG CAG GAA TCA CAC AGA GC 3'

annealing temperature: 57°C

Htr2c (860 bp)

forward: for1 5' ATC GCT GGA CCG GTA TGT AG 3'

reverse: rev2 5' GAC GAA AGC AAA GTG TTC GTG 3'

annealing temperature: 57°C

Htr3a (653 bp)

forward: for1 5' CTT GCT GCC CAG TAT CTT CC 3'

reverse: rev2 5' AGC ACA GCC AGC AGG TAG ATG 3'

annealing temperature: 59°C

Htr3b (767 bp)

forward: for2 5' TGG CAC CAT TAG AAA CCA CAA G 3'

reverse: rev2 5' CCC GAG TTC GAA GAG AGT TG 3'

annealing temperature: 57°C

Htr4 (904 bp)

forward: for3 5' TGA GTT CCA ACG AGG GTT TC 3'

reverse: rev3 5' CTG CCT TGG TCT CTG TCC TC 3'

annealing temperature: 60°C

Htr5a (781 bp)

forward: for1 5' GCC ACA TTC ACT TGG AAC CTG 3'

reverse: rev2 5' AGG AAC ACA GGG GAC TGA TG 3'

annealing temperature: 57°C

Htr5b (996 bp)

forward: for1 5' CTC TTG CTT CGC CAC CTA TC 3'

reverse: rev1 5' AAA CAC GCC AAT CAA GAT CC 3'

annealing temperature: 55°C

Htr6 (751 bp)

forward: for2 5' TTC TTC CTG GTG TCG CTC TTC 3'

reverse: rev2 5' AGT ATC CCA GCC ATG TGA GG 3'

annealing temperature: 58°C

Htr7 (811 bp)

forward: for2 5' CCC TGA AAC TTG CTG AGA GG 3'

reverse: rev1 5' CTC CCT GCT CAT AAC ACA CC 3'

annealing temperature: 58°C

Maoa (876 bp)

forward: for3 5' AAA CCA TGA CGG ATC TGG AG 3'

reverse: rev4 5' CTC TCA GGT GGA AGC TCT GG 3'

annealing temperature: 57°C

Maob (875 bp)

forward: for1 5' TGA GCG GCT GAT ACA CTT TG 3'

reverse: rev2 5' GCT TCT TGG GAG TTC AGC AC 3"

annealing temperature: 57°C

Tph1 (673 bp)

forward: for1 5' CAA AGA CCA TTC CTC CGA AAG 3'

reverse: rev1 5' CCA CAG GAC GGA TGG AAA AC 3'

annealing temperature: 57°C

Primers used for the synthesis of in-situ hybridization (ISH) probes

Htr3a (996bp)

forward: for2 5' TCA CCG GAA GAA GTG AGG TC 3'

reverse: rev1 5' AGA GAC TGG GGT TGC TCA GATG 3'

annealing temperature: 59°C

Tph1 (1024bp)

forward: for1 5' CAA AGA CCA TTC CTC CGA AAG 3'

reverse: rev2 5' GAT CAA AGG GCT TGA CTT TG 3'

annealing temperature: 55°C

Maoa (977bp)

forward: for1 5' CAA GCA TTG CTC CTT GTC AG 3'

reverse: rev1 5' AAA CAC ATG GGC TGT ACT GG 3'

annealing temperature: 57°C

Maob (875bp)

forward: for1 5' TGA GCG GCT GAT ACA CTT TG 3'

reverse: rev2 5' GCT TCT TGG GAG TTC AGC AC 3'

annealing temperature: 57°C

Primers used for the expression construct *T-cod*

T-cod (1320bp)

forward: T-cod_clal_for 5' ATCGATATGAGCTCGCCGGGCACAGAGAGC 3'

reverse: T-cod_xhol_rev 5' ATCTCGAGTCATAGATGGGGGTGACACAGGT 3'

annealing temperature: 67°C

Subcloning of PCR products and bacteria culture

For the subcloning of PCR products the desired sequences were ligated into the pGEMTeasy vector and transformed into chemically competent XL1-blue cells. The vector has its multiple cloning site within the coding region of β-galactosidase, so that clones can be selected by color screening.

Ligation of PCR products into cloning vectors

PCR-products were ligated into the linearized pGEMTeasy vector with the help of T4 ligase. In a standard reaction, 5µl of ligation buffer, 1µl of vector and 1µl of T4 ligase were combined with 3µl of fresh PCR product. The reaction was incubated for 1h at RT or overnight at 4°C and then transformed into bacteria.

Transformation and clonal selection

The ligated vectors were transformed into chemically competent bacteria using the heat shock method. Different volumes (typically 100, 150, 250µl) of transformed bacteria were plated on LB-agar selective plates (100µg/ml ampicillin / 0.5mM IPTG / 80µg/ml X-Gal) and incubated overnight. The white color of the clones indicated insertion of a PCR product into the multiple cloning site. These clones were selected for further amplification and analysis using a mini-prep procedure.

Cloning of the T-cod sequence into the CS^{2+} expression vector

The Cs^{2+} expression vector was specially designed for gain-of-function experiments in *Xenopus laevis*. It contains a Cytomegalovirus-promoter followed by a polylinker and a SV40 polyadenylation site. The desired sequence was cloned into the multiple cloning site and with theT6 polymerase in vitro capped RNA was synthesized. Before cloning the vector was linearized with a restriction enzyme and subsequently extracted with phenol and chloroform. Ligation was catalyzed by a 0.5µl T4-DNA-ligase together with 2.5µl 2x ligation buffer, 2µl CS^{2+} and 2µl of the PCR product of T-cod. Ligation was incubated for 3d at 4°C.

Amplification of gene sequences

Partial sequences of genes described in databases (NCBI, MGI) were cloned and analyzed for their expression patterns in mouse embryos. The following protocols were taken from and used as described in (Feistel 2006).

Isolation and handling of nucleic acids

Preparation of small amounts of plasmid DNA (mini-prep)

Plasmid DNA from *E. coli* cultures was isolated using a modified alkaline lysis protocol. All centrifugation steps were done at 4°C. 3ml of selective LB medium (100µg/ml Ampicillin) were inoculated with a single bacteria colony from a selective plate and grown overnight with vigorous shaking at 37°C. 2ml of the culture were poured into a microcentrifuge tube and bacteria were pelleted in a microcentrifuge at

6000g for 15min. The supernatant was discarded and the pellet resuspended by heavy vortexing in 100µl P1 buffer. When the bacteria suspension appeared uniform, 200µl of P2 buffer were added and the tube was inverted several times to thoroughly mix the reagents. Alkaline lysis was allowed to proceed for 5min and was then stopped by neutralizing with 150µl of P3, again inverting the tube several times. After 20min of incubation on ice, the lysate was cleared from the fluffy white precipitate containing genomic DNA, cell debris, proteins and potassium dodecyl sulphate by centrifugation in a microcentrifuge at full speed for 10min. 400µl of the clear supernatant were transferred to a fresh microcentrifuge tube and mixed well with 1ml of 100% Ethanol to precipitate the plasmid DNA. After precipitation for 30min at -20°C the plasmid DNA was pelleted by centrifuging at full speed for 10min. The pellet was washed in 70% ethanol, centrifuged briefly, dried and resuspended in 50µl sterile DDW.

Preparation of medium amounts of plasmid DNA (midi-prep)

100ml of selective LB medium (100µg/ml ampicillin) were inoculated with 1ml of a positively tested bacteria culture and grown overnight in a 1000ml conical flask with vigorous shaking at 37°C. Bacteria were harvested by centrifugation, lysed and DNA was purified following the Promega “PureYield Plasmid Midiprep System” using the vacuum method.

Measuring the concentration of nucleic acids

The concentration of nucleic acids in aqueous solutions was determined via spectrophotometry. The ratio of absorption (A) at 260nm and 280nm wavelength indicated the purity of the solution (pure nucleic acid solution: 1.8 for DNA, 2.0 for RNA). The content of either DNA or RNA was inferred from the A_{260} value with 1 unit corresponding to 50µg/µl DNA and 40µg/µl RNA.

Restriction enzyme digests of DNA

To check for insertion of the correct PCR product after mini-prep, inserts were released from the plasmids by digestion with a restriction enzyme cutting on both sides of the multiple cloning site. EcoRI was mostly used for the pGEMTeasy vector. Typically to 10µl of plasmid-DNA 2µl 10x buffer and 0.5µl enzyme were added, the mixture was filled up with 7.5µl sterile DDW to a final volume of 20µl and incubated at 37°C for 2hrs. After digestion the whole volume of the reaction was analyzed on a

1% agarose gel. For linearization digests typically 20µg of plasmid-DNA was used in a 100µl reaction. 4µl of restriction enzyme were used and the digestion was incubated overnight at 37°C. 3µl (approximately 600ng) of the digestion were controlled on a 1% agarose gel.

Agarose gel analysis

The products of each reaction were checked on a standard 1% agarose gel supplemented with an end concentration 0,4µl/ml ethidium bromide solution.

Synthesis of capped RNA

For the synthesis of capped RNA the Ambion kit mMESSAGE mMACHINE (High yield capped RNA Transcription kit) was used. For the reaction 4µl nuclease free H_2O, 10µl 2xNTP/CAP (ATP, 10mM; CTP, 10mM; UTP, 10mM; GTP, 2mM, cap analog, 8mM), 2µl 10xbuffer, 2µl linearized CS^{2+} containing the coding sequence of mouse *T* (≈ 2 µg) and 2µl enzyme mixture (containing SP6 RNA polymerase) were mixed. After incubation for 2h at 37°C, 1µl DNase was added with a subsequent incubation of 15min. mRNA was then twice phenol-chloroform extracted and precipitated in isopropyl alcohol. Afterwards the concentration of the mRNA was determined via spectrophotometry and the quality of the mRNA was estimated using an agarose gel.

Whole mount in situ hybridization

In vitro transcription of RNA probes

For in vitro transcription of RNA probes 200ng linearized plasmid with the insert of interest was used as a template. Depending on the orientation of the insert, 20u of either Sp6 or T7 polymerase were added to a mixture of template, 4µl Transcription Buffer, 0.5µl (= 20units) RNasin, 2µl DTT and 2µl 10x Dig-Mix. Sterile DDW was added to a final volume of 20µl and the mixture was incubated at 37°C for 2hrs. After transcription, 1µl of the transcription was mixed with 8µl sterile DDW and 1µl 10x Loading Buffer and checked on a 1% agarose gel for integrity of the product. 115µl 100% EtOH and 3.75µl 4M LiCl were added to the incubated transcription mixture and RNA was precipitated at -20°C for at least 30min. The tube was then centrifuged

at full speed in a tabletop centrifuge at 4°C for 20min, the resulting pellet was rinsed in 70% EtOH and centrifuged again for 5min. The pellet was allowed to dry shortly before it was resuspended in 50µl of a 1:1 mixture of sterile DDW and formamide. The resuspended RNA was stored at -80°C until further use.

In situ hybridization

Whole mount in situ hybridization was used to detect the expression pattern of specific genes in mouse and *Xenopus* embryos.

Day 1: On the first day of the procedure, tissue was prepared for taking up the antisense RNA probe, which hybridizes to the endogenous target RNA. Embryos were rehydrated from storage in 100% methanol through a graded series of 75%, 50% and 25% methanol in PBS$^-$. Embryos were washed three times for 5min in PBS$^-$w and then the tissue was permeabilized for 5-15min in 10µg/µl Proteinase K in PBS$^-$w at RT. Digestion was stopped in 2mg/ml glycine followed by three washing steps in PBS$^-$w for 5min each. The tissue was then refixed for 15min at RT in 4% PFA supplemented with 0.2% glutaraldehyde. After washing three times in PBS$^-$w for 5min the embryos were transferred into a 1:1 mixture of hybridization solution and PBS$^-$w. After equilibration in 100% hybridization solution, a pre-hybridization period in 900µl hybridization solution at 65°C for 2-3hrs eliminated endogenous phosphatases. Depending on the concentration of the RNA, about 1µl of antisense probe (~20ng) diluted in 100µl hybridization solution was added to the vial and the embryo was incubated with the probe overnight at 70°C.

Day 2: On the second day excess antisense probe was removed in high stringency washing steps and the tissue was prepared for incubation with the anti-digoxygenin antibody. In a first step, the hybridization solution containing the antisense probe was replaced by 800µl hybridization solution without probe and embryos were washed in it for 5min at 70°C. In three steps each 400µl of 2xSSC (pH 4.5) were added and the embryo was washed twice in 2xSSC (pH 7) at 70°C afterwards. The washing steps in SSC were followed by four washing intervals in MABw, twice at RT for 10min and another two times at 70°C for 30min. Afterwards, embryos were washed three times in PBS$^-$w at RT for 10min each and were then pre-incubated in antibody-blocking buffer at 4°C for 2hrs. In a second tube, the anti-digoxygenin antibody coupled to alkaline phosphatase was diluted 1/10,000 and pre-blocked for the same time. After the 2hrs of pre-incubation, the blocking buffer was replaced with the antibody-

solution and the embryos were incubated with the antibody overnight at 4°C on a laboratory shaker.

Day 3: On the third day, unbound antibody was removed in extensive washing steps and the staining reaction was started. Embryos were rinsed and then washed five times for 45min each in PBS$^-$w containing 0.1% BSA. The washing in BSA was followed by two washing steps with PBS$^-$w for 30min each and embryos were then transferred into AP1 buffer, which adjusts the pH of the tissue for the optimal reaction of the alkaline phosphatase. AP1 buffer was changed twice and then replaced by a 1:1 mixture of AP1 buffer and BMPurple, the substrate for the alkaline phosphatase. The staining process was controlled and stopped by washing in PBS$^-$w, when the expected signal had reached a dark blue to violet color. A gradual methanol series intensified the signal and the embryos were afterwards stored in 100% methanol at -20°C.

Histological analysis of embryos after in situ hybridization

After rehydration embryos were equilibrated in a small volume of embedding medium (~1ml). 2ml of embedding medium were mixed shortly but vigorously with 140µl of glutaraldehyde and poured into a square mold formed of two glass brackets. The mixture was allowed to harden and the equilibrated embryo was transferred upon the surface of the block, excess embedding medium was carefully removed. Another 2ml of embedding medium mixed with glutaraldehyde were poured into the mold so that the embryo was now sandwiched between two layers of embedding mix. The hardened block was trimmed with a razor blade and glued onto a plate. The plate was mounted into the holder of the vibratome and 30µm thick sections were prepared. The sections were arranged onto glass slides, embedded with mowiol and protected with glass cover slips.

Scanning electron microscopy

Embryos were freshly dissected in PBS$^+$ and immersion fixed in a mixture of 2% paraformaldehyde (PFA) and 2,5% glutaraldehyde overnight at 4°C. The specimens were washed three times for 10 minutes in 0,1M phosphate buffer (PB) and were then postfixed for 1hr in 1% OsO_4 in 1M PB at 4°C. After extensive washing embryos were gradually dehydrated in an ethanol series and stored in 100% EtOH at 4°C until submitted to the drying procedure. Critical point drying was performed using CO_2 as drying agent. Embryos were sputter with gold and viewed under a Zeiss DSM 940A.

Statistical analysis

The statistical analysis was performed using the 2x2 Chi-square test (*Xenopus* experiments) and the Mann-Whitney-U test (CBF analysis) of the program Statistica (Stat-soft).

Buffers, Solutions and Media

For in situ hybridization:

Phosphate Buffered Saline 10x (PBS, 1l)

80g NaCl

2g KCl

14.4g Na_2HPO_4

2.4g KH_2PO_4

800ml DDW

adjust pH to 7.4, add DDW to 1L, autoclave.

PBSw (500ml)

500ml PBS^-

500µl Tween20.

Alkaline Phosphatase Buffer (AP1, 1l)

100ml 1M TRIS pH 9.5

20ml 5M NaCl

50ml 1M MgCl

add DDW to 1l.

Maleic Acid Buffer 5x (MAB, 1l)

58.05g (100mM) Maleic Acid

43.83g (150mM) NaCl

800ml DDW

adjust pH to 7.5 with 10N NaOH, add DDW to 1l, autoclave.

Sodium Sodium Citrate Buffer 20x (SSC, 1l)

175.3g NaCl

88.2g Sodium citrate

800ml DDW

adjust pH to 7.0, add DDW to 1l, autoclave.

Hybridization solution (1l)

10g Boehringer Block

500ml Formamide

250ml SSC 20x

Heat to 65°C for 1 hour

120ml DDW

100ml Torula RNA (10mg/ml in DDW; filtered)

2ml Heparin (50mg/ml in 1x SSC pH 7)

5ml 20% Tween-20

10ml 10% CHAPS

10ml 0.5M EDTA

Antibody Blocking Buffer

10% Heat Inactivated Goat Serum

1% Boehringer Block

0.1% Tween-20

dissolve in PBS at 70°C, vortexing frequently, then filter (0.45µm).

For frog experiments:

5xMBSH (1l)

25.7g NaCl

0.375g KCl

1g $NaHCO_3$

1g $MgSO_4/7H_2O$

0.39g $(CaNO_3)^2/4H_2O$

0.3g $CaCl_2/2H_2O$

11.9g Hepes

5 ml Penicillin/Streptomycin

10xMEMFA (500ml)

2M MOPS (pH 7.4)

200ml 100mM EGTA

10ml 1M $MgSO_4$

add DDW to 1l, autoclave.

1xMEMFA

10 % 10xMEMFA

10 % Formaldehyd 37%

80 % H_2O.

Gurdon's buffer

88mM NaCl

15mM HEPES

1mM KCl

15mM Tris-HCl, pH 7.6

Ficoll

2% Ficoll diluted in 1xMBSH

Cystein

2% Cystein diluted in DDW. Adjust pH to 7.99.

For bacteria culture:

Super Optimal Catabolite repression medium (S.O.C.)

0.5% Yeast extract

2.0% Tryptone

10mM NaCl

2.5mM KCl

10mM $MgCl_2$

10mM $MgSO_4$

20mM Glucose

autoclave

Lysogeny Broth (LB) medium

1% Tryptone

1% NaCl

0.5% Yeast extract

adjust pH to 7.0, autoclave.

LB agar

1% Tryptone

1% NaCl

0.5% Yeast extract

adjust pH to 7.0, add 15g/l agar before autoclaving.

For electron microscopy:

Sörensen phosphate buffer (PB)

Stock solution A: 0.2M NaH_2PO_4

Stock solution B: 0.2M Na_2HPO_4

for 0.1M pH 7.4: 19ml A, 81ml B, 100ml H_2O

for 0.1M pH 7.0: 39ml A, 61ml B, 100ml H_2O

For DNA preparation:

P1

50mM TRIS HCl

10mM EDTA pH 8

add RNaseA (DNase free) to a final concentration of 100µg/ml

P2

0,2M NaOH

1% SDS

P3

3M Potassium acetate, pH 5.5

For other applications:

Embedding medium for vibratome sections

2.2g Gelatine

135g Bovine Serum Albumin

90g Saccharose

dissolve in 450ml PBS.

Mowiol (Mounting medium)

96g Mowiol 488

24g Glycerol

24ml DDW

stir for 2h, then add

48ml TRIS 0.2M pH 8.5

stir for 20min at 50°C

centrifuge for 15min at 5000rpm, keep supernatant

and store at -20°C.

Tris Acetate EDTA Buffer (TAE)

40mM Tris-acetate

2mM EDTA

adjust pH to 8.0.

Sources of supply

Chemicals and lab-ware:

Acetic acid	AppliChem, Darmstadt
Agarose	Roth, Karlsruhe
Albumin faraktion V	AppliChem, Darmstadt
Ampicillin	AppliChem, Darmstadt
Anti-Digoxigenin-AP	Roche, Mannheim
BM Purple	Roche, Mannheim
Boehringer Block	Roche, Mannheim
Bovine serum albumin	AppliChem, Darmstadt
BSA	AppliChem
CAS-Block	Zymed (Invitrogen) Karlsruhe
CHAPS	Sigma, Schnelldorf
Chloroform	Merck, Darmstadt
Cystein	Roth, Karlsruhe
Desoxynucleosidtriphosphate (dNTPs)	Promega, Mannheim
Dig-Mix	Roche, Mannheim
Dimethylsulfoxid (DMSO)	Roth, Karlsruhe
Disodium hydrogen phosphate	AppliChem, Darmstadt
Dithioreitol (DTT)	Promega, Mannheim
Glass slides	Roth, Karlsruhe
Glass coverslips	Roth, Karlsruhe
DigMix	Roche, Mannheim
DTT	Promega, Mannheim
DMSO	Roth, Karlsruhe
EDTA	Roth, Karlsruhe
Ethanol	Roth, Karlsruhe
Ethidiumbromide	Roth, Karlsruhe
Epinephrinehydrochloride	Sanofi-Aventis, Frankfurt
Ethyl-p-Aminobenzoat (Benzocain)	Sigma, Schnelldorf
Ethylendiamintetraessigsäure EDTA	Roth, Karlsruhe
Ethylenguanintetraessigsäure EGTA	Roth, Karlsruhe

F10 medium	Gibco (Invitrogen) Karlsruhe
Fetal bovine serum	Sigma, Schnelldorf
Ficoll	AppliChem, Darmstadt
FluoSphere Fluorescent beads 500nm	Invitrogen, (Molecular Probes), Karlsruhe,
Formaldehyd	AppliChem, Darmstadt
Forceps (#3, #5)	Fine Science Tools, Heidelberg
Formamide	Roth, Karlsruhe
Gelatine	Roth, Karlsruhe
Glucose	AppliChem, Darmstadt
Glutaraldehyde	AppliChem, Darmstadt
Glycerol	Roth, Karlsruhe
Glycin	AppliChem, Darmstadt
Goat serum	Sigma, Schnelldorf
GR113808	Sigma, Schnelldorf
Grids	Plano, Wetzlar
HCG (human chorionic gonadotropin)	Sigma, Schnelldorf
HCl (37%)	Merck, Darmstadt
Hepes	AppliChem, Darmstadt
Heparin	Sigma, Schnelldorf
Injection-needle Sterican (0,4x20 mm)	B. Braun, Melsungen
Injection syringe F1, 1ml	B. Braun, Melsungen
Lambda-DNA	Promega, Mannheim
Lead nitrate	Serva, Heidelberg
Ligase (T4-Ligase)	Promega, Mannheim
Lithium chloride	Serva, Heidelberg
Loading Buffer	AppliChem, Darmstadt
LY-278,584	Sigma, Schnelldorf
Magnesium chloride	Roth, Karlsruhe
Magnesium sulfate	AppliChem, Darmstadt
Maleic acid	Roth, Karlsruhe
Methanol	Roth, Karlsruhe
Microcentrifuge tubes	Sarstedt, Nümbrecht
Objective slides	Roth, Karlsruhe
Oligonucleotides	Operon, Cologne
Osmium tetroxide	Plano, Wetzlar

Parafilm	Roth, Karlsruhe
Paraformaldehyde	AppliChem, Darmstadt
PBS+ (10x)	Gibco (Invitrogen) Karlsruhe
Penicillin/Streptomycin	Gibco (Invitrogen) Karlsruhe
pGEM-T-Easy-Vektor	Promega, Mannheim
Phenol/chloroform (Rotiphenol)	Roth, Karlsruhe
Plastic pipettes	Sarstedt, Nümbrecht
2-Propanol	Roth, Karlsruhe
Propylenoxide	Serva, Heidelberg
Proteinase K	Roth, Karlsruhe
Rhodamine dextran	Molecular Probes (Invitrogen), Karlsruhe
RNAse A	Roth, Karlsruhe
RNAsin	Promega, Mannheim
Saccharose	AppliChem, Darmstadt
SDZ-205,557	Sigma, Schnelldorf
Sodium acetate	Roth, Karlsruhe
Sodium chloride	Roth, Karlsruhe
Sodium citrate	Roth, Karlsruhe
Sodium dihydrogen phosphate	AppliChem, Darmstadt
Sodium hydroxide	AppliChem, Darmstadt
Sp6-RNA-Polymerase	Promega, Mannheim
Syringe filters	Whatman, Dassel
T7-RNA-Polymerase	Promega, Mannheim
Taq-DNA-Polymerase (Go-Taq)	Promega, Mannheim
Torula RNA	Sigma, Schnelldorf
TRIS base	AppliChem, Darmstadt
TRIS HCl	AppliChem, Darmstadt
Triton-X100	Serva, Heidelberg
Tryptone	AppliChem, Darmstadt
Tween-20	AppliChem, Darmstadt
X-Gal	Roth, Karlsruhe

Kits:

DNA-Purification-Kit (Easy-Pure)	Biozym, Hessisch Oldendorf

mMESSAGE mMACHINE SP6	Ambion, Darmstadt
pGEM-T Easy Vector System	Promega, Mannheim
PureYield Plasmid Midiprep System	Promega, Mannheim
peqGOLD TriFast	peqlab, Erlangen

Proteins and Antibodies:

Restriction enzymes and buffers	Promega, Mannheim
Modifying enzymes and buffers	Promega, Mannheim
Mouse anti-acetylated tubulin	Sigma, Schnelldorf
Anti-digoxigenin	AP Roche, Mannheim

Special Hardware:

Peltier Thermal Cycler PTC-200	Biozym, Hessisch Oldendorf
Vibratome	Leica, Bensheim
Stereo microscope	Zeiss, Oberkochen
Zeiss DSM 940A	Zeiss, Oberkochen
LSM 5 Pascal	Zeiss, Oberkochen
Axioplan 2	Zeiss, Oberkochen
Critical point dryer CPD 030	Balzers, Austria
Sputter coater SCD 050	Balzers, Austria

Animals:

Mice

Mice of the mouse-line C57Bl/6j were obtained from Harlan Winkelmann, Borchen and bred in the animal facility of the Institute of Zoology, University of Hohenheim since 2003.

Mice of the mouse-line Deleter were provided by K. Rajewski, University of Cologne and bred in the animal facility of the Institute of Zoology, University of Hohenheim since 2003.

Mice of the mouse-line *mT-Gsc* were generated by K. Deissler in the Institute of Toxicology and Genetics, Karlsruhe and bred in the animal facility of the Institute of Zoology, University of Hohenheim since 2003.

Mice of the mouse-line *T* were provided by B. G. Herrmann, Max-Planck-Institute, Berlin and bred in the animal facility of the Institute of Zoology, University of Hohenheim since 2005.

Mice of the mouse-line *sert* were provided by H. K. Biesalski, Department of Biological Chemistry and Nutrition, University of Hohenheim and bred in the animal facility of the Institute of Zoology, University of Hohenheim in 2007.

All mice were kept species-appropriate in the animal facility of the Institute of Zoology at a 12h light-cycle. Animals had free disposal of water and food (Ssniff R/M H, Ssniff, Soest)

Frogs

Adult African clawed frogs (*Xenopus laevis*) were obtained from Guy Pluck, Xenopus express, Ancienne Ecole de Vernassal, Le Bourg 43270, Vernassal, Haute-Loire, France. They were and kept species-appropriate at a 12h light-cycle in the animal facility of the Institute of Zoology, University of Hohenheim.

References

Abdelkhalek, H. B., Beckers, A., Schuster-Gossler, K., Pavlova, M. N., Burkhardt, H., Lickert, H., Rossant, J., Reinhardt, R., Schalkwyk, L. C., Muller, I., Herrmann, B. G., Ceolin, M., Rivera-Pomar, R. and Gossler, A. (2004). "The mouse homeobox gene Not is required for caudal notochord development and affected by the truncate mutation." Genes Dev 18(14): 1725-36.

Abramoff, M. D., Magelhaes, P. J. and Ram, S. J. (2004). "Image Processing with ImageJ." Biophotonics International 11(7): 36-42.

Afzelius, B. A. (1976). "A human syndrome caused by immotile cilia." Science 193(4250): 317-9.

Alberts, B., Johnson, A., Lewis, J., Raff, M., Roberts, K. and Walter, P. (2002). "Molecular biology of the cell." Garland Science, New York.

Amack, J. D. and Yost, H. J. (2004). "The T box transcription factor no tail in ciliated cells controls zebrafish left-right asymmetry." Curr Biol 14(8): 685-90.

Andre, P. (2004). "Analyse von Gastrulationsdefekten nach Fehlexpression von *goosecoid* im Primitivstreifen der Maus." Diploma thesis at the Universität Hohenheim.

Ang, S. L., Wierda, A., Wong, D., Stevens, K. A., Cascio, S., Rossant, J. and Zaret, K. S. (1993). "The formation and maintenance of the definitive endoderm lineage in the mouse: involvement of HNF3/forkhead proteins." Development 119(4): 1301-15.

Artinger, M., Blitz, I., Inoue, K., Tran, U. and Cho, K. W. (1997). "Interaction of goosecoid and brachyury in Xenopus mesoderm patterning." Mech Dev 65(1-2): 187-96.

Augustine-Rauch, K. A., Zhang, Q. J., Leonard, J. L., Chadderton, A., Welsh, M. J., Rami, H. K., Thompson, M., Gaster, L. and Wier, P. J. (2004). "Evidence for a molecular mechanism of teratogenicity of SB-236057, a 5-HT1B receptor inverse agonist that alters axial formation." Birth Defects Res A Clin Mol Teratol 70(10): 789-807.

Beckers, A., Alten, L., Viebahn, C., Andre, P. and Gossler, A. (2007). "The mouse homeobox gene Noto regulates node morphogenesis, notochordal ciliogenesis, and left right patterning." Proc Natl Acad Sci U S A 104(40): 15765-70.

Beddington, R. S. (1994). "Induction of a second neural axis by the mouse node." Development 120(3): 613-20.

Beddington, R. S., Jaenisch, R., Smith, J.C., McLaren, A.L., Lawson, and K.A. and Herrmann, B. G. (1992). "Three-dimensional representation of gastrulation in the mouse." Ciba Found Symp 165: 55–60.

Bengel, D., Murphy, D. L., Andrews, A. M., Wichems, C. H., Feltner, D., Heils, A., Mossner, R., Westphal, H. and Lesch, K. P. (1998). "Altered brain serotonin homeostasis and locomotor insensitivity to 3, 4-methylenedioxymethamphetamine ("Ecstasy") in serotonin transporter-deficient mice." Mol Pharmacol 53(4): 649-55.

Bhattacharya, A., Dang, H., Zhu, Q. M., Schnegelsberg, B., Rozengurt, N., Cain, G., Prantil, R., Vorp, D. A., Guy, N., Julius, D., Ford, A. P., Lester, H. A. and Cockayne, D. A. (2004). "Uropathic observations in mice expressing a constitutively active point mutation in the 5-HT3A receptor subunit." J Neurosci 24(24): 5537-48.

Blatt, E. N., Yan, X. H., Wuerffel, M. K., Hamilos, D. L. and Brody, S. L. (1999). "Forkhead transcription factor HFH-4 expression is temporally related to ciliogenesis." Am J Respir Cell Mol Biol 21(2): 168-76.

Blum, M., Andre, P., Muders, K., Schweickert, A., Fischer, A., Bitzer, E., Bogusch, S., Beyer, T., van Straaten, H. W. and Viebahn, C. (2007). "Ciliation and gene expression distinguish between node and posterior notochord in the mammalian embryo." Differentiation 75(2): 133-46.

Blum, M., Beyer, T., Weber, T., Vick, P., Andre, P., Bitzer, E. and Schweickert, A. (2009). "Xenopus, an ideal model system to study vertebrate left-right asymmetry." Dev Dyn 238(6): 1215-25.

Blum, M. and Fischer, A. (2003). "Die Links-Rechts-Asymmetrie der Wirbeltiere." Biospektrum(4): 356-359.

Blum, M., Gaunt, S. J., Cho, K. W., Steinbeisser, H., Blumberg, B., Bittner, D. and De Robertis, E. M. (1992). "Gastrulation in the mouse: the role of the homeobox gene goosecoid." Cell 69(7): 1097-106.

Blumberg, B., Wright, C. V., De Robertis, E. M. and Cho, K. W. (1991). "Organizer-specific homeobox genes in Xenopus laevis embryos." Science 253(5016): 194-6.

Bockaert, J., Claeysen, S., Compan, V. and Dumuis, A. (2004). "5-HT4 receptors." Curr Drug Targets CNS Neurol Disord 3(1): 39-51.

Bonasera, S. J., Chu, H. M., Brennan, T. J. and Tecott, L. H. (2006). "A null mutation of the serotonin 6 receptor alters acute responses to ethanol." Neuropsychopharmacology 31(8): 1801-13.

Boucher, D. M., Schaffer, M., Deissler, K., Moore, C. A., Gold, J. D., Burdsal, C. A., Meneses, J. J., Pedersen, R. A. and Blum, M. (2000). "goosecoid expression represses Brachyury in embryonic stem cells and affects craniofacial development in chimeric mice." Int J Dev Biol 44(3): 279-88.

Brennan, J., Norris, D. P. and Robertson, E. J. (2002). "Nodal activity in the node governs left-right asymmetry." Genes Dev 16(18): 2339-44.

Brody, S. L., Yan, X. H., Wuerffel, M. K., Song, S. K. and Shapiro, S. D. (2000). "Ciliogenesis and left-right axis defects in forkhead factor HFH-4-null mice." Am J Respir Cell Mol Biol 23(1): 45-51.

Broun, M., Sokol, S. and Bode, H. R. (1999). "Cngsc, a homologue of goosecoid, participates in the patterning of the head, and is expressed in the organizer region of Hydra." Development 126(23): 5245-54.

Campione, M., Steinbeisser, H., Schweickert, A., Deissler, K., van Bebber, F., Lowe, L. A., Nowotschin, S., Viebahn, C., Haffter, P., Kuehn, M. R. and Blum, M. (1999). "The homeobox gene Pitx2: mediator of asymmetric left-right signaling in vertebrate heart and gut looping." Development 126(6): 1225-34.

Casey, B. (1998). "Two rights make a wrong: human left-right malformations." Hum Mol Genet 7(10): 1565-71.

Casey, B. (2001). "Genetics of human situs abnormalities." Am J Med Genet 101(4): 356-8.

Chapman, D. L., Agulnik, I., Hancock, S., Silver, L. M. and Papaioannou, V. E. (1996). "Tbx6, a mouse T-Box gene implicated in paraxial mesoderm formation at gastrulation." Dev Biol 180(2): 534-42.

Chapman, D. L., Cooper-Morgan, A., Harrelson, Z. and Papaioannou, V. E. (2003). "Critical role for Tbx6 in mesoderm specification in the mouse embryo." Mech Dev 120(7): 837-47.

Chapman, D. L. and Papaioannou, V. E. (1998). "Three neural tubes in mouse embryos with mutations in the T-box gene Tbx6." Nature 391(6668): 695-7.

Cho, K. W., Blumberg, B., Steinbeisser, H. and De Robertis, E. M. (1991). "Molecular nature of Spemann's organizer: the role of the Xenopus homeobox gene goosecoid." Cell 67(6): 1111-20.

Choi, D. S., Ward, S. J., Messaddeq, N., Launay, J. M. and Maroteaux, L. (1997). "5-HT2B receptor-mediated serotonin morphogenetic functions in mouse cranial neural crest and myocardiac cells." Development 124(9): 1745-55.

Clements, D., Taylor, H. C., Herrmann, B. G. and Stott, D. (1996). "Distinct regulatory control of the Brachyury gene in axial and non-axial mesoderm suggests separation of mesoderm lineages early in mouse gastrulation." Mech Dev 56(1-2): 139-49.

Compan, V., Zhou, M., Grailhe, R., Gazzara, R. A., Martin, R., Gingrich, J., Dumuis, A., Brunner, D., Bockaert, J. and Hen, R. (2004). "Attenuated response to stress and novelty and hypersensitivity to seizures in 5-HT4 receptor knock-out mice." J Neurosci 24(2): 412-9.

Conlon, F. L., Lyons, K. M., Takaesu, N., Barth, K. S., Kispert, A., Herrmann, B. and Robertson, E. J. (1994). "A primary requirement for nodal in the formation and

maintenance of the primitive streak in the mouse." Development 120(7): 1919-28.

Conlon, F. L. and Smith, J. C. (1999). "Interference with brachyury function inhibits convergent extension, causes apoptosis, and reveals separate requirements in the FGF and activin signalling pathways." Dev Biol 213(1): 85-100.

Conlon, F. L., Wright, C. V. and Robertson, E. J. (1995). "Effects of the TWis mutation on notochord formation and mesodermal patterning." Mech Dev 49(3): 201-9.

Copp, A. J., Greene, N. D. and Murdoch, J. N. (2003). "The genetic basis of mammalian neurulation." Nat Rev Genet 4(10): 784-93.

Cote, F., Fligny, C., Bayard, E., Launay, J. M., Gershon, M. D., Mallet, J. and Vodjdani, G. (2007). "Maternal serotonin is crucial for murine embryonic development." Proc Natl Acad Sci U S A 104(1): 329-34.

Crossley, P. H. and Martin, G. R. (1995). "The mouse Fgf8 gene encodes a family of polypeptides and is expressed in regions that direct outgrowth and patterning in the developing embryo." Development 121(2): 439-51.

Cunliffe, V. and Smith, J. C. (1992). "Ectopic mesoderm formation in Xenopus embryos caused by widespread expression of a Brachyury homologue." Nature 358(6385): 427-30.

Davenport, J. R. and Yoder, B. K. (2005). "An incredible decade for the primary cilium: a look at a once-forgotten organelle." Am J Physiol Renal Physiol 289(6): F1159-69.

De Robertis, E. M., Blum, M., Niehrs, C. and Steinbeisser, H. (1992). "Goosecoid and the organizer." Dev Suppl: 167-71.

De Robertis, E. M., Larrain, J., Oelgeschlager, M. and Wessely, O. (2000). "The establishment of Spemann's organizer and patterning of the vertebrate embryo." Nat Rev Genet 1(3): 171-81.

Deißler, K. (2002). "Koditionale ubiquitäre Expression des Homöoboxgens *goosecoid* im Primitivstreifen der Maus." Dissertation at the Universität Karlsruhe.

Dobrovolskaïa-Zavadskaïa, N. (1927). "Sur la mortification spontanèe de la queue chez la souris nouveau-nèe et sur l'existence d'un caractëre heriditaire 'non-viable'." C. R. Soc. Biol. 97: 114-116.

Downs, K. M. and Davies, T. (1993). "Staging of gastrulating mouse embryos by morphological landmarks in the dissecting microscope." Development 118(4): 1255-66.

Echelard, Y., Epstein, D. J., St-Jacques, B., Shen, L., Mohler, J., McMahon, J. A. and McMahon, A. P. (1993). "Sonic hedgehog, a member of a family of putative signaling molecules, is implicated in the regulation of CNS polarity." Cell 75(7): 1417-30.

Essner, J. J., Vogan, K. J., Wagner, M. K., Tabin, C. J., Yost, H. J. and Brueckner, M. (2002). "Conserved function for embryonic nodal cilia." Nature 418(6893): 37-8.

Ewald, A. J., Peyrot, S. M., Tyszka, J. M., Fraser, S. E. and Wallingford, J. B. (2004). "Regional requirements for Dishevelled signaling during Xenopus gastrulation: separable effects on blastopore closure, mesendoderm internalization and archenteron formation." Development 131(24): 6195-209.

Feistel, K. (2006). "Determination of Laterality in the Rabbit Embryo: Studies on Ciliation and Asymmetric Signal Transfer." Dissertation at the Universität Hohenheim.

Feistel, K. and Blum, M. (2006). "Three types of cilia including a novel 9+4 axoneme on the notochordal plate of the rabbit embryo." Dev Dyn 235(12): 3348-58.

Fludzinski, P., Evrard, D. A., Bloomquist, W. E., Lacefield, W. B., Pfeifer, W., Jones, N. D., Deeter, J. B. and Cohen, M. L. (1987). "Indazoles as indole bioisosteres: synthesis and evaluation of the tropanyl ester and amide of indazole-3-carboxylate as antagonists at the serotonin 5HT3 receptor." J Med Chem 30(9): 1535-7.

Fujimoto, H. and Yanagisawa, K. O. (1983). "Defects in the archenteron of mouse embryos homozygous for the T-mutation." Differentiation 25(1): 44-7.

Fujinaga, M. and Baden, J. M. (1991). "Critical period of rat development when sidedness of asymmetric body structures is determined." Teratology 44(4): 453-62.

Fujinaga, M. and Baden, J. M. (1991). "Evidence for an adrenergic mechanism in the control of body asymmetry." Dev Biol 143(1): 203-5.

Fujinaga, M., Hoffman, B. B. and Baden, J. M. (1994). "Receptor subtype and intracellular signal transduction pathway associated with situs inversus induced by alpha 1 adrenergic stimulation in rat embryos." Dev Biol 162(2): 558-67.

Fujinaga, M., Maze, M., Hoffman, B. B. and Baden, J. M. (1992). "Activation of alpha-1 adrenergic receptors modulates the control of left/right sidedness in rat embryos." Dev Biol 150(2): 419-21.

Fukumoto, T., Blakely, R. and Levin, M. (2005). "Serotonin transporter function is an early step in left-right patterning in chick and frog embryos." Dev Neurosci 27(6): 349-63.

Fukumoto, T., Kema, I. P. and Levin, M. (2005). "Serotonin signaling is a very early step in patterning of the left-right axis in chick and frog embryos." Curr Biol 15(9): 794-803.

Gaio, U., Schweickert, A., Fischer, A., Garratt, A. N., Muller, T., Ozcelik, C., Lankes, W., Strehle, M., Britsch, S., Blum, M. and Birchmeier, C. (1999). "A role of the

cryptic gene in the correct establishment of the left-right axis." Curr Biol 9(22): 1339-42.

Galili, N., Baldwin, H. S., Lund, J., Reeves, R., Gong, W., Wang, Z., Roe, B. A., Emanuel, B. S., Nayak, S., Mickanin, C., Budarf, M. L. and Buck, C. A. (1997). "A region of mouse chromosome 16 is syntenic to the DiGeorge, velocardiofacial syndrome minimal critical region." Genome Res 7(1): 17-26.

Giovannini, N. and Rungger, D. (2002). "Antisense inhibition of Xbrachyury impairs mesoderm formation in Xenopus embryos." Dev Growth Differ 44(2): 147-59.

Goldberg, J. I., Koehncke, N. K., Christopher, K. J., Neumann, C. and Diefenbach, T. J. (1994). "Pharmacological characterization of a serotonin receptor involved in an early embryonic behavior of Helisoma trivolvis." J Neurobiol 25(12): 1545-57.

Grailhe, R., Waeber, C., Dulawa, S. C., Hornung, J. P., Zhuang, X., Brunner, D., Geyer, M. A. and Hen, R. (1999). "Increased exploratory activity and altered response to LSD in mice lacking the 5-HT(5A) receptor." Neuron 22(3): 581-91.

Griffin, K. J. and Kimelman, D. (2003). "Interplay between FGF, one-eyed pinhead, and T-box transcription factors during zebrafish posterior development." Dev Biol 264(2): 456-66.

Gruneberg, H. (1958). "Genetical studies on the skeleton of the mouse. XXIII. The development of brachyury and anury." J Embryol Exp Morphol 6(3): 424-43.

Hamada, H., Meno, C., Watanabe, D. and Saijoh, Y. (2002). "Establishment of vertebrate left-right asymmetry." Nat Rev Genet 3(2): 103-13.

Hamilton, D. L. and Abremski, K. (1984). "Site-specific recombination by the bacteriophage P1 lox-Cre system. Cre-mediated synapsis of two lox sites." J Mol Biol 178(2): 481-6.

Hartwell, K. A., Muir, B., Reinhardt, F., Carpenter, A. E., Sgroi, D. C. and Weinberg, R. A. (2006). "The Spemann organizer gene, Goosecoid, promotes tumor metastasis." Proc Natl Acad Sci U S A 103(50): 18969-74.

Heisler, L. K., Chu, H. M., Brennan, T. J., Danao, J. A., Bajwa, P., Parsons, L. H. and Tecott, L. H. (1998). "Elevated anxiety and antidepressant-like responses in serotonin 5-HT1A receptor mutant mice." Proc Natl Acad Sci U S A 95(25): 15049-54.

Hensen, V. (1876). "Beobachtungen über die Befruchtung und Entwicklung des Kaninchens und Meerschweinchens." Z Anat Entwicklungsgeschichte 1: 213-273; 353-423.

Herrmann, B. G. (1992). "Action of the Brachyury gene in mouse embryogenesis." Ciba Found Symp 165: 78-86; discussion 86-91.

Herrmann, B. G. and Kispert, A. (1994). "The T genes in embryogenesis." Trends Genet 10(8): 280-6.

Hilfinger, A., Chattopadhyay, A. K. and Julicher, F. (2009). "Nonlinear dynamics of cilia and flagella." Phys Rev E Stat Nonlin Soft Matter Phys 79(5 Pt 1): 051918.

Hoess, R. H. and Abremski, K. (1984). "Interaction of the bacteriophage P1 recombinase Cre with the recombining site loxP." Proc Natl Acad Sci U S A 81(4): 1026-9.

Joubin, K. and Stern, C. D. (1999). "Molecular interactions continuously define the organizer during the cell movements of gastrulation." Cell 98(5): 559-71.

Keller, R. and Danilchik, M. (1988). "Regional expression, pattern and timing of convergence and extension during gastrulation of Xenopus laevis." Development 103(1): 193-209.

Kienle, S. (2006). "Analyse der entodermalen Defekte nach Fehlexpression von *goosecoid* im Primitivstreifen der Maus." Diploma thesis at the Universität Hohenheim.

Kinder, S. J., Tsang, T. E., Wakamiya, M., Sasaki, H., Behringer, R. R., Nagy, A. and Tam, P. P. (2001). "The organizer of the mouse gastrula is composed of a dynamic population of progenitor cells for the axial mesoderm." Development 128(18): 3623-34.

King, T., Beddington, R. S. and Brown, N. A. (1998). "The role of the brachyury gene in heart development and left-right specification in the mouse." Mech Dev 79(1-2): 29-37.

Kispert, A., Ortner, H., Cooke, J. and Herrmann, B. G. (1995). "The chick Brachyury gene: developmental expression pattern and response to axial induction by localized activin." Dev Biol 168(2): 406-15.

Konig, P., Krain, B., Krasteva, G. and Kummer, W. (2009). "Serotonin increases cilia-driven particle transport via an acetylcholine-independent pathway in the mouse trachea." PLoS One 4(3): e4938.

Kuhn, R. and Torres, R. M. (2002). "Cre/loxP recombination system and gene targeting." Methods Mol Biol 180: 175-204.

Kwan, K. M. and Kirschner, M. W. (2003). "Xbra functions as a switch between cell migration and convergent extension in the Xenopus gastrula." Development 130(9): 1961-72.

Latinkic, B. V. and Smith, J. C. (1999). "Goosecoid and mix.1 repress Brachyury expression and are required for head formation in Xenopus." Development 126(8): 1769-79.

Latinkic, B. V., Umbhauer, M., Neal, K. A., Lerchner, W., Smith, J. C. and Cunliffe, V. (1997). "The Xenopus Brachyury promoter is activated by FGF and low

concentrations of activin and suppressed by high concentrations of activin and by paired-type homeodomain proteins." Genes Dev 11(23): 3265-76.

Lauder, J. M., Wilkie, M. B., Wu, C. and Singh, S. (2000). "Expression of 5-HT(2A), 5-HT(2B) and 5-HT(2C) receptors in the mouse embryo." Int J Dev Neurosci 18(7): 653-62.

Lee, J. D. and Anderson, K. V. (2008). "Morphogenesis of the node and notochord: the cellular basis for the establishment and maintenance of left-right asymmetry in the mouse." Dev Dyn 237(12): 3464-76.

Levin, M. (2004). "The embryonic origins of left-right asymmetry." Crit Rev Oral Biol Med 15(4): 197-206.

Levin, M. (2006). "Is the early left-right axis like a plant, a kidney, or a neuron? The integration of physiological signals in embryonic asymmetry." Birth Defects Res C Embryo Today 78(3): 191-223.

Levin, M., Johnson, R. L., Stern, C. D., Kuehn, M. and Tabin, C. (1995). "A molecular pathway determining left-right asymmetry in chick embryogenesis." Cell 82(5): 803-14.

Lewandoski, M. (2001). "Conditional control of gene expression in the mouse." Nat Rev Genet 2(10): 743-55.

Logan, M., Pagan-Westphal, S. M., Smith, D. M., Paganessi, L. and Tabin, C. J. (1998). "The transcription factor Pitx2 mediates situs-specific morphogenesis in response to left-right asymmetric signals." Cell 94(3): 307-17.

Lowe, L. A., Supp, D. M., Sampath, K., Yokoyama, T., Wright, C. V., Potter, S. S., Overbeek, P. and Kuehn, M. R. (1996). "Conserved left-right asymmetry of nodal expression and alterations in murine situs inversus." Nature 381(6578): 158-61.

Luu, O., Nagel, M., Wacker, S., Lemaire, P. and Winklbauer, R. (2008). "Control of gastrula cell motility by the Goosecoid/Mix.1/ Siamois network: basic patterns and paradoxical effects." Dev Dyn 237(5): 1307-20.

Maisonneuve, C., Guilleret, I., Vick, P., Weber, T., Andre, P., Beyer, T., Blum, M. and Constam, D. B. (2009). "Bicaudal C, a novel regulator of Dvl signaling abutting RNA-processing bodies, controls cilia orientation and leftward flow." Development 136(17): 3019-30.

Mathieu, J., Griffin, K., Herbomel, P., Dickmeis, T., Strahle, U., Kimelman, D., Rosa, F. M. and Peyrieras, N. (2004). "Nodal and Fgf pathways interact through a positive regulatory loop and synergize to maintain mesodermal cell populations." Development 131(3): 629-41.

McGrath, J., Somlo, S., Makova, S., Tian, X. and Brueckner, M. (2003). "Two populations of node monocilia initiate left-right asymmetry in the mouse." Cell 114(1): 61-73.

Meno, C., Gritsman, K., Ohishi, S., Ohfuji, Y., Heckscher, E., Mochida, K., Shimono, A., Kondoh, H., Talbot, W. S., Robertson, E. J., Schier, A. F. and Hamada, H. (1999). "Mouse Lefty2 and zebrafish antivin are feedback inhibitors of nodal signaling during vertebrate gastrulation." Mol Cell 4(3): 287-98.

Meno, C., Saijoh, Y., Fujii, H., Ikeda, M., Yokoyama, T., Yokoyama, M., Toyoda, Y. and Hamada, H. (1996). "Left-right asymmetric expression of the TGF beta-family member lefty in mouse embryos." Nature 381(6578): 151-5.

Meno, C., Shimono, A., Saijoh, Y., Yashiro, K., Mochida, K., Ohishi, S., Noji, S., Kondoh, H. and Hamada, H. (1998). "lefty-1 is required for left-right determination as a regulator of lefty-2 and nodal." Cell 94(3): 287-97.

Meyers, E. N. and Martin, G. R. (1999). "Differences in left-right axis pathways in mouse and chick: functions of FGF8 and SHH." Science 285(5426): 403-6.

Mucchielli, M. L., Mitsiadis, T. A., Raffo, S., Brunet, J. F., Proust, J. P. and Goridis, C. (1997). "Mouse Otlx2/RIEG expression in the odontogenic epithelium precedes tooth initiation and requires mesenchyme-derived signals for its maintenance." Dev Biol 189(2): 275-84.

Nagy, A., Gertsenstein, M., Vintersten, K. and Behringer, R. (2003). "Manipulating the Mouse Embryo." A laboratory Manual, Cold Spring Hartbor Laboratory Press.

Nebigil, C. G., Choi, D. S., Dierich, A., Hickel, P., Le Meur, M., Messaddeq, N., Launay, J. M. and Maroteaux, L. (2000). "Serotonin 2B receptor is required for heart development." Proc Natl Acad Sci U S A 97(17): 9508-13.

Nguyen, T., Chin, W. C., O'Brien, J. A., Verdugo, P. and Berger, A. J. (2001). "Intracellular pathways regulating ciliary beating of rat brain ependymal cells." J Physiol 531(Pt 1): 131-40.

Niehrs, C. (2004). "Regionally specific induction by the Spemann-Mangold organizer." Nat Rev Genet 5(6): 425-34.

Niehrs, C., Keller, R., Cho, K. W. and De Robertis, E. M. (1993). "The homeobox gene goosecoid controls cell migration in Xenopus embryos." Cell 72(4): 491-503.

Nonaka, S., Shiratori, H., Saijoh, Y. and Hamada, H. (2002). "Determination of left-right patterning of the mouse embryo by artificial nodal flow." Nature 418(6893): 96-9.

Nonaka, S., Tanaka, Y., Okada, Y., Takeda, S., Harada, A., Kanai, Y., Kido, M. and Hirokawa, N. (1998). "Randomization of left-right asymmetry due to loss of nodal cilia generating leftward flow of extraembryonic fluid in mice lacking KIF3B motor protein." Cell 95(6): 829-37.

Nonaka, S., Yoshiba, S., Watanabe, D., Ikeuchi, S., Goto, T., Marshall, W. F. and Hamada, H. (2005). "De novo formation of left-right asymmetry by posterior tilt of nodal cilia." PLoS Biol 3(8): e268.

Okada, Y., Nonaka, S., Tanaka, Y., Saijoh, Y., Hamada, H. and Hirokawa, N. (1999). "Abnormal nodal flow precedes situs inversus in iv and inv mice." Mol Cell 4(4): 459-68.

Okada, Y., Takeda, S., Tanaka, Y., Belmonte, J. C. and Hirokawa, N. (2005). "Mechanism of nodal flow: a conserved symmetry breaking event in left-right axis determination." Cell 121(4): 633-44.

Oki, S., Hashimoto, R., Okui, Y., Shen, M. M., Mekada, E., Otani, H., Saijoh, Y. and Hamada, H. (2007). "Sulfated glycosaminoglycans are necessary for Nodal signal transmission from the node to the left lateral plate in the mouse embryo." Development 134(21): 3893-904.

Rivera-Perez, J. A., Mallo, M., Gendron-Maguire, M., Gridley, T. and Behringer, R. R. (1995). "Goosecoid is not an essential component of the mouse gastrula organizer but is required for craniofacial and rib development." Development 121(9): 3005-12.

Saijoh, Y., Oki, S., Ohishi, S. and Hamada, H. (2003). "Left-right patterning of the mouse lateral plate requires nodal produced in the node." Dev Biol 256(1): 160-72.

Saint-Jore, B., Puech, A., Heyer, J., Lin, Q., Raine, C., Kucherlapati, R. and Skoultchi, A. I. (1998). "Goosecoid-like (Gscl), a candidate gene for velocardiofacial syndrome, is not essential for normal mouse development." Hum Mol Genet 7(12): 1841-9.

Saka, Y., Tada, M. and Smith, J. C. (2000). "A screen for targets of the Xenopus T-box gene Xbra." Mech Dev 93(1-2): 27-39.

Saudou, F., Amara, D. A., Dierich, A., LeMeur, M., Ramboz, S., Segu, L., Buhot, M. C. and Hen, R. (1994). "Enhanced aggressive behavior in mice lacking 5-HT1B receptor." Science 265(5180): 1875-8.

Sbalzarini, I. F. and Koumoutsakos, P. (2005). "Feature point tracking and trajectory analysis for video imaging in cell biology." J Struct Biol 151(2): 182-95.

Schier, A. F. and Shen, M. M. (2000). "Nodal signalling in vertebrate development." Nature 403(6768): 385-9.

Schulte-Merker, S., Hammerschmidt, M., Beuchle, D., Cho, K. W., De Robertis, E. M. and Nusslein-Volhard, C. (1994). "Expression of zebrafish goosecoid and no tail gene products in wild-type and mutant no tail embryos." Development 120(4): 843-52.

Schweickert, A., Deissler, K., Britsch, S., Albrecht, M., Ehmann, H., Mauch, V., Gaio, U. and Blum, M. (2008). "Left-asymmetric expression of Galanin in the linear heart tube of the mouse embryo is independent of the nodal co-receptor gene cryptic." Dev Dyn 237(12): 3557-64.

Schweickert, A., Weber, T., Beyer, T., Vick, P., Bogusch, S., Feistel, K. and Blum, M. (2007). "Cilia-driven leftward flow determines laterality in Xenopus." Curr Biol 17(1): 60-6.

Schwenk, F., Baron, U. and Rajewsky, K. (1995). "A cre-transgenic mouse strain for the ubiquitous deletion of loxP-flanked gene segments including deletion in germ cells." Nucleic Acids Res 23(24): 5080-1.

Shiratori, H. and Hamada, H. (2006). "The left-right axis in the mouse: from origin to morphology." Development 133(11): 2095-104.

Shook, D. R., Majer, C. and Keller, R. (2004). "Pattern and morphogenesis of presumptive superficial mesoderm in two closely related species, Xenopus laevis and Xenopus tropicalis." Dev Biol 270(1): 163-85.

Smith, J. C., Price, B. M., Green, J. B., Weigel, D. and Herrmann, B. G. (1991). "Expression of a Xenopus homolog of Brachyury (T) is an immediate-early response to mesoderm induction." Cell 67(1): 79-87.

Spemann, H. and Mangold, H. (1924). "Über Induktion von Embryonalanlagen durch Implantation artfremder Organisatoren." Arch Mikrosk Anat Entwicklungsmech 100: 599–638.

Stubbs, J. L., Oishi, I., Izpisua Belmonte, J. C. and Kintner, C. (2008). "The forkhead protein Foxj1 specifies node-like cilia in Xenopus and zebrafish embryos." Nat Genet 40(12): 1454-60.

Sulik, K., Dehart, D. B., Iangaki, T., Carson, J. L., Vrablic, T., Gesteland, K. and Schoenwolf, G. C. (1994). "Morphogenesis of the murine node and notochordal plate." Dev Dyn 201(3): 260-78.

Tabin, C. J. and Vogan, K. J. (2003). "A two-cilia model for vertebrate left-right axis specification." Genes Dev 17(1): 1-6.

Tada, M., O'Reilly, M. A. and Smith, J. C. (1997). "Analysis of competence and of Brachyury autoinduction by use of hormone-inducible Xbra." Development 124(11): 2225-34.

Tada, M. and Smith, J. C. (2000). "Xwnt11 is a target of Xenopus Brachyury: regulation of gastrulation movements via Dishevelled, but not through the canonical Wnt pathway." Development 127(10): 2227-38.

Takeda, S., Yonekawa, Y., Tanaka, Y., Okada, Y., Nonaka, S. and Hirokawa, N. (1999). "Left-right asymmetry and kinesin superfamily protein KIF3A: new insights in determination of laterality and mesoderm induction by kif3A-/- mice analysis." J Cell Biol 145(4): 825-36.

Tam, P. P. (1998). "Postimplantation mouse development: whole embryo culture and micro-manipulation." Int J Dev Biol 42(7): 895-902.

Tanaka, Y., Okada, Y. and Hirokawa, N. (2005). "FGF-induced vesicular release of Sonic hedgehog and retinoic acid in leftward nodal flow is critical for left-right determination." Nature 435(7039): 172-7.

Tecott, L. H., Sun, L. M., Akana, S. F., Strack, A. M., Lowenstein, D. H., Dallman, M. F. and Julius, D. (1995). "Eating disorder and epilepsy in mice lacking 5-HT2c serotonin receptors." Nature 374(6522): 542-6.

Theiler, K. (1972). "The house mouse." Springer, Berlin, Heidelberg, New York.

Tsukui, T., Capdevila, J., Tamura, K., Ruiz-Lozano, P., Rodriguez-Esteban, C., Yonei-Tamura, S., Magallon, J., Chandraratna, R. A., Chien, K., Blumberg, B., Evans, R. M. and Belmonte, J. C. (1999). "Multiple left-right asymmetry defects in Shh(-/-) mutant mice unveil a convergence of the shh and retinoic acid pathways in the control of Lefty-1." Proc Natl Acad Sci U S A 96(20): 11376-81.

Turing, A. M. (1952). "The chemical basis of morphogenesis." Phil. Trans. R. Soc. Lond. B 237(641): 37-72.

Ulmer, B. (2008). "Die Rolle des Homeoboxgens Goosecoid im PCP-Signalweg." Diploma thesis at the Universität Hohenheim.

Varlet, I., Collignon, J. and Robertson, E. J. (1997). "nodal expression in the primitive endoderm is required for specification of the anterior axis during mouse gastrulation." Development 124(5): 1033-44.

Vick, P., Schweickert, A., Weber, T., Eberhardt, M., Mencl, S., Shcherbakov, D., Beyer, T. and Blum, M. (2009). "Flow on the right side of the gastrocoel roof plate is dispensable for symmetry breakage in the frog Xenopus laevis." Dev Biol 331(2): 281-91.

Wada, Y., Mogami, Y. and Baba, S. (1997). "Modification of ciliary beating in sea urchin larvae induced by neurotransmitters: beat-plane rotation and control of frequency fluctuation." J Exp Biol 200(Pt 1): 9-18.

Waddington, C. H. (1933). "Induction by the primitive streak and its derivatives in the chick." J Exp Biol 10: 38–46.

Waddington, C. H. and Schmidt, G. A. (1933). "Induction by heteroplastic grafts of the primitive streak in birds." Wilhelm Roux' Arch Entwicklungsmech 128: 522–563.

Wakamiya, M., Lindsay, E. A., Rivera-Perez, J. A., Baldini, A. and Behringer, R. R. (1998). "Functional analysis of Gscl in the pathogenesis of the DiGeorge and velocardiofacial syndromes." Hum Mol Genet 7(12): 1835-40.

Wallingford, J. B., Fraser, S. E. and Harland, R. M. (2002). "Convergent extension: the molecular control of polarized cell movement during embryonic development." Dev Cell 2(6): 695-706.

Weisstaub, N. V., Zhou, M., Lira, A., Lambe, E., Gonzalez-Maeso, J., Hornung, J. P., Sibille, E., Underwood, M., Itohara, S., Dauer, W. T., Ansorge, M. S., Morelli, E., Mann, J. J., Toth, M., Aghajanian, G., Sealfon, S. C., Hen, R. and Gingrich, J. A. (2006). "Cortical 5-HT2A receptor signaling modulates anxiety-like behaviors in mice." Science 313(5786): 536-40.

Wemmer, K. A. and Marshall, W. F. (2004). "Flagellar motility: all pull together." Curr Biol 14(23): R992-3.

Wilkinson, D. G., Bhatt, S. and Herrmann, B. G. (1990). "Expression pattern of the mouse T gene and its role in mesoderm formation." Nature 343(6259): 657-9.

Witkin, J. M., Baez, M., Yu, J., Barton, M. E. and Shannon, H. E. (2007). "Constitutive deletion of the serotonin-7 (5-HT(7)) receptor decreases electrical and chemical seizure thresholds." Epilepsy Res 75(1): 39-45.

Wolpert, L., Beddington, R., Brockes, J., Jessell, T., Lawrence, P. and Mayerovitz, E. (1998). "Principles of development." Oxford University press Inc., New York.

Yamada, G., Mansouri, A., Torres, M., Stuart, E. T., Blum, M., Schultz, M., De Robertis, E. M. and Gruss, P. (1995). "Targeted mutation of the murine goosecoid gene results in craniofacial defects and neonatal death." Development 121(9): 2917-22.

Yan, Y. T., Gritsman, K., Ding, J., Burdine, R. D., Corrales, J. D., Price, S. M., Talbot, W. S., Schier, A. F. and Shen, M. M. (1999). "Conserved requirement for EGF-CFC genes in vertebrate left-right axis formation." Genes Dev 13(19): 2527-37.

Yao, J. and Kessler, D. S. (2001). "Goosecoid promotes head organizer activity by direct repression of Xwnt8 in Spemann's organizer." Development 128(15): 2975-87.

Ybot-Gonzalez, P., Savery, D., Gerrelli, D., Signore, M., Mitchell, C. E., Faux, C. H., Greene, N. D. and Copp, A. J. (2007). "Convergent extension, planar-cell-polarity signalling and initiation of mouse neural tube closure." Development 134(4): 789-99.

Yu, X., Ng, C. P., Habacher, H. and Roy, S. (2008). "Foxj1 transcription factors are master regulators of the motile ciliogenic program." Nat Genet 40(12): 1445-53.

Zeitz, K. P., Guy, N., Malmberg, A. B., Dirajlal, S., Martin, W. J., Sun, L., Bonhaus, D. W., Stucky, C. L., Julius, D. and Basbaum, A. I. (2002). "The 5-HT3 subtype of serotonin receptor contributes to nociceptive processing via a novel subset of myelinated and unmyelinated nociceptors." J Neurosci 22(3): 1010-9.